The Jordan Journal of Earth and Environmental Sciences (JJEES)

JJEES is an international peer-reviewed research journal, issued by the Deanship of Academic Research and Graduate Studies, the Hashemite University, in corporation with, the Jordanian Scientific Research Support Fund, the Ministry of Higher Education and Scientific Research.

SUBMISSION ADDRESS:

Professor **Eid A. Al-Tarazi**
Deanship of Academic Research and Higher Studies
Hashemite University, P.O. Box 150458, Postal Code 13115, Zarqa, Jordan.
Phone: +962-5-3903333 ext. 4385
E-Mail: jjees@hu.edu.jo

Hashemite Kingdom of Jordan

Hashemite University

Jordan Journal of Earth and Environmental Sciences

JJEES

An International Peer-Reviewed Scientific Journal

Financed by Scientific Research Support Fund

http:// jjees.hu.edu.jo/

ISSN 1995-6681

المجلة الأردنية لعلوم الأرض والبيئة
Jordan Journal of Earth and Environmental Sciences (JJEES)
http://jjees.hu.edu.jo

Hashemite University

Deanship of Scientific Research and Graduate Studies

TRANSFER OF COPYRIGHT AGREEMENT

Journal publishers and authors share a common interest in the protection of copyright: authors principally because they want their creative works to be protected from plagiarism and other unlawful uses, publishers because they need to protect their work and investment in the production, marketing and distribution of the published version of the article. In order to do so effectively, publishers request a formal written transfer of copyright from the author(s) for each article published. Publishers and authors are also concerned that the integrity of the official record of publication of an article (once refereed and published) be maintained, and in order to protect that reference value and validation process, we ask that authors recognize that distribution (including through the Internet/WWW or other on-line means) of the authoritative version of the article as published is best administered by the Publisher.

To avoid any delay in the publication of your article, please read the terms of this agreement, sign in the space provided and return the complete form to us at the address below as quickly as possible.

Article entitled:---

Corresponding author: ---

To be published in the journal: Jordan Journal of Earth & Environmental Sciences (JJEES)

I hereby assign to the Hashemite University the copyright in the manuscript identified above and any supplemental tables, illustrations or other information submitted therewith (the "article") in all forms and media (whether now known or hereafter developed), throughout the world, in all languages, for the full term of copyright and all extensions and renewals thereof, effective when and if the article is accepted for publication. This transfer includes the right to adapt the presentation of the article for use in conjunction with computer systems and programs, including reproduction or publication in machine-readable form and incorporation in electronic retrieval systems.
Authors retain or are hereby granted (without the need to obtain further permission) rights to use the article for traditional scholarship communications, for teaching, and for distribution within their institution.

☐ I am the sole author of the manuscript

☐ I am signing on behalf of all co-authors of the manuscript

☐ The article is a 'work made for hire' and I am signing as an authorized representative of the employing company/institution

Please mark one or more of the above boxes (as appropriate) and then sign and date the document in black ink.

Signed:____ Name printed: ____

Title and Company (if employer representative) : ____

Date: __________________________________

Data Protection: By submitting this form you are consenting that the personal information provided herein may be used by the Hashemite University and its affiliated institutions worldwide to contact you concerning the publishing of your article.

Please return the completed and signed original of this form by mail or fax, or a scanned copy of the signed original by e-mail, retaining a copy for your files, to:

Hashemite University
Deanship of Scientific Research and Graduate Studies
Zarqa 13115 Jordan
Fax: +962 5 3903338
Email: jjees@hu.edu.jo

Subscription

Jordan Journal of Earth & Environmental Sciences (ISSN 1995-6681)
An International Peer- Reviewed Research Journal
Published by the deanship of Research and Graduate Studies- The Hashemite University

Name:	الاســـــــــــــــم:
Specialty:..	التخصـــــــــــــص:
Address:...	العنـــــــــــــوان:
P.O. Box:..	صنــدوق البريـــــد:
City & Postal Code:	المدينة: الرمز البريدي:
Country:...	الـــــــــــــــدولة:
Phone:...	رقــم الهاتـــــــف:
Fax No:..	رقــم الفاكـــــــس:
E-mail:...	البريـــد الإلكترونــي:
Method of payment:	طريقـــــة الدفـــع:
Amount Enclosed:...	المبلـــغ المرفـــق:
Signature:..	التوقيـــــــــــع:

Cheques should be paid to Deanship of Research and Graduate Studies- The Hashemite University

I would like to subscribe to the Journal:

For

- ☐ One year
- ☐ Two years
- ☐ Three years

One year Subscription Rates

	Inside Jordan	Outside Jordan
Individuals	10JD	70$
Students	5JD	35$
Institutions	20JD	90$

Correspondence

Subscriptions and sales:

Prof. Dr. Eid Al-Tarazi
The Hashemite University
P.O. Box 330127- Zarqa 13115 - Jordan
Tel. +962-(0) 795651567 (mobile)
+962-5-3903333 -4385 (office)
Fax: +962 5 3903338
Email: jjees@hu.edu.jo

Editorial Preface

We are pleased to publish the second issue of the fifth volume of the *Jordan Journal of Earth and Environmental Sciences*, a scientific, peer-reviewed and indexed journal issued by the Higher Scientific Research Committee and supported by the Scientific Research Support Fund of the Ministry of Higher Education and Scientific Research in Jordan, under the supervision of the Deanship of Academic Research and Graduate Studies at the Hashemite University.

Editor-in-Chief and all members of the editorial board extend their sincere thanks and gratitude to all those who contributed to publishing this journal and making it a success.

The editorial boards are always striving to continue their endeavors to publish scientific, refereed research projects that are of interest to researchers in academic and professional institutions locally, regionally and internationally. We hope that such institutions keep providing us with their unique research projects. We will, as always, handle all research projects with utmost accuracy, honesty and professionalism with all the due care and speed of publishing, following the due scientific and academic standards. We will continue our efforts to publish our journal regularly to serve researchers and achieve the objectives we set for our magazine. We are also doing our best to get accreditation at a global level.

Prof. Eid Abdel Rahman Al-Tarazi
Chairman of the Editorial Board
Faculty of Natural Resources and Environment
The Hashemite University

JJEES

Volume 5, Number 2, December. 2013
ISSN 1995-6681
Pages 45- 52

Jordan Journal of Earth and Environmental Sciences

Dissolution Cavities of Karren type in the Algal Limestone Member of Al Bayda Formation, Sector (3), Wadi Az Zad, Al Jabal Al Akhdar, NE Libya

Omar B. Elfigih[1,*] and Mohamed Y. Elgheriani[2]

[1] Assistant Professor, Petroleum Geologist, University of Benghazi, Faculty of Science, Department of Earth Sciences

[2] Geologist, University of Benghazi, Faculty of Science, Department of Earth Sciences,

Received 23 April, 2013; Accepted 9 Nov., 2013

Abstract

The study area of Wadi Az Zad is characterized by landforms of relatively stepped terraced escarpment and karst isolated hills.At least three distinct karst features are recognized in the selected measured traverses in the surface exposure of the Algal Limestone Member at Wadi Az Zad which are: Groove karren, Circular karren, and Kluft karren.

Histograms of the Algal Limestone Member at the studied traverses (T1-T3) have revealed some relationships of the recognized karren types with their elevation, lithology, topography and number of karrens or density variations. For instance, the observed densities of these surface cavities vary widely from high density of about (5.2-15.8) karren/m^2 for circular type which is found to be associated with flat area and grainstone facies, to an intermediate density of about (1.6-3.2) karren/m^2 for groove type which is found to exist mostly in relatively slope areas and in mudstone facies, and eventually to low density of about (0.5-1.5) karren/m^2 for kluft type which is found to be associated with relatively fractured (heavily jointed) and of wackstone – packstone facies.

These surface dissolution cavities are evident to be associated with lithologic and structural characters of the Algal Limestone facies in the study area.

Keywords: Al Jabal Al Akhdar, Algal Limestone, Karren, Wadi Az Zad

1. Introduction

Karst features are the foremost examples of surface water erosion on this planet. The sculpturing and removal of limestone rocks is predominantly by solution, aided in some cases by soil transmission or piping, eventually causing collapse. Surface karst features are small landforms created by solution of the surface of the rock (Selby, 1985). In general, also karst landforms (minor and major) are best developed in limestone and dolomites. Karst surface morphologies exist at a variety of scales. Inevitably then, a wide variety of geomorphological techniques and methods are employed in karst morphometric analysis (McIlroy de la Rosa, 2012; McIlroy de la Rosa et al., 2012).

Carbonate rocks of Algal limestone member in sector (3) (Fig.1) crop-out over approximately (75%) of the study area, and are characterized by surface features which are formed mainly through surface runoff and aided by integrated conduit flow systems through surface joints and even porous, leached grainstones.

We observed and measured karst features in Wadi Az Zad; we were constrained by conditions of the exposures to measuring features of the limestone surface rather than of land surface. In general, we found that the solution features on the surface of the limestone are smaller than dolines or caves of meso-karren type (Eren et al., 2010) and too small to create permanent depressions in the overlying sediment cover because the rate of dissolution is certainly much slower than the rates of surface phenomena like intensive bioturbation. The high density (number/unit area) of small solution features (karren types) on the surface of the Algal Limestone Member and sparse land-surface depressions or sinkholes are, in part, a consequence of the differences in lithology, structure, runoff, and the mechanism of dissolution of the various facies types of this limestone.

The objective of this study is to outline some of the diagnostic surface karst features in the Algal Limestone Member of sector (3), and to reveal their relationship to lithological changes and minor structural features.

* Corresponding author. e-mail: oelfigih@yahoo.com.

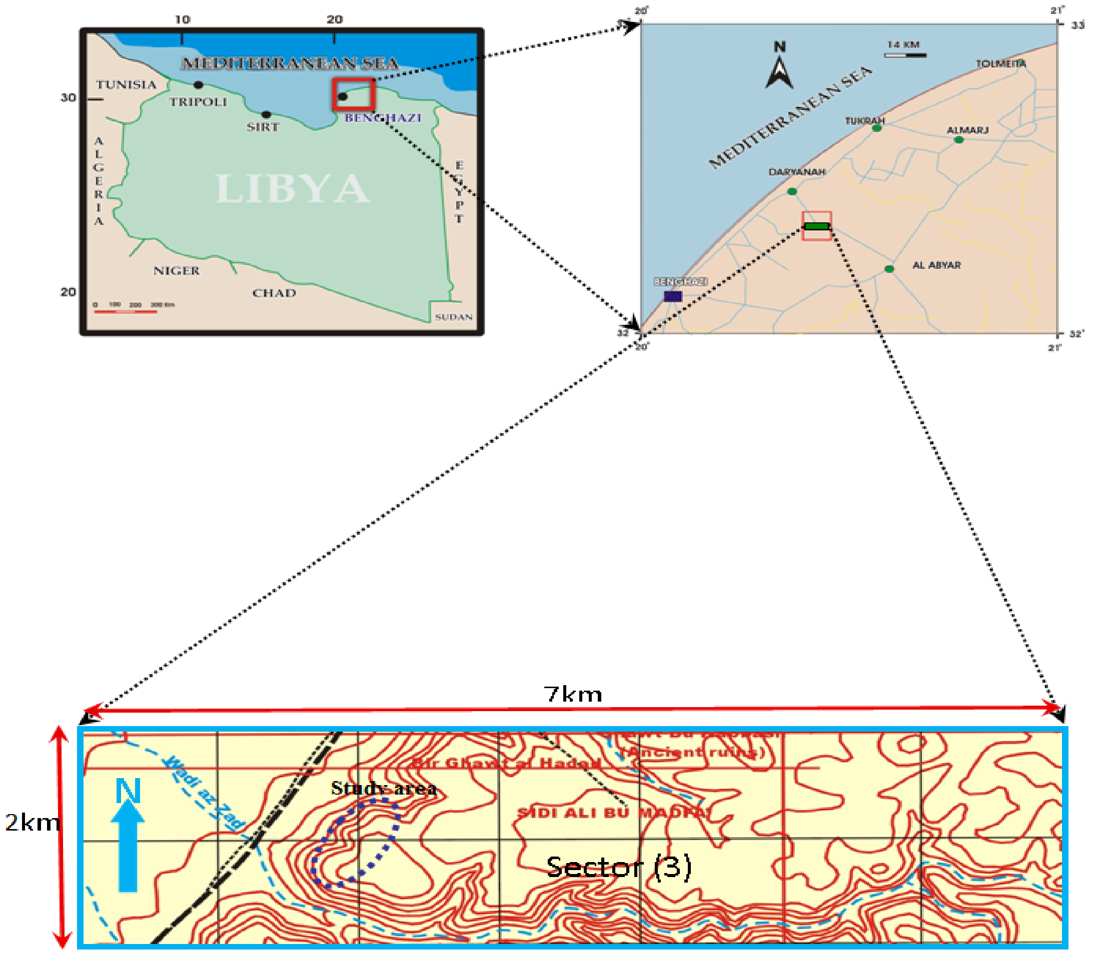

Figure 1 .Location map of sector (3) area, showing studied escarpment (dashed circle), Wadi Az Zad, Al Jabal Al Akhdar, NE Libya.

2. Geologic Setting

2.1. Geologic Units

Karst formation is an active and on-going process in the Algal Limestones of Wadi Az Zad in Tansoloukh area. Horizontal solution cavities that cut across evident bedding surfaces are present at several elevations.

Shahhat Marl Member and Algal Limestone Member (Early Oligocene) are exposed in the study area (Fig.2) and are potentially active in karst processes. The Shahhat Marl is the oldest rock unit exposed in the study area and represent the basal sedimentation unit corresponds to major transgression in the area (Rohlich, 1974). It is mainly yellow to whitish yellow marl and marly bioclastic limestone (mudstone to wackstone texture), and soft. It contains two to three marly beds, a few meters thick, wedges-out east of Wadi Az Zad. Fossils include benthonic foraminifera, echinoids, bryozoans, and mollusks. Remnants of marine organisms, as shell fragments that formed this unit, were composed originally of aragonite.

The primary biogenic aragonite has been dissolved, leaving behind molds of the organisms and creating a well-connected secondary porosity. The Algal Limestone sediments, overlying the Shahhat Marl in the field area, consists of thick-bedded to massive, white to creamy, white fossiliferous microcrystalline, chalky to medium grained Algal limestone (mudstone-grainstone texture). It is characterized by the presence of flat-like to ball-like shapes of algae (corralline red algae) of the genus Lithothamnium (Pietesz, 1968; Barr and Weeger, 1972; Muftah and Erhoma, 2002) , mollusk, nummulites and some bryozoan fragments are also present, usually embedded in sparite, but micritic matrix is occasionally very well developed at some places, which may suggest deposition in an inner-neritic conditions of shallow marine environment (Rohlich, 1974).

2.2. Depositional History

Several studies describe the geologic history of the study area, and summarize the depositional history of Al Jabal Al Al Akhdar and Cyrenica platform of northeast Libya (Klitzsch, 1970; Rohlich, 1980; El Arnauti and Shelmani, 1985; Abulsamad and Barbieri, 1999; El Hawat and Abdulsamad, 2004; El Arnauti *et al*., 2008; Yanilmaz *et al*., 2008). Carbonate and evaporite sediments were deposited on Al Jabal Al Akhdar and Cyrenica platform from the Early Cretaceous to the Late Paleogene when the deposition of transgressive carbonate rocks were followed by progressed Neogene sedimentation of regressive, highly agitated glauconitic to Oolitic limestones (grainstones) of Early to Late Miocene to local erosion and local reworking in the Late Miocene. Significant deposition may have been absent during the Pliocene and was certainly absent during the Pleistocene. Quaternary sedimentation may have been limited to reworking of Miocene deposits, local fluvial deposition as debris flow, and the deposition of terrace deposits were also topping the sequence.

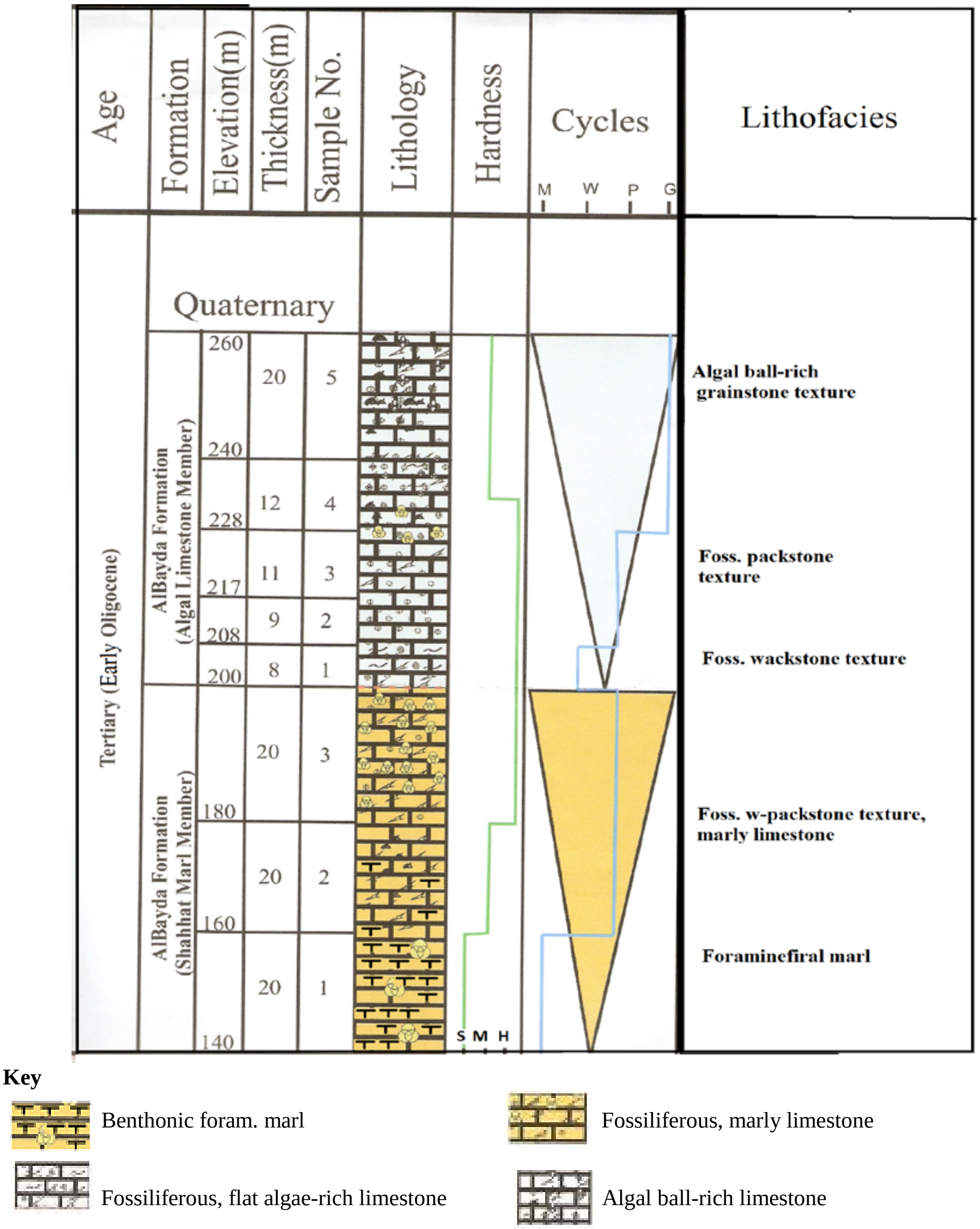

Figure 2, Generalized lithostratigraphic column of exposed pre-Quaternary deposits in Wadi Az Zad, sector (3), Al Jabal Al Akhdar, NE Libya

3. Structural Attitudes of Algal Limestone

The exposed Algal Limestone rocks are of horizontal to semi-horizontal bedding characterized by regional low dip of about 2º -5º SW. These beds are well jointed at some places and characterized by two major regional joint-trends oriented NW-SE and NE-SW. These regional fracture trends may be attributed to tensional stresses associated with the formation of Al Jabal Al Akhdar. According to Rholich (1974; 1980), two different episodes of uplift occurred during (Late Cretaceous to Late Miocene). Other possible minor trend of joints oriented E-W was also recognized, which might have contributed partially to the formation of the existent escarpment as a result of some compression and inversion tectonics in parts of Al Jabal Al Akhdar (Guiraud and Bosworth, 1999; Guiraud et al., 2005). A direct surface measurement of the joint patterns in the Algal Limestone is in general possible. Moreover, the linear features are observable on a regional scale on topographic maps and aerial photographs representing wadies parallelism and orientation, as the water flows northwest in the direction of the regional dip and discharges along the present-day coast. The joints and some minor fractures in the wackestone-packstone facies are responsible for the development of linear solution features (Kluft type) that form from the downward percolation of surface water along the joints and fractures.

4. Database

Several traverses have been taken through the outcrop of Algal Limestone Member in the study area (Fig.3) where lithology and mainly structural features have been detected and noted in a geological column. We examined, photographed, described, and counted surficial karst features exposed in three traverses (T1-T3), but safety and access limitations prevented in situ measurements of spacing and distance; so we counted these karst features across known distances. The sampling area is relatively reasonable; it is of about 480m^2 (6m x 80m), so the distribution and characteristics of the recorded solution features may be representative, in general, of small-scale karst features on the surface of the studied Algal Limestone. This Karren study involves the comparison of different parameters of the same form, allowing the researcher to deduce how the topographic and stratigraphic position of the karst terrain may influence the development of mesoscale forms. According to Tóth (2009), for any given karren form, characteristic parameters such as width, depth, and length should be chosen and compared with measurements of the same karren form under different conditions.

This study took into consideration main literatures on karstification, Jenings (1971), Sweeting (1973), White (1988, 1990), Abdulalim and Sobhi (2002), Waltham (2005), Lundberg and Ginés, (2009), Cucchi (2009), Tóth, (2009), Ford and Williams (2007) and Ginés et al. (2009) and inspection of karst features in the field and some discussions with an experienced consultant.

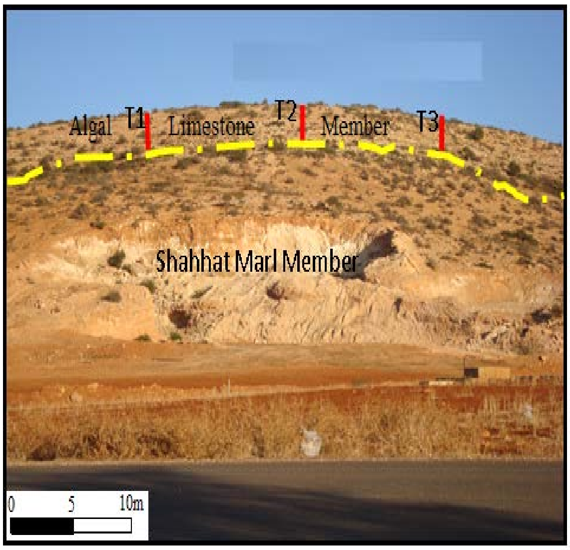

Figure 3. Studied escarpment composed of Shahhat Marl Member at the base which is used as quarry and Algal Limestone Member at the top in which studied traverses (T1,T2 and T3) can be seen, sector (3), Wadi Az Zad (Looking SE).

5. Observations

The evidence for regional karstification in the study area is extensive and there is no reason to preclude karst conditions in the Algal Limestone Member.

The following observations indicate that dissolution cavities of karst features do exist:

1. Extensive caliche in the exposed rock.
2. Solution-controlled vugular porosity.
3. Irregular surface features and of strong surface runoff.

On field observations, karren types were observed at the studied facies of the Algal Limestone Member.

Based on field observations, there are three main types of karrens, namely Groove karren, Circular karren and Kluft karren (Table 1).

5.1. Karren Processes

Falling droplets, sheet and channeled runoff, film flow, and pounded water may create small-scale dissolution forms (Karren), where rain falls onto limestone and break onto it (Ford *et al*., 1988; Bogli, 1980) gave detailed classification and discussion on surface dissolution features and their processes in limestone.

5.2. Groove karren

Longitudinal linear, groove like channels are few, (0.5cm-3.6cm) deep, (1cm-4cm) wide, but they are of (13cm-50cm) long, found at various elevations at (190m, 220m, 240m, 250m and 260m) in hard, fine- grained (mudstone to wackestone) facies they form because of strong runoff on steep slopes. (Figs.4 a,b), in cross-section AB (Fig. 5) they are of angular sharp base.

5.3. Circular karren

Circular in plane like features of localized dissolution action, these karst forms are found in flat areas because water stands (stagnates) for a longer time, thus giving the dissolution enough time to act vertically down in a pan shape, other than the mentioned grooves which form on the steep slopes due to running water.

They are few, (1cm-45cm) wide to few (1cm-40cm) deep and (0.5cm-25cm) long. They are found at various elevations (180m, 190m, 200m, 225m, 230m and 240m), usually associated with packstone to grainstone facies (Figs.6a,b), in cross-section (Fig.7), and they are rounded features.

5.4. Kluft karren

Straight or sinuous channels or film flow features are few, (0.3cm-0.5cm) deep, (0.5cm-1cm) wide, and about (36cm-180cm) long. They are found at various elevations (190m, 200m, 243m, 257m and 260m), usually associated with wackstone to packstone facies of relatively flat, parallel to bedding plane to highly jointed areas. (Figs.8a, b).

Table 1. Field observations and types of karrens in Algal Limestone Member, sector (3).

Elevation (M)	Facies			- Groove karren					+ Circular karren					* Kluft karren				
				No.	Area(M²)	L (cm)	W (cm)	D (cm)	No.	Area (M²)	L (cm)	W (cm)	D (cm)	No.	Area(M²)	L (cm)	W (cm)	D (cm)
260	- Mudstone		* W-P	18	9.5	13-20	2-4	0.5-1						5	4	90-180	0.5-1	0.5
257			* W-P											8	15	50-63	1	0.5
250	- Mudstone			8	2.5	20-50	1-4	1										
243			* W-P											6	10	36-60	0.5	0.5
240	- Mudstone	+ Grainstone		12	7	25-40	2-3	0.5-1	163	24	1-8	1-2	1.5-3					
230		+ Grainstone							73	14	2.4	3-4	1.5-3					
225		+ Grainstone							350	48	1-3	1.7-4	2-4					
220	- Mudstone			9	4.5	15-40	2-4.5	1-3.6										
200		+ Grainstone	* W-P						335	28	2-25	3.6-45	5-40	5	10	1,20	1	0.5
190		+ Grainstone	* W-P	10	6	13-35	2-3	1-3	400	25.3	2.6-7	5.5-7	2-4	12	8	73-90	0.5-1	0.3-0.5
180		+ Grainstone							200	26	0.5-1.2	1.5-3.8	1-3					

Key:
- Groove karren associated with mudstone facies.
+ Circular karren associated with grainstone facies.
* Kluft karren associated with wackestone to packstone facies.
L= Length of karren features.
W= Width of karren features.
D= Depth of karren features.

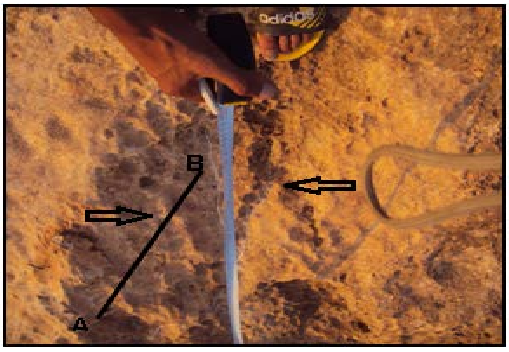

Figure 4a, Groove karren (arrows) in mudstone facies of Algal Limestone Member at elevation 220m

Figure 4b.Groove karren in mudstone facies of Algal Limestone Member at elevation 290m.

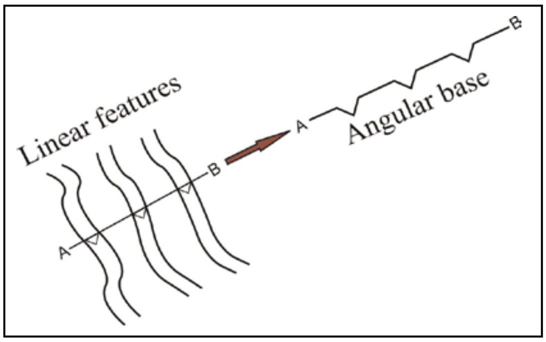

Figure 5, Cross section through groove karrens, showing linear features (grooves) of angular base on steep slopes due to running water.

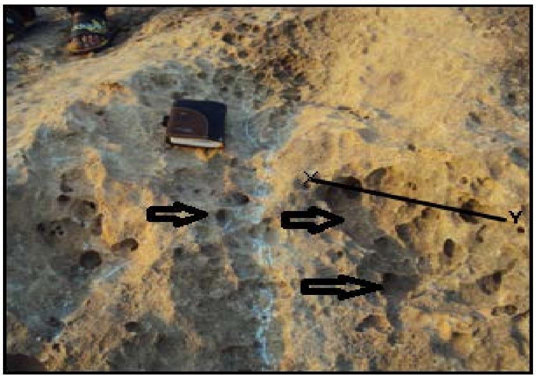

Figure 6a, Deep (2-4 cm) circular karren (arrows) in grainstone facies of Algal Limestone Member at elevation 190m.

  - Volume 5, Number 2 (ISSN 1995-6681)

Figure 6b, Oversized (25cm) long circular karren in grainstone facies of Algal Limestone Member at elevation 200m.

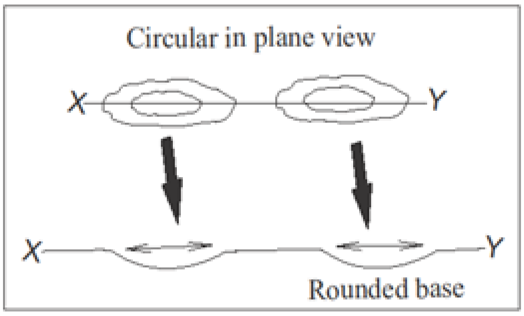

Figure 7. Cross-section through circular karrens found in flat areas, as water standing longer time, dissolution acts vertically down in a pan shape of rounded base**.**

Figure 8a. Kluft karren (arrow) in wackestone to packstone facies,parallel to bedding plane of Algal Limestone Member.

Figure 8b, Kluft karren (arrows) in wackestone to packstone faciesof Algal Limestone Member associated with joint >150cm long at elevation 190m.

6. Histograms Construction

Various histograms (Fig.9) have been constructed to show a relationship of observed karren types with some parameters such as:

1. Relationship between karren types with elevation:
   a. Elevation of groove karren at 190m, 220m, 240m, 250m and 260m.
   b. Elevation of circular karren at 180m, 190m, 200m, 225m, 230m and 240m.
   c. Elevation of kluft karren at 190m, 200m, 243m, 257m and 260m.

So, the elevation of groove (gr.) and kluft karrens (kl.) are relatively observed in higher elevation and characterized by mud-supported steep slope and of relatively extensive jointed areas relatively. However, circular karren (cir.) as evidenced in the studied section (Fig. 2) to occupy lower elevation (240m and below) represented by porous grainstone facies which is getting tighter of crystalline nature at higher elevation (260m). Actually, short distances (in vertical and lateral directions) within and between studied, traverses have revealed sudden facies changes effecting the spatial changes of karren types in an unpredictable fashion.

2. Relationship between karren types with lithology:
   a. The groove karren present only in mudstone.
   b. The circular karren present only in grainstone.
   c. The kluft karren present only in wackestone to packstone, which formed of enlarging of pre-existing joints by the dissolution action of acidic water.

Lithology of the Algal Limestone Member has a profound effect on karstification, and the formation of different karren types, as calcite dissolves more readily than other carbonates due to its higher solubility (Martinez and White 1999). Karstification can also take place where the Algal Limestone Member changes in facies (Fig.2) from benthonic foraminiferal marl, to fossiliferois marly limestone, to fossiliferous algal limestone. As mud to grains ratio decreases, a circular karren type dominates the outcrop surface, as in this facies, water standing for a period of time, percolates down with the help of the relatively porous texture of this unit. On the other hand, if mud to grains ratio increases, groove karren dominates the exposed surface because of strong runoff on steep slopes and the relative decease in porosity of this facies; thus this facie is usually characterized by mudstone-wackestone texture. As the exposed Algal Limestone is characterized by joints and fractures, formed during periods of uplift (Rohlich, 1980), governs the orientation of the kluft karren type in mudstone-packstone facies, increasing their secondary permeability, rainwater, during humid periods, begins to dissolve the carbonate along these structural weakness planes.

3. Relationship between karren types with topography:
   a. The groove karren exist only in slope areas.
   b. The circular and kluft karrens exist only in flat areas.

4. Relationship between karren types with density (number of karren per unit area):

Karren types in the study area are different in density, and show tendency of high to low density from circular to groove to kluft type.

According to White (1988), the karst feature density (Dd for doline and kd for karren in our case) could be defined as: the number of karren (Nk) in the karst area with the dimension of inverse area or per unit area (Ak), (Kd =Nk/Ak).

The studied area which is suitable for sampling is about 240m^2 , so the distribution and characteristics of the surface dissolution features recorded in the photographs (Figs.4-8) are mostly representative in general of the karren features and their in-situ measured spacing and distance on the exposed surface of the Algal Limestone Member of Wadi Az Zad.

The observed densities of these surface cavities (Table 2) vary widely as following:

Measured high density of about (5.2-15.8) karren/m2 for circular type, which is found to be associated with flat area and grainstone facies.

An intermediate density of about (1.6-3.2) karren/m^2 for groove type which is found to be mostly in relatively slope areas and of mudstone facies.

Low density of about (0.5-1.5) karren/m^2 for kluft type which is found to be associated with relatively fractured (heavily jointed) and wackestone–packstone facies.

Table 2. Karren density measurement in Algal Limestone Member, sector (3). (Kd= Nk/Ak after White 1988).

Elevation (M)	K.type	No.	Area (M^2)	$K_d = \frac{N_k}{A_k}$
260	Groove	18	9.5	1.8
	Kluft	5	4	1.2
257	Kluft	8	15	0.5
250	Groove	8	2.5	3.2
243	Kluft	6	10	0.6
240	Groove	12	7	1.7
	Circular	163	24	6.8
230	Circular	73	14	5.2
225	Circular	350	48	7.2
220	Groove	9	4.5	2
200	Kluft	5	10	0.5
	Circular	335	28	12
190	Groove	10	6	1.6
	Kluft	12	8	1.5
	Circular	400	25.3	15.8
180	Circular	200	26	7.6

Key: K.type= karren type.

K_d: karren density.

N_k: Number of karren.

A_k: Area of karren.

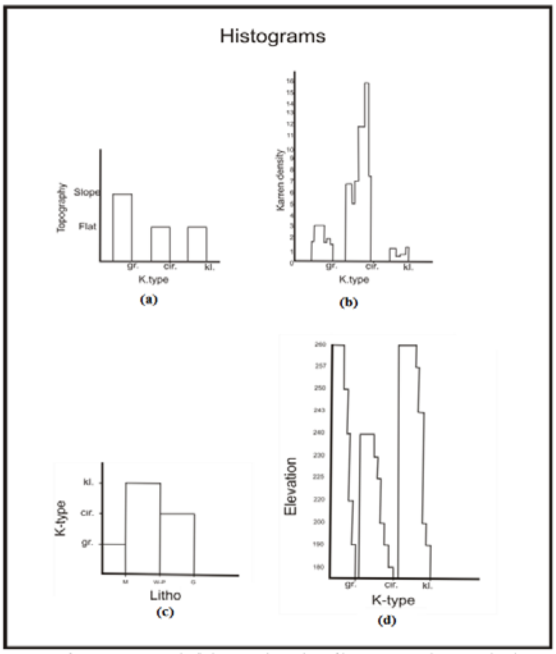

Figure 9. Histograms (a-d) showing relationships of karren types with topography, density, lithology and elevation, in Algal Limestone Member, sector (3).

7. Conclusion

Based on field observations and literature review, the Algal Limestone facies in sector (3) area, Tansulukh region are dominated by minor surface dissolution karstic features like cavities. Histograms have shown some relationships of these karstic features (karren types) with some parameters such as lithology, topography and density. The observed dissolution karstic features are found to be mainly controlled by lithologic change; as mud to grains ratio decreases, circular karren type dominates the outcrop surface where water standing for a period of time, percolates down with the help of the relatively porous packstone-grainstone texture. On the other hand, if mud to grains ratio increases, groove karren will dominate the exposed surface because of the strong runoff on steep slopes and the relative decease in porosity of this mudstone-wackestone facies. Structural attitudes and characters of the exposed Algal Limestone Member in the study area have an impact on the type of karren; as joints and fractures, formed during periods of uplift, govern the orientation of the kluft karren type in mudstone-packstone facies and increasing their secondary permeability through extensive joints to dissolve the carbonate along these structural weakness planes.

Acknowledgement

The authors would like to thank Prof. Dr. A. El Hawat and Prof. Dr. A. El Arnauti, Earth Sciences Department Benghazi University, for their reading of an early draft of this paper and their fruitful suggested comments.

Thanks also extended to the anonymous reviewers for their constructive criticism of the manuscript.

References

[1] Abdulsamad, E. and Barbieri, R.,(1999). Foraminifera distribution and paleoecological interpretation of the Eocene-Miocene carbonate at Al Jabal al Akhdar (northeast Libya), Journal of Micropaleontology, 18, p..45-65, England.

[2] Abdulalim S. and Sobhi J., (2002). Middle Pleistocene karst evolution in the state of Qatar, Arabian Gulf, Journal of cave and karst studies, 64 (2), pp.132-139.

[3] Bogli, A., (1980). Karst hydrology and physical speleology: Berlin, springer. Verlag 284p.

[4] Barr F., T., and Weager A., A., (1972). Stratigraphic nomenclature of the Sirte Basin, Libya, 179p., Petrl. Expl. Soc. Libya, Tripoli.

[5] Cucchi, F. (2009) Kamenitzas. In: Ginés, A., Knez, M., Slabe, T., Dreybrodt, W. (eds.) (2009) *Karst Rock Features: Karren Sculpturing*. Ljubljana: ZRC Publishing.

[6] El Arnauti, A. and Shelmani, M., 1985. Stratigraphy and structural setting, In: B. Thusu and B. Owens (Eds.), Palynostratigraphy of Northeast Libya, Jour, Brit. Micropal, Sco, London.

[7] El Arnauti A., Lawrece S. R., Mansouri A. L., Sengor A. M., Soulsby A. and Hassan H., (2008). Structural styles in NE Libya, Geology of the East Libya, V. IV, pp. 153-178.

[8] El Hawat, A. S. and Abdulsamad, E.O., (2004). The geology of Cyrenaica, a field seminar, Earth science society of Libya ,1pp.

[9] Eren, M. and Hatipoglu-Bagci, Z. (2010) "Karst surface features of the hard laminated crust (caliche hardpan) in the Mersin area, southern Turkey". *Acta Carsologica*. 39 (1): 93-102.

[10] Ford D. C., Arthur N. Plamer and William B. White, (1988). Landform development, karst, Vol.0-2 hydrology, the geology of North America.

[11] Ford, D.C. and Williams, P. (2007) *Karst Hydrogeology and Geomorphology*. Chichester: Wiley.

[12] Ginés, A., Knez, M., Slabe, T., Dreybrodt, W. (eds.) (2009) *Karst Rock Features: Karren Sculpturing*. Ljubljana: ZRC Publishing.

[13] Guiraud R. and Bosworth W., (1999). Phanerozoic geodynamic evolution of northeastern Africa and the northwestern Arabian platform, *Tectonophysics* 315, pp. 73–108.

[14] Guiraud R., Bosworth W., Thierry J., Delplanque A., (2005). Phanerozoic geological evolution of Northern and Central Africa: An overview, Journal of African Earth Sciences 43 (2005) 83–143

[15] Jenings, J. N., (1971). Karst, M. I. T. press, Cambridge, Mass. 252pp.

[16] Klitzsch, E., (1970). The structural development of parts of North Africa since Cambrian time. In: Geol. Libya (ed. C. Grey).

[17] Lundberg, J. and Ginés, A. (2009) Rillenkarren. In: Ginés, A., Knez, M., Slabe, T., Dreybrodt, W. (eds.) (2009) *Karst Rock Features: Karren Sculpturing*. Ljubljana: ZRC Publishing.

[18] Martinez, M.I., & White, W., 1999, A laboratory investigation of the relative dissolution rates of the Lirio limestone and the Isla de Mona dolomite, and implications for cave and karst development on Isla de Mona: Journal ofCave and Karst Studies, v. 61, p. 7-12

[19] McIlroy de la Rosa. (2012) " Karst Landform Classification Techniques". In: Geomorphological Techniques, Chap. 3, Sec. 6.1 (2012), British Society for Geomorphology (BSG), ISSN 2047-0371, pp.1-15.

[20] McIlroy de la Rosa, J.P., Warke, P.A., Smith, B.J. (2012) "Microscale biopitting by the endolithic lichen *Verrucaria baldensis* and its proposed role in mesoscale solution basin development on limestone". *Earth Surface Processes and Landforms*. 37: 374-384.

[21] Muftah A. and Erhoma H., (2002). Coralline red algae of the Algal Limestone Member of Al Bayda Formation, NE Libya biostratigraphic and paleoenvironmental significant, 6th international conference on geology of the Arab world, Cairo University, vol. II, p.637.

[22] Pietersz, C. R., (1968). Proposed nomenclature for rock units in northern Cyrenaica. In: F.T. Barr (ed.), Geology and archaeology of northern Cyrenaica, Libya. Petrl. Expl. Soc. Libya, Tripoli, Libya, pp.125-130.

[23] Rohlich, P., (1974). Geological map of Libya, 1:250,000, Al Bayda sheet NI34-15, explanatory booklet; Indust. Resear. Cent., Tripoli, Libya, 70pp.

[24] Rohlich , P., (1980). Tectonic development of Al Jabal Al Akhdar, in M. J. Salem and M. Buscrewil, eds. Proc. Sypm, Geology of Libya, V.II. P.P 923-931.

[25] Selby, M. J., (1985). Earth's changing surface. Clarendon press. Oxford, 607pp.

[26] Sweeting M. M., (1973). Karst landforms, Columbia University Press, New York.

[27] Tóth, G. (2009) Some methodologies on karren research. In: Ginés, A., Knez, M., Slabe, T., Dreybrodt, W. (eds.) (2009) *Karst Rock Features: Karren Sculpturing*. Ljubljana: ZRC Publishing.

[28] Waltham T., (2005). Karst terrains, In: Fookes P. G., Lee M. and Milligan G. (eds.), Geomorphology for engineer, Whittles publishing, Caithness, pp.662-687.

[29] White W. B., (1988). Geomorphology and hdrology of karst terrains. Oxford University Press, 464pp.

[30] White W. B., (1990). Surface and near surface karst landforms. Geological Society of America, special paper 252pp.

[31] Yanilmaz E., Huffman D. P., Martin M. and Gutteridge P., (2008). Facies analysis and depositional systems of defined sedimentary sequences from Precambrian to Late Miocene in NE Libya, Geology of East Libya, V. IV, pp. 3-84.

JJEES

Volume 5, Number 2, December. 2013
ISSN 1995-6681
Pages 53- 61

Jordan Journal of Earth and Environmental Sciences

A Preliminary Assessment of Soil Pollution in Some Parts of Jalingo Metropolis, Nigeria Using Magnetic Susceptibility Method.

Kanu, Maxwell O., M.Sc.[1,*], Meludu, Osita C., PhD[2] and Oniku, S. A., PhD[2]

[1] Department of Physics, Taraba State University, P. M. B. 1167, Jalingo, Taraba State, Nigeria.

[2] Department of Physics, Modibbo Adama University of Technology, P.M.B. 2076, Yola, Adamawa State, Nigeria.

Received 12 Nov., 2012; accepted 8 Oct., 2013

Abstract

An investigation of magnetic properties using magnetic susceptibility and frequency dependent susceptibility was conducted on 36 soil samples from parts of Jalingo, Taraba State, N-E Nigeria. The purpose was to assess the level of soil pollution and identify pollution hotspots using magnetic proxy parameters. The results of the mass specific low frequency magnetic susceptibility measurements show significant enhancement with values ranging from 67.8 - 495.3 x 10^{-6} m^3kg^{-1} with a mean value of 191.61 x 10^{-6} m^3kg^{-1} for the Jalingo College of Education JCOE data; 520.1 – 1612.8 x 10^{-6} m^3kg^{-1} with a mean value of 901.34 x 10^{-6} m^3kg^{-1} for the Jalingo Main Market, JMM and 188.5- 1203.6 x10^{-6} m^3kg^{-1} with an average value of 574 92 x 10^{-6} m^3kg^{-1} for the Jalingo Motor Park JMP. The significant magnetic enhancement indicates high concentration of ferrimagnetic minerals in the soil and thus increases pollution. The magnetic susceptibility of the different land use studies decreased in the order commercial area (market) > motor park > official area. The results of the percentage frequency dependence susceptibility showed that most of the samples have a mixture of superparamagnetic SP and coarse multidomains grains or superparamagnetic grains < 0.05μm. In the JCOE samples, the value of percentage frequency dependent susceptibility ($\chi_{fd}\%$) ranges from 2.68 – 13.80% with an average value of 8.67%. Five samples (that is about 30%) are virtually all SP grains as they have $\chi_{fd}\%$ in the range of 12 – 14 %, while other samples have values in the range of 2 – 10 % indicating the presence of a mixture of SP and Multi Domain MD magnetic grains. In the Jalingo Main Market (JMM) samples, seven samples fall within the medium range of 2 – 10 % and may be said to have a mixture of SP and coarse MD grains; three samples have low $\chi_{fd}\%$ of < 2% implying that they have no SP grains while only one sample has high $\chi_{fd}\%$ of 10.04 % meaning that the dominant magnetic component of this soil is SP ferrimagnetic grains. For the JMP samples, about 70% of the samples have $\chi_{fd}\%$ value in the medium range, and this can be interpreted as soils with admixture of SP and coarser non-SP grains or < 0.005μm SP grains. Two samples (about 20%) of the JMP samples have $\chi_{fd}\%$ > 10%, indicating soils where virtually all the iron component is SP grains, while about 10% of the samples contains no SP grains. Generally, most of the samples in the studied area contain a mixture of SP and MD magnetic grains.

Key words: Soil Pollution, Magnetic Susceptibility, Frequency Dependent Susceptibility, Mineral Magnetic, Ferrimagnetic

1. Introduction

The adverse effect of human impact, especially atmospheric pollution in the environment has increased in recent years and has become a subject of global concern. So, pollution has become a subject widely investigated from various fields, such as geology, geophysics, chemistry, and agriculture. Atmospheric pollution has been identified as one of the most harmful factors for ecosystems (Petrovsky and Elwood, 1999). The various pollution sources, whether industrial, vehicular and domestic emissions, usually contain heavy metals and toxic elements. When these pollutants are released into the atmosphere, they are incorporated into the environment or in living organism such as vegetation, animals and human beings, posing serious risks to human health. Pope and Dockery (2006) showed that long-term exposure to

* Corresponding author. e-mail: maxiexpress007@gmail.com.

airborne pollutants can lead to respiratory and cardiovascular diseases. Before now organic lead compounds (tetraethyl lead and tetramethyl lead) were extensively used as additives in gasoline, but at present unleaded gasoline is used in most countries of the world. Africa has contributed substantially to global lead pollution (Nduka and Orisakwe, 2010). In Nigeria, gasoline, with an average lead content of 0.66g/l, is still in use (Fakayode and Olu-Owolabi, 2003). The national consumption of petrol in the country is estimated at 20 million litres per day, with about 150 people/car/city, therefore, close to 15,000 kg of lead is emitted into the environment through combustion. The release of lead into the environment is further compounded by the poor road network, dilapidated nature of existing roads and the large volume of importation of fairly used vehicles, which leads to a high number of irreparable and decomposing automobile parts littered on the roadsides. These contaminants that are released into the atmosphere, soils and sediments are rich in magnetic particles, resulting in magnetic enhancement of the urban soils and sediments. A measure of the amount of magnetic enhancement is expressed by its magnetic susceptibility and in recent years, it has been successfully used to monitor anthropogenic pollution, especially heavy metal pollution in soils (Strzyszcz and Maigiera, 1998; Petrovsky *et al*., 2000; Gautam *et al*., 2004; Canbay, 2010, Sandeep, 2012; among others).

Magnetic susceptibility is defined as the ratio of the total magnetization induced in a sample to the intensity of the magnetic field that produces the magnetization (Mullins, 1977). Magnetic susceptibility measures the concentration of magnetic crystals, grain size and the shape and type of the magnetic minerals present in a sample. Magnetic minerals present in soils may either be obtained from the parent rocks (lithogenic origin) during pedogenesis, or because of anthropogenic activities. The magnetic mineral content of the soil can broadly be expressed by its magnetic susceptibility. Magnetic susceptibility can be used to identify the type of mineral and the amount of iron bearing minerals contained in a material (Dearing, 1999). When the contribution of lithogenesis and pedogenesis to the overall magnetic properties of soils are minimal, magnetic susceptibility measurements become very important for monitoring environmental (anthropogenic) pollution. Soils are sinks to anthropogenic pollutants released into the atmosphere. Accumulation of anthropogenic ferrimagnetic particles, originating from oxidation process during combustion of fossil fuels, results in significant enhancement of topsoil magnetic susceptibility. The most important magnetic mineral is magnetite and in the atmosphere it can originate from combustion (and other industrial) processes (Petrovsky *et al*., 2000). One source of atmospheric pollution is road traffic. Hopke *et al.* (1980) found that Lead, Cadmium, Chromium, Cobalt and Arsenide, the primary constituents of automobile exhaust are in association with high-density magnetic particles (presumably magnetite). The iron particles results from car body rusting or ablation from the interior of car exhaust systems and breaks.

In Nigeria, most pollution studies (for example Fakayode and Olu-Owolabi, 2003; Adie and Osibanjo, 2009; Nduka and Orisakwe, 2010; among others) have been conducted using the traditional chemical analysis. Studies of magnetic proxies for pollution in Nigeria are scarce. This is a preliminary attempt to studying soil pollution using magnetic susceptibility in some parts of Taraba State, North-East Nigeria. The study aims at mapping and providing information on the level of soil pollution using magnetic proxy parameters. This study does not consider the relationship between heavy metal and magnetic susceptibility; it only utilizes the fast, nondestructive, and cost effective magnetic analyses as a preliminary tool to assess pollution hotspots. Further studies will hopefully consider the traditional, cost and time consuming geochemical technique on specific samples that are found to be highly polluted using the magnetic technique.

2. Materials and Methods

2.1. Geographical and Geological setting of the Study Area

Jalingo, the study area, is the administrative headquarters of Taraba State which is located between latitude 6°30' and 8°30' North of the equator and between 9°00' and 12°00' East of the Greenwich meridian (Figure 1). The state has a tropical wet and dry climate, dry season lasts for a minimum of five months (November to March) while the wet season spans from April to October. It has an annual rainfall of about 8000 mm. Jalingo is a city with no major industry. The major pollution source is the emission from traffic and power generating sets and other human activities such as indiscriminate dumping of waste, bush burning, household heating systems, etc.

The study area is underlain by the undifferentiated Basement Complex rocks, which consist mainly of the migmatites, gneisses and the Older Granites. Tertiary to Recent basalts also occurs in the area. The undifferentiated Basement Complex, particularly the migmatites, generally varies from coarsely mixed gneisses to diffused textured rocks of variable grain size and are frequently porphyroblastic (Macleod *et al*., 1971). This rock unit constitutes principally the undifferentiated igneous and metamorphic rocks of Precambrian age (Grant, 1971.)

The Pan African Older Granites are equally widespread in the area. They occur either as mafic or intermediate intrusives (Turner, 1964). Different kinds of textures, ranging from fine to medium to coarse grains, can be noticed on the Older Granites (McCurry, 1976). Other localized occurrences of minor rock types include some doleritic and pegmatitic rocks mostly occurring as dykes and vein. These occurrences are common to both the undifferentiated Basement Complex and the Older Granite rocks (Carter *et al*., 1963; McCurry, 1976). The Tertiary basalts, on the other hand, are found in the Mambila Plateau mostly comprised of trachytic lavas and extensive basalts, which occur around Nguroje (du Preez, 1965).

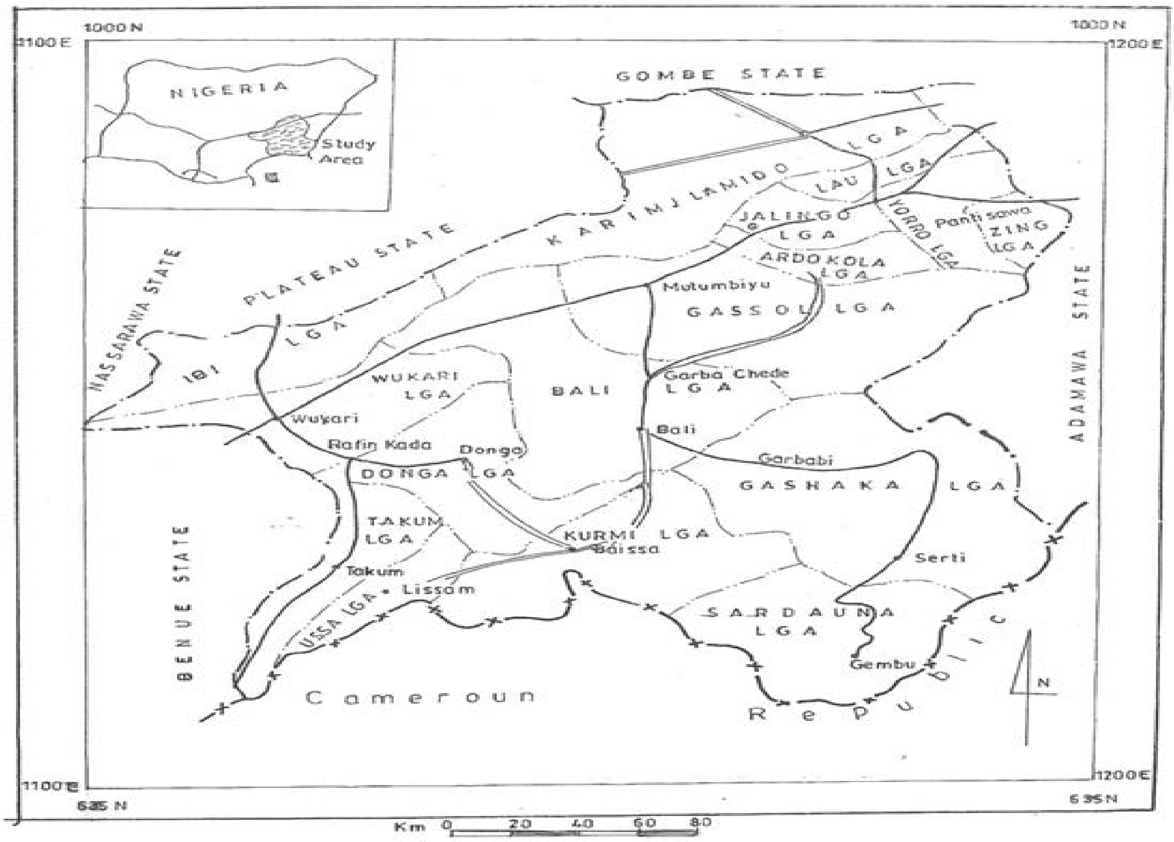

Figure 1. Map of study area (insert: map of Nigeria, showing study area).

2.2. Sampling and Analysis

Topsoil samples (0- 2 cm) were collected from three different locations using a plastic material to avoid contamination. The samples locations were determined using a 12 Channel Garmin Global Positioning System (GPS 12). A total of 36 samples were randomly collected, 15 samples from an official area, 10 samples from a motor park and 11 samples from a commercial area. The Jalingo College of Education (JCOE), which has been in existence for more than 25 years, was chosen to represent a school environment. The Jalingo Motor Park (JMP) has been in operation for more than 15 years with a land area of about 250 square meters with more than 500 vehicles moving in and out daily. The Jalingo Main Market (JMM), which is the major commercial centre of the city, has an area of about 500 square meters and was built more than two decades ago. Many commercial activities take place in this market and vehicular movement around the market area has been on the rise over the years.

The samples were air dried at a temperature of 30°C in the laboratory for several days to avoid any chemical reactions. They were then ground using agate mortar and sieved using a 1 mm sieve mesh (Kim *et al*., 1999) and stored in plastic containers for further laboratory measurements. The mass specific magnetic susceptibility measurements were then carried out on the sieved samples packaged in a 10 ml plastic container at laboratory temperature. Measurements of magnetic susceptibility were made at both low (0.47 kHz) and high (4.7 kHz) frequencies using MS2 dual frequency susceptibility meter. All measurements were conducted at the 1.0 sensitivity setting. Each sample was measured three times with an air reading before and after each series for drift correction. The mass specific frequency dependence susceptibility χ_{fd} was obtained from the relation:

$$\chi_{fd} = \chi_{lf} - \chi_{hf} \quad (1)$$

Where χ_{lf} and χ_{hf} are the low frequency and high frequency susceptibility, respectively.

This parameter is sensitive only to a very narrow grain size range crossing the superparamagnetic/single domain threshold (~ 20 – 25 nm for maghemite) (Worm and Jackson, 1999). For natural samples, which generally exhibit a continuous and nearly constant grain size distribution, χ_{fd} can be used as a proxy for relative changes in concentration in pedogenic fined – grained magnetic particles (Liu *et al*., 2005). The relative χ_{fd} also called Percentage frequency dependent susceptibility (χ_{fd}%) was then calculated following Dearing (1999) as:

$$\chi fd\ (\%) = \left(\frac{\chi^{lf} - \chi^{hf}}{\chi^{lf}}\right) \times 100 \quad (2)$$

The magnetic map of the study area was obtained using a computer software program, surfer 7.0.

3. Results and Discussion

The results of the mass specific low field magnetic susceptibility, frequency dependence, and percentage frequency dependence of the samples are displayed in tables 1 - 3. The value of low frequency mass specific magnetic susceptibility ranges from 67.8 - 495.3 x 10^{-6} m^3kg^{-1} with a mean value of 191.61 x 10^{-6} m^3kg^{-1} for the JCOE data. The JMM has low frequency magnetic susceptibility values ranging from 520.1 – 1612.8 x 10^{-6} m^3kg^{-1} with a mean value of 901.34 x 10^{-6} m^3kg^{-1}, while the JMP has a low frequency magnetic susceptibility ranging from 188.5- 1203.6 x$10^{-6}m^3kg^{-1}$ with an average value of 574. 92 x 10^{-6} m^3kg^{-1}. The results obtained are comparable to urban soils in Shanghai, China, which has a magnetic susceptibility value ranging from 127.3 – 1959 x 10^{-8} m^3kg^{-1} (Hu *et al*., 2006). The magnetic susceptibility of the different land use studies decreased in the order commercial area (market) > motor park > official area. The differences in the values of magnetic susceptibility in the different areas are caused by the difference in the type and strength of human activity in these areas. The high magnetic susceptibility values of the JMM may be attributed to the high commercial activity in the market, tiny pieces of rusted metal parts that might be thrown to the ground and anthropogenic sources due to the high volume of traffic within the market area.

Table 1: Jalingo College of Education (JCOE) data.

Sample	Mass (g)	Latitude (N)	Longitude (E)	χ_{lf} x10^{-6} m^3kg^{-1}	X_{hf} x 10^{-6} m^3kg^{-1}	χ_{fd} x 10^{-6} m^3kg^{-1}	χ_{fd} (%)
JCOE 1	16.29	8°54.080’	11°19.052’	226.7	197.0	29.7	13.10
JCOE 2	17.91	8°54.067’	11°19.078’	359.5	309.9	48.6	13.80
JCOE 3	18.31	8°54.104’	11°19.078’	175.7	171.0	4.7	2.68
JCOE 4	17.94	8°54.119’	11°19.044’	132.8	123.4	9.4	7.08
JCOE 5	18.58	8°54.129’	11°19.021’	200.8	182.4	18.4	9.16
JCOE 6	17.03	8°54.135’	11°19.009’	136.9	125.2	11.7	8.55
JCOE 7	19.72	8°54.111’	11°18.992’	156.7	149.7	7.0	4.47
JCOE 8	18.96	8°54.122’	11°18.962’	131.1	122.7	8.4	6.41
JCOE 9	17.70	8°54.078’	11°19.005’	495.3	437.2	58.1	11.73
JCOE 10	19.62	8°54.162’	11°19.087’	309.6	286.1	23.5	7.59
JCOE 11	18.95	8°54.186’	11°19.102’	81.0	74.0	8.6	9.31
JCOE 12	19.07	8°54.193’	11°19.072’	67.8	62.0	5.8	8.55
JCOE 13	18.26	8°54.191’	11°19.038’	110.8	96.8	14.0	12.64
JCOE 14	19.20	8°54.165’	11°19.049’	141.7	136.4	5.3	3.74
JCOE 15	17.11	8°54.220’	11°18.961’	147.1	130.5	16.6	11.28

Table 2: Jalingo Main Market (JMM) data.

Sample	Mass (g)	Latitude (N)	Longitude (E)	χ_{lf} x10^{-6} m^3kg^{-1}	X_{hf} x 10^{-6} m^3kg^{-1}	χ_{fd} x 10^{-6} m^3kg^{-1}	χ_{fd} (%)
JMM 1	16.63	8°53.714’	11°21.605’	658.3	622.3	36.0	5.47
JMM 2	18.06	8°53.711’	11°21.526’	520.1	510.0	10.1	1.94
JMM 3	18.05	8°53.678’	11°21.547’	1182.7	1115.9	66.8	5.65
JMM 4	16.87	8°53.703’	11°21.555’	1321.4	1229.2	92.2	6.98
JMM 5	15.79	8°53.692’	11°21.607’	623.5	599.8	23.7	3.80
JMM 6	17.44	8°53.689’	11°21.603’	571.5	568.7	2.8	0.49
JMM 7	17.13	8°53.690’	11°21.600’	556.1	549.7	6.4	1.15
JMM 8	17.17	8°53.651’	11°21.578’	1612.8	1503.4	109.4	6.78
JMM 9	16.28	8°53.619’	11°21.601’	656.6	611.9	44.7	6.81
JMM 10	17.41	8°53.591’	11°21.610’	1120.9	1008.4	112.5	10.04
JMM 11	18.10	8°53.548’	11°21.631’	1090.8	1020.3	70.5	6.46

Table 3: Jalingo Motor Park (JMP) data.

Sample	Mass (g)	Latitude (N)	Longitude (E)	χ_{lf} x10^{-6} m^3kg^{-1}	X_{hf} x 10^{-6} m^3kg^{-1}	χ_{fd} x 10^{-6} m^3kg^{-1}	χ_{fd} (%)
JMP1	17.86	8°56.267’	11°20.328’	401.7	349.3	52.4	13.04
JMP 2	18.15	8°56.301’	11°20.323’	842.4	811.8	30.6	3.63
JMP 3	18.57	8°56.306’	11°20.305’	444.3	418.7	25.6	5.76
JMP 4	16.90	8°56.300’	11°20.283’	286.0	261.5	24.5	8.57
JMP 5	18.38	8°56.290’	11°20.303’	442.6	440.1	2.5	0.56
JMP 6	17.46	8°56.277’	11°20.286’	188.5	167.7	21.8	11.03
JMP 7	18.34	8°56.265’	11°20.281’	466.7	453.3	13.4	2.87
JMP 8	17.86	8°56.274’	11°20.301’	903.9	855.3	48.6	5.38
JMP 9	18.94	8°56.257’	11°20.317’	1203.6	1149.9	53.7	4.46
JMP 10	17.71	8°56.242’	11°20.300’	569.5	550.5	19.0	3.34

Gautam *et al.* (2004) classified soils into three broad categories based on their magnetic susceptibility (MS) values as follows: 'normal' (MS < 10 x 10^{-6} m^3kg^{-1}), 'moderately magnetic' (MS 10 – 100 x 10^{-6} m^3kg^{-1}), and 'highly magnetic' (MS >100 x 10^{-6} m^3kg^{-1}). From the above classification, the soils from JMM and JMP can be said to be highly magnetic, while those of JCOE ranges from moderate to highly magnetic. The high values indicate high concentration of ferrimagnetic minerals in the soil. Previous studies showed that differences in variations in magnetic susceptibility are caused by differences in geology (lithogenic/geogenic), soil forming processes (pedogenesis), and the anthropogenic input of magnetic material (Thompson and Oldfield, 1986; and Dearing *et al*., 1996). The higher magnetic enhancement in JMM and JMP is caused by the higher volume of traffic in and around these areas and other human activities. Vehicular emissions comprise different fractions of particles formed in the engine in the exhaust pipes and released into the environment. These emissions are of magnetic character, which is determined by the enhancement in the MS. The moderate values of MS obtained from JCOE samples are expected since the area is an official area with less traffic. The high values obtained in some samples are attributed to emissions from vehicles and power-generating sets, as power is epileptic in this city. Most businesses are operated using private alternating current generators.

The magnetic susceptibility map of the study area is displayed in figure 2. The map shows a magnetic enhancement at the top NE and the NW regions.

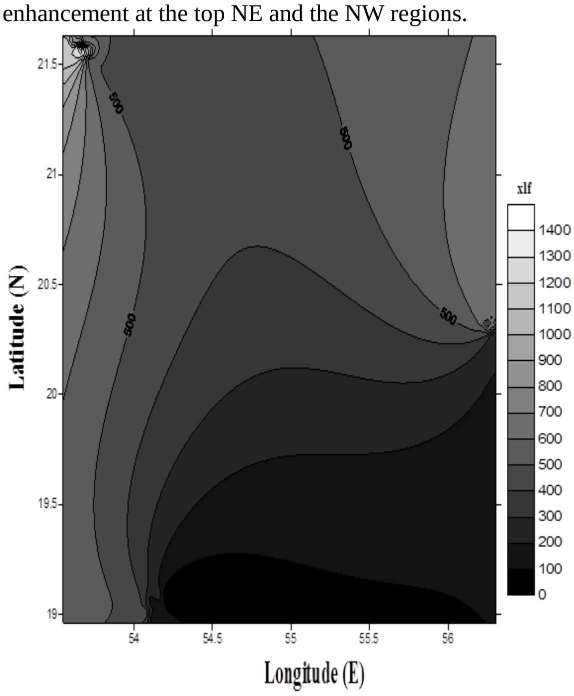

Figure 2: Contour map showing distribution of MS in the studied area.

Figure 3 shows the 3-D map of the distributions pattern of mass normalized MS (χ_{lf} x10^{-6} m^3kg^{-1}) for the surface soils studied. From the diagram, two high susceptibility peaks can be observed around the NW and NE regions. These regions correspond to the market area where a lot of human activities, including emissions from power generating sets, take place and the motor park where large emissions from car exhausts are experienced. Another MS contrast is observed around the SS region. This may correspond to the JCOE region where the lowest MS values are observed.

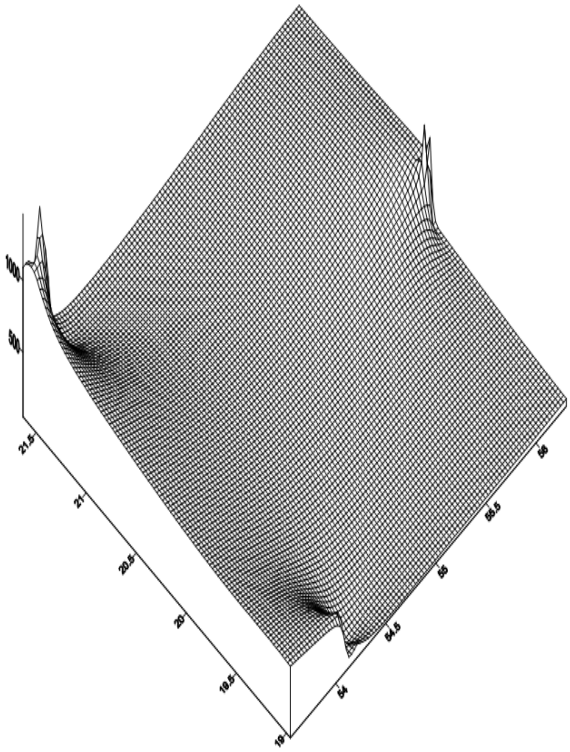

Figure 3: 3-D map of mass normalized MS (χ_{lf} x10^{-6} m^3kg^{-1}) showing distributions pattern for the surface soils studied.

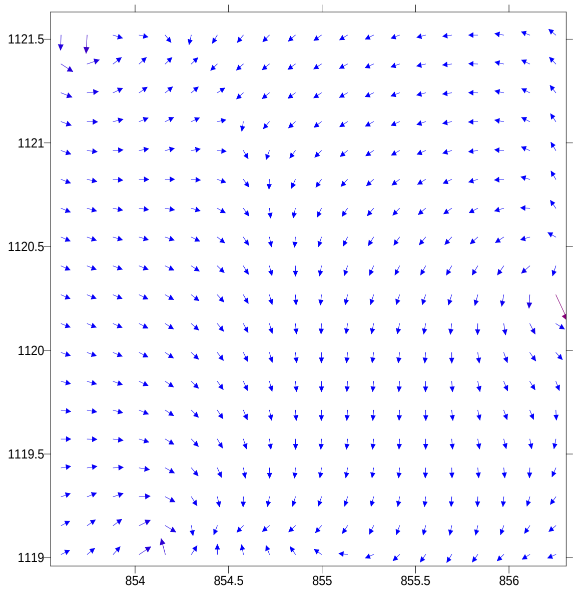

Figure 4: Vector map of the studied area.

A vector map can depict the local gradients of a topographic surface. In the vector map shown in figure 4, each arrow shows a slope direction and a magnitude associated with the location at which the arrow is drawn. The arrow points in the direction of steepest ascent and the size of the arrows are scaled to the magnitude of the local slopes. The slopes are gentle suggesting the surface run -

off as a major control of transportation and re-deposition of the anthropogenically loaded topsoil during rainy season.

Generally, the magnetic susceptibility measured at high frequencies (4.7 kHz) has lower values than the low frequency (0.47 kHz) magnetic susceptibility measurements (Dearing *et al*., 1996; Dearing, 1999). This is further confirmed about soils in Jalingo Metropolis, as shown in figures 5 to 7. Measurements made at these two frequencies at a constant applied field are generally used to detect the presence of ultrafine ferrimagnetic (also called super paramagnetic fraction of less than 0.03 µm) minerals occurring as crystals and to some extent the single domain (approximately greater than 0.03 to less than 0.06 µm fractions) (Sangode *et al*., 2010). Higher frequency measurements do not allow super paramagnetic grains to react with the applied magnetic field, as it changes more quickly than the required relaxation time for super paramagnetic grains. As a result, in higher frequency, lower values of MS are encountered and the difference is used to estimate the super paramagnetic ferromagnetic particles (Sangode, *et al*., 2010). When super paramagnetic minerals are present in a soil sample, the MS values at high frequency are slightly lower than the values of MS at low frequency. If there are no super paramagnetic (SP) minerals, the two measurements are identical (Dearing, 1999).

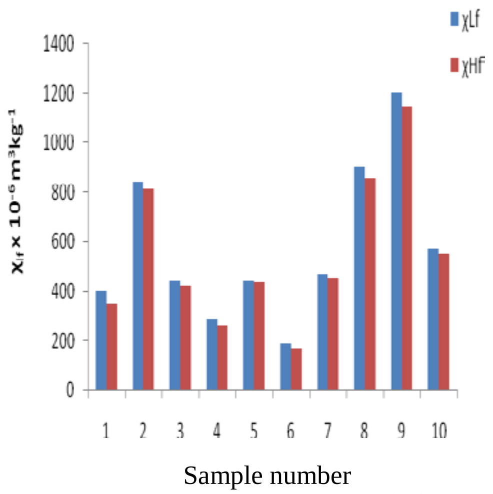

Figure 5: Magnetic susceptibility values (x 10^{-6} m^{3}kg^{-1}) for JMP samples both at high and low frequency.

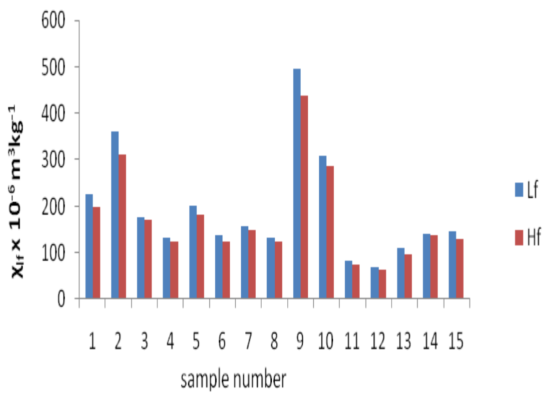

Figure 6: Magnetic susceptibility values (x 10^{-6} m^{3}kg^{-1}) for JCOE samples both at high and low frequency.

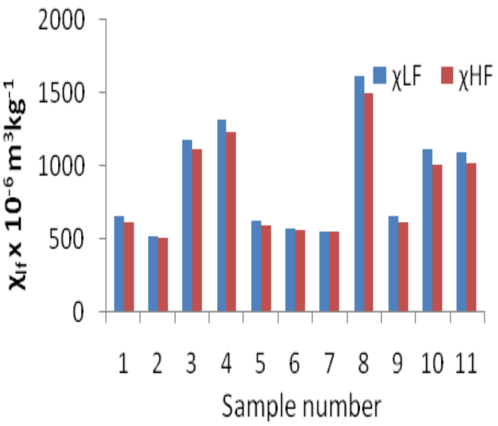

Figure 7: Magnetic susceptibility values (x 10-6 m3kg-1) for JMM samples both at high and low frequency.

There is a great difference between measured values of χLF and χHF , which indicates the presence of admixture of SP minerals in the studied soil. This difference is expressed by the frequency dependent MS (χfd) shown in tables 1-3. The values of varied between 4.7 – 58.1 x 10^{-6}m^{3}kg^{-1} with an average of 17.99 x 10^{-6}m^{3}kg^{-1} for the JCOE, 2.8 – 112.5 x 10^{-6}m^{3}kg^{-1} with a mean value of 52.28 x 10^{-6}m^{3}kg^{-1} for JMM and 2.5- 53.7 x 10^{-6}m^{3}kg^{-1} with a mean of 29.21 x 10^{-6}m^{3}kg^{-1} for the JMP. According to Dearing (1999), the mass specific frequency dependent susceptibility ranges from ~30 x 10^{-6}m^{3}kg^{-1} in stable single domain (SSD) grains to 75 – 160 x 10^{-6}m^{3}kg^{-1} in the SP range. From this information, the majority of the samples studied falls within the SSD range, while only about 20% from the JMM are in the SP range.

Figure 8 relates the χLF and χHF values in the topsoil samples of JMP. The graph shows a linear relationship between χlf and χHF with very significant correlation coefficient.

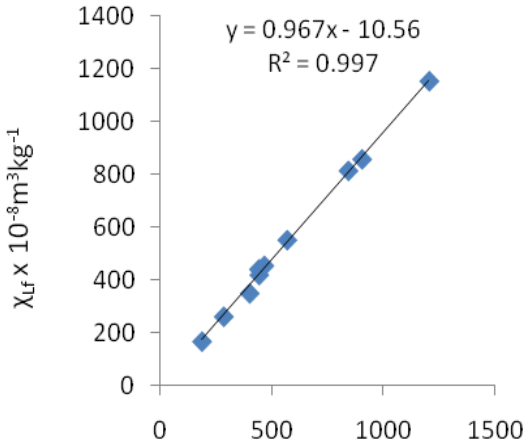

Figure 8: Relation between low frequency and high frequency susceptibility for Jalingo motor park.

Figures 9 -11 compare the χ_{fd} and χ_{LF} values in the topsoil samples. An increase in MS appears to be related to an increase in the χ_{fd}. According to Foster *et al.* (1994), such linear correlation indicates that with increasing magnitude the susceptibility is more controlled by the contribution from the fine magnetic fraction. The JMM and JCOE were more correlated with correlation coefficients of 0.84 and 0.85, respectively.

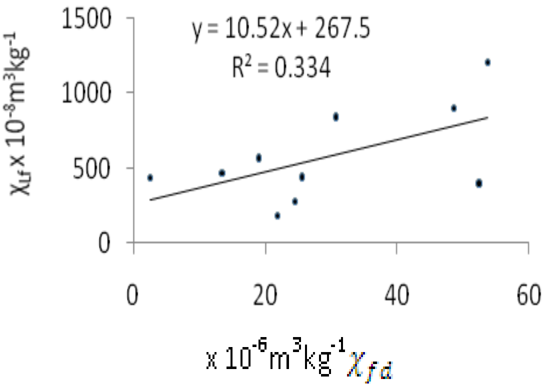

Figure 9: Linear regression between χ_{fd} and χ_{LF} for JMP.

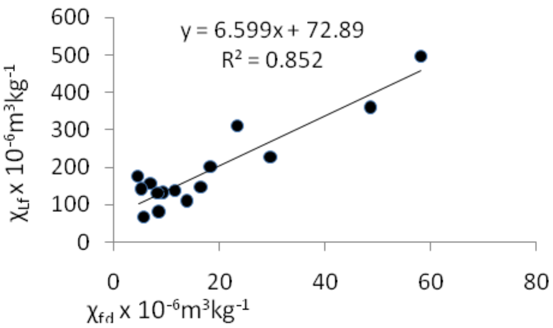

Figure 10: Linear regression between χ_{fd} and χ_{Lf} for JCOE samples.

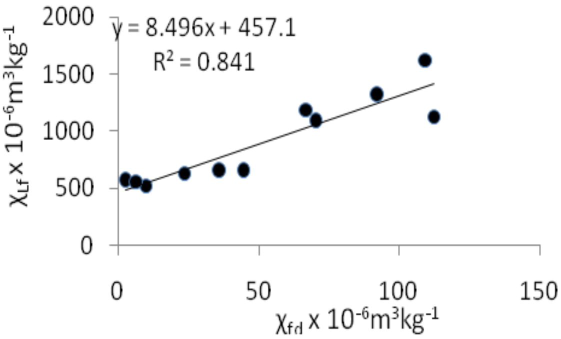

Figure 11: Linear regression between χ_{fd} and χ_{LF} JMM samples.

Percentage frequency dependent susceptibility $\chi_{fd}\%$ is used to approximate the total concentration of SP grains, while coarse multi domain (MD) magnetic grains are frequency independent as they show similar susceptibility values at low and high frequencies. Dearing (1999) proposed a model for the interpretation of percentage frequency dependence as follows:

$\chi_{fd}\%$	Interpretation
< 2%	Virtually no SP grains
2 – 10%	Admixture of SP and coaser non-SP (MD) grains or SP grains < 0.005μm
10 – 14%	Virtually all (> 75%) SP grains
>14%	Rare values, erroneous measurement, anisotropy, weak samples or contamination

Based on the semi quantitative model above by Dearing (1999), the results of this work demonstrated that about 67% of the samples have a mixture of SP and coarse grains or SP grains < 0.05μm. In the JCOE samples, the value of $\chi_{fd}\%$ ranges from 2.68 – 13.80% with an average value of 8.67%. Five samples (that is about 30%) are virtually all SP grains as they have $\chi_{fd}\%$ in the range of 12 – 14 %, while other samples have values in the range of 2 – 10 % indicating the presence of a mixture of SP and MD magnetic grains. In the JMM samples, seven samples fall within the medium range of 2 – 10 % and may be said to have a mixture of SP and coarse MD grains, three samples have low $\chi_{fd}\%$ of < 2% implying that they have no SP grains, while only one sample has high $\chi_{fd}\%$ of 10.04 % meaning that the dominant magnetic component of this soil sample are SP ferrimagnetic grains. For the JMP samples, about 70% of the samples have $\chi_{fd}\%$ value in the medium range and this can be interpreted as soils with admixture of SP and coarser non-SP grains or < 0.005μm SP grains. About 20% of the JMP samples are soils where virtually all the iron component are SP grains, while about 10% of the samples contains no SP grains. Generally, most of the samples in the studied area contain a mixture of SP and MD magnetic grains.

Figures 12 – 14 are the respective scattergram of χ_{lf} - $\chi_{fd}\%$ for JMP, JCOE and JMM showing typical sample positions for the various domains and sources.

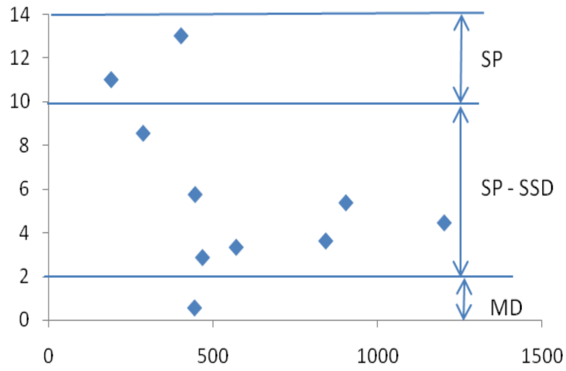

Figure 12: A schematic - scattering diagram showing typical positions of samples from JMP.

The JMP samples showed negative correlation between χ_{lf} and $\chi_{fd}\%$ while the JCOE and JMM samples showed positive correlation. The negative correlation observed in the JMP samples indicates that the main susceptibility variations are due to magnetic enhancement because of industrial and anthropogenic pollution. The negative correlation between χ_{lf} and $\chi_{fd}\%$ further shows that pedogenic SP grains contribute little to the magnetic enhancement of urban soils, the magnetic enhancement is mainly contributed by coarse magnetic grains from industrial and anthropogenic pollution. Similar results were also obtained by Lu *et al*. (2007) for urban topsoils from Luoyang and Lu and Bai (2008) for urban soils from Hangzhou. The positive correlation of the JMM and JCOE samples indicates that the MS enhancement is due to SP ferromagnetic grains. The MS of soils derived from sedimentary rocks usually increase with an increase in frequency dependent susceptibility (Lu 2003). Many authors (Zhu *et al*., 2001; Wang *et al*., 2003; among others) also reported a positive correlation between χ_{lf} $and\ \chi_{fd}\%$ for Chinese loess and paleosols.

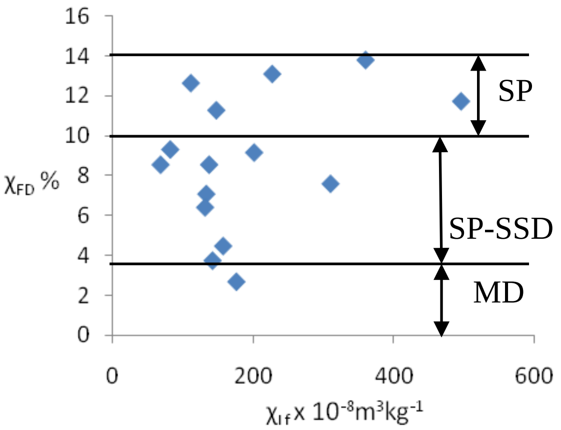

Figure 13. A schematic χ_{lf} - $\chi_{fd}\%$ scattering diagram showing typical positions of samples from JCOE.

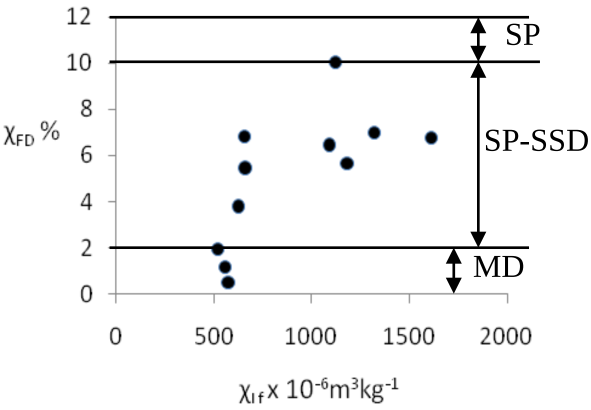

Figure 14: A schematic χ_{lf} - $\chi_{fd}\%$ scattering diagram showing typical positions of samples from JMM.

4. Conclusion

This paper presents preliminary results of magnetic susceptibility studies of soils in Jalingo, Taraba State, Nigeria and is probably the first study of this kind in this area.

The results of the mass specific low frequency magnetic susceptibility ranges from 67.8 - 495.3 x 10^{-6} m^3kg^{-1} with a mean value of 191.61 x 10^{-6} m^3kg^{-1} for the JCOE data; 520.1 – 1612.8 x 10^{-6} m^3kg^{-1} with a mean value of 901.34 x 10^{-6} m^3kg^{-1} for the JMM and 188.5-1203.6 x$10^{-6}m^3kg^{-1}$ with an average value of 574.92 x 10^{-6} m^3kg^{-1} for the JMP. The results showed significant magnetic enhancement, which indicates high concentration of ferrimagnetic minerals in the soil. The magnetic susceptibility of the different land use studies decreased in the order commercial area (market) > motor park > official area. The significant magnetic enhancement also indicates that the study area is polluted; pollution distribution can be known by analysis of magnetic susceptibility. Since the MS method is cheap, fast and capable of measuring a very wide area within a short time, it can be used as a preliminary tool to detect highly polluted areas before the application of the time consuming and expensive geochemical method on select representative sampling.

A linear positive correlation between MS and χ_{fd} was obtained. This indicates that the MS is controlled by the contribution from the fine magnetic fraction in the soil.

The results of the percentage frequency dependence showed that most of the samples have a mixture of SP and coarser non-SP grains. The average value of χ_{fd} (%) are 8.67%, 5.05% and 5.86% for the JCOE, JMM and JMP, respectively. Specifically, 24 samples had a mixture of SP and MD grains, eight (8) samples were in the SP grain size range while four (4) samples were within the MD range

References

[1] Adie, G. U. and Osibanjo, O. (2009): Assessment of soil-pollution by slag from an automobile battery manufacturing plant in Nigeria. *African Journ. Of Environmental Science and Technology*, Vol.3 (9), pp. 239 – 250.

[2] Canbay, M. (2010): Investigation of the Relationship between Heavy metal Contamination of soils and its Magnetic Susceptibility. *International Journ. of Physical Sciences* Vol. 5(5), pp.393 – 400.

[3] Carter, J.D., Barber, W. and Tait, E. A. (1963): The Geology of parts of Adamawa, Bauchi and Bornu Provinces in Northeastern Nigeria. Bull. No. 30, Geological Survey of Nigeria, 108.

[4] Dearing, J. A. (1999): Environmental Magnetic Susceptibility, Using thr Bartington MS2 System. Second edition, England: Chi Publishing.

[5] Dearing, J. A., Dann, R. J. L., Hay, K., Lees, J. A., Loveland, P. J., Maher B. A, and O'Grady, K. (1996): Frequency Dependent Susceptibility Measurements of Environmental Materials. *Geophys. J. Int.*, Vol. 124, 228 – 240.

[6] du Perez, J. W. and Barber, W. (1965): The Distinction of Chemical Quality of Ground Water in Northern Nigeria. Bull. 36, Geological Survey of Nigeria, 93.

[7] Fakayode, S. O. and Olu-Owolabi B. I. (2003): Heavy metal contamination of roadside topsoil in Osogbo, Nigeria.: its Relationship to Traffic Density and Proximity to Highways *.Environ. Geol.* 44: 150 -157.

[8] Foster, T. H., Evans, M. E., Heller, F. (1994): The Frequency Dependence of Low Field Susceptibility in Loess Sediments, *Geophys. J. Int.*, Vol. 28, 223 – 246.

[9] Gautam, P., Blaha, U. and Appel, E. (2004): Integration of Magnetic Properties and Heavy Metal Chemistry to Quantify Environmental Pollution in Urban Soils, Kathmandu, Nepal. Extended Abstract: 19th Himalaya-Karakoram –Tibet Workshop, Niseko, Japan.

[10] Gautam, P., Blaha U. and Appel, E. (2005): Magnetic Susceptibility of Dust Loaded Leaves as a Proxy of Traffic -Related Heavy Metal Pollution in Kathmandu, Nepal. *Phy. Chem. Earth*, 29: 2201 -2211.

[11] Grant, N. K. (1961): A Compilation of Radiomaetric Age from Nigeria. Journ. Of Mining Geology, 6: 37-54.

[12] Hopke, P. K., Lamb, R. E., and Natush, D. F. S. (1980): Multielemental Characteraterization of Urban Roadway Dust. *Env. Sci. Technol.* 14: 164 – 172.

[13] Hu, X. F., Su, Y., Ye, R., Li, X. Q. and Zhang, G.L. (2006): Magnetic properties of the urban soils in Shanghai and their environmental implications. *Catena*, 70: 428-436.

[14] Kim, W., Doh, S. J. and Yu, Y. (1999): Anthropogenic contribution of magnetic particulates in urban roadside dust. *Atmospheric Environment*. 43: 3137-3144.

[15] Liu, Q. S., Maher, B. A., Yu, Y., Deng, C. I., Zhu, R. X. and Zhao, X. X. (2005): Quantifying Grain Size Distribution of Pedogenic Magnetite Particles in Chinese Loess and its Significance for Pedogenesis. *J. Geophys. Res.* 110: B11102, doi: 10.1029/2005JB003726.

[16] Lu, S. G. (2003): Chinese Soil Magnetism and Environment. Higher Education Press, Beijing (in Chinese).

[17] Lu, S. G., Bai, S. Q. and Xue, Q. F. (2007): Magnetic Particles as Indicators of Heavy Metals Pollution in Urban Soils: A case Study from the City of Luoyang, China. *Geophys. Journ. Inter*. 171: 603 – 612.

[18] Lu, S. G. and Bai, S. Q. (2008): Magnetic Characterization and Magnetic Mineralogy of the Hangzhou Urban Soils and its Environmental Implications. *Chinese Journal of Geophys.* Vol 51. No. 3, pp. 549 – 557.

[19] Macleod, W. N., Turner, D. C. and Wright, E. P. (1971): The Geology of the Jos Plateau. Geological Survey of Nigeria, Bull. No. 32, 18.

[20] McCurry, P. (1976): A Generalized Review of the Geology of the Precambrian to lower Paleozoic Rocks, Northern Nigeria: In Kogbe, C. A. (ed.), Geology of Nigeria, Elizabethan Press, Lagos. Pp. 13 -38.

[21] Mullins C. E., (1977): Magnetic Susceptibility of the Soil and its significance in Soil Science: a Review, *J. Soil Sci.* 28: 223 – 246.

[22] Nduka, J. K. and Orisakwe,O. E. (2010): Assessment of Environmental Distribution of Lead in Some Municipalities of South – Eastern Nigeria. Int. *Journ. of Environ. Research and Public Health* 7(6): 3501 – 2513.

[23] Petrovsy, E. and Ellwood, B. B. (1999): Magnetic Monitoring of Air, Land and Water pollution. In: Maher, B. A. and Thompson, R. (eds.) Quaternary Climates, Environments and Magnetism. UK: Cambridge University Press, pp. 279 – 319.

[24] Petrovsky, E., Kapicka. A. Jordanova, N., Knab, M. and Hoffmann, V. (2000): Low Field Magnetic Susceptibility: A Proxy Method in Estimating increased Pollution of different Environmental Systems. *Environ. Geol*. 39: 312 – 318.

[25] Pope, C. A. and Dockery, D. W. (2006): Health effects of fine particulate air pollution: Lines that connect. *Journal of the Air and Waste Management Association*, 56: 709-742.

[26] Sangode, S. J., Vhatkar, K., Patil, S. K., Meshram, D.C., Pawar, N. J., Gudadhe, S.S., Badekar, A. G. and Kumaravel, V. (2010): Magnetic Susceptibility Distribution in the Soils of Pune Metropolitan Region: Implications to Soil Magnetometry of Anthropogenic Loading. *Current Science*, Vol. 98, No. 4, PP. 516 -527.

[27] Stzyszcz, Z. T. and Magiera, T. (1998): Magneic Susceptibility and Heavy Metals Contamination in Soils of Southern Poland. *Phys. Chem. Earth* 23(9-10):1127 -1131.

[28] Thompson , R. and Oldfield, F. (1986): Environmental Magnetism. Allen and Unwin, London.

[29] Turner, D. C. (1964): Notes on Fieldwork of the Basement Rocks of 1: 250,000 Sheets 7 and 8. Geol. Survey of Nigeria Report No. 5503.

[30] Wang, X. Y., Lu, Z., Deng, C. L., Tan, H. B. and Song, Y. G. (2003): Paleoclimate Significance of Mineral Magnetic Properties of Loess Sediments in Northern Qingai-Tibetan Plateau. *Chinese Sci. Bull*. 48: 2126 – 2133.

[31] Worm, H. U. and Jackson, M. (1999): The Superparamagnetism of Yucca Mountain Tuff. *J. Geophys. Res*. 104: 25415 – 25425.

[32] Zhu, R. X., Deng, C. I. and Jackson, M. J. (2001): A Magnetic Investigation along a NW-SE transect of the Chinese Loess Plateau and its Implications. *Phys. Chem. Earth.* 26: 867 - 872.

JJEES
Jordan Journal of Earth and Environmental Sciences
Volume 5, Number 2, December. 2013
ISSN 1995-6681
Pages 63- 71

Geoelectrical and Hydrogeochemical Assessment of the Groundwater Potentials of Ehandiagu, Enugu State, Southeastern Nigeria

O.S. Onwuka[1], A.C.Ekwe[2] and Adimonye, O.J[1]

[1]*University of Nigeria, Nsukka,*

[2]*Federal University Ndufu Alike, Ikwo, Ebonyi State, Nigeria.*

Received 11 April, 2013; Accepted 10 Oct., 2013

Abstract

Geoelectrical, hydrogeochemical investigations were carried out in order to determine the groundwater potentials of Ehandiagu in Enugu state, southeastern Nigeria. Ehandiagu is underlain by the Nkporo Shale, which is a low permeability formation. Four vertical electrical sounding (VES), employing the Schlumberger electrode configuration, was carried out in the study area, with a maximum electrode separation of 580m. The VES data were modeled with the IPI2 WIN software. The VES curves were predominantly of the QH type. The lithologic succession consists of lateritic top soil, weathered bedrock, fractured shale (the aquifer) and compact carbonaceous shale. Results show that the depth to water ranges between 6.82m and 20.7m while aquifer thicknesses range between 8.95m and 26.26m. The depth to water obtained from hand-dug wells varies between 6.20m and 15.18m. Aquifer hydraulic conductivity and transmissivity were calculated to be 2.62 x 10^{-3} m/day and 4.31 x 10^{-2} m^2/day respectively. These parameters were used to classify the aquifer as moderately good to poor aquifer. Hydrogeochemical analysis of groundwater samples collected from twelve (12) hand-dug wells in the study area reveals that weathering is the major process that controls the groundwater chemistry and the water type is Sodium-Potassium-Bicarbonate. The concentration of heavy metals (Mn, Fe, Pb) were found to be above the acceptable limits for potability and the SO_4^{2-} concentration is very low, probably due to sulphate reduction. Both sulphate reduction and high heavy metal concentration suggest a geochemical reducing environment.

Keywords: Ehandiagu, Groundwater Chemistry, Hydraulic Conductivity, Transmissivity, Vertical Electrical Sounding.

1. Introduction

Ehandiagu is located in the eastern part of the Anambra Basin, between latitudes 6°46′ and 6°50′N, and longitudes 7°32' and 7°35'E (Fig. 1). The terrain is generally flat. Few ephemeral streams exist in the area, and groundwater is not readily available due to the existence of impermeable bedrock in the area. There are several hand-dug wells in Ehandiagu, but there are no boreholes. Ehandiagu has become important lately because of the renewed interest in the exploration of oil and gas in the Nigerian inland basins. There is, therefore, a need to evaluate the potentials of the underlying formation in the area to supply groundwater as a more dependable alternative to surface water, in anticipation that development projects may quickly come up in the area. This is the reason for this work.

Relationships between aquifer characteristics and electrical parameters of geoelectric layers, as well as the chemical quality of groundwater, have been studied and reviewed by many authors. Igboekwe *et al.* (2006) delineated potential aquifer zones in Kwaibo watershed in Ikwuano and Umuchieze area, based on the high hydraulic conductivity and transmissivity values in most parts of the watershed. Ofoma *et al.* (2006) delineated 6-7 geoelectric layers in Nsukka and observed that the water table falls within the lower parts of the layers at a depth of about 110m. The primary objective of this work is to determine aquifer characteristics such as aquifer depth, thickness, hydraulic conductivity and transmissivity from both hydrogeological and geophysical data, and to assess the quality of the groundwater with a view to determining the potability.

2. Geology and Hydrogeology

Ehandiagu is located within the Anambra Basin, which flanks the Benue Trough to the east. The Anambra Basin originated in the Santonian stage by the contemporaneous subsidence of the Anambra platform and the uplift of the Abakaliki-Benue anticlinorium (Murat, 1972). This basin is funnel shaped and filled with texturally and mineralogically mature sediments of the Cretaceous age. The stratigraphic packaging of the Anambra Basin is divided into two, namely: Nkporo Group and the Coal Measures. The Nkporo Group comprises Nkporo Shale, Enugu Shale and Owelli Sandstone. Ehandiagu is directly underlain by the Nkporo Shale (Fig.1).

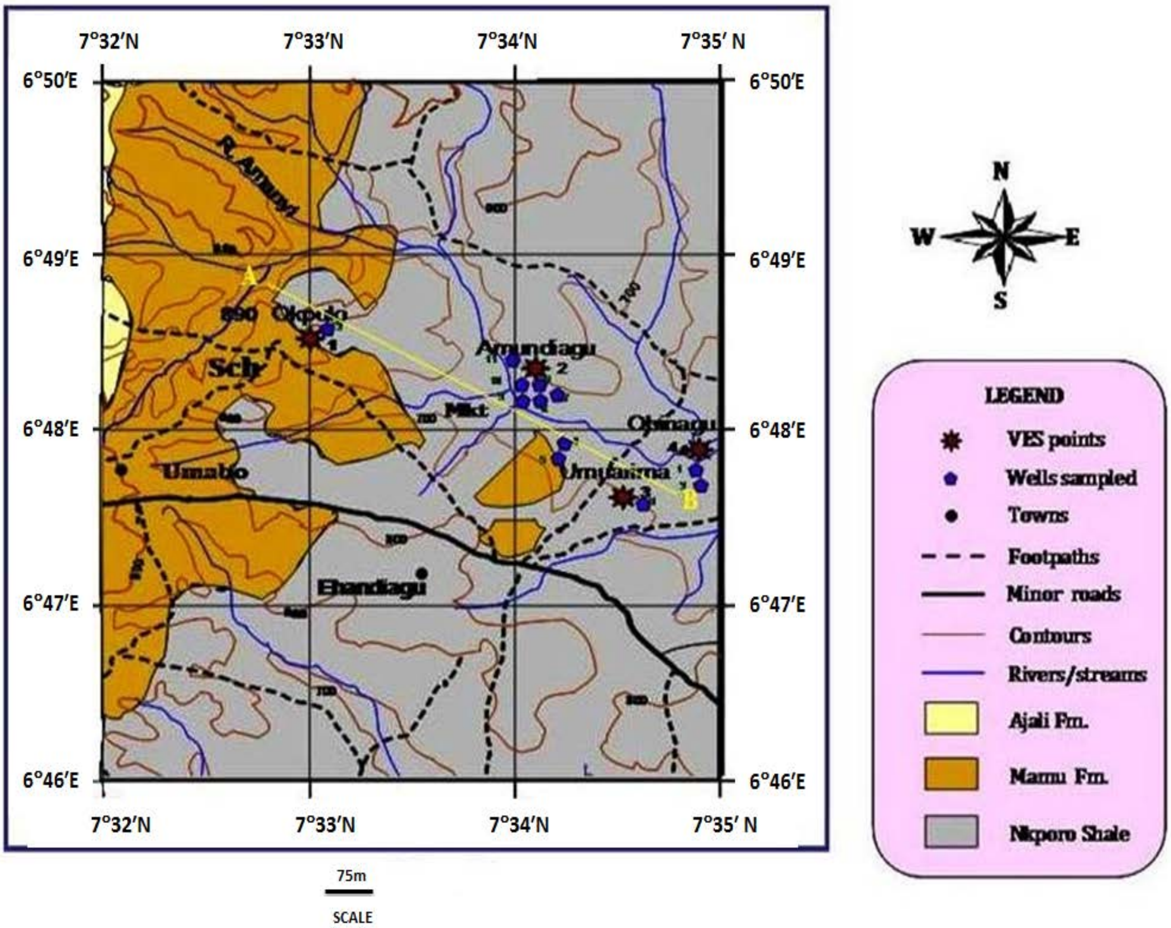

Figure 1. Location and geologic map of the study area**.**

The Nkporo Shale and the Enugu Shale are known to be aquicludes (Offodile, 2002). Outcrops of the Nkporo Shale are scarce but cored samples from boreholes show that the formation consists of dark shales and mudstones, with sparse intercalations of sandstones. The shales have weathered to lateritic clay regolith that overlies fractured and fresh bedrock in Ehandiagu. The regolith and the fractured bedrock constitute the only known aquifer in the study area. The impermeable bedrock underlying the study area favors the existence of ephemeral springs and streams. This condition underscores the importance of groundwater in Ehandiagu. The geologic and groundwater situations in Ehandiagu compares positively with those of Enugu town (Onwuka et al., 2009). Enugu town is directly underlain by the Enugu Shale, a lateral equivalent of the Nkporo Shale.

3. Methods of Study

Vertical electrical sounding survey and hydrogeochemical studies were employed in this work.

3.1. Vertical Electrical Sounding (VES)

VES is a method of resistivity survey that provides information on the variation of the resistivity of subsurface materials with depth. The instrumentation of VES is simple; field logistics are easy and straightforward while the analysis of data is less tedious and economical (Zhody et al., 1974; Ekine and Osobonye, 1996; Ako and Olorunfemi, 1989). Resistivity measurements are normally made by injecting current into the ground through two current electrodes and measuring the resulting potential difference at two potential electrodes. From the current (I) and voltage (V) values, an apparent resistivity (ρa) value is calculated using the formula:

where K is the geometric factor, which depends on the arrangement of the four electrodes (Loke, 1999).

The electrode arrangement used in this study was the Schlumberger method because fieldwork is easier while master curves and software for result analysis are more

$$\rho_a = K \frac{V}{I}$$

readily available. In the Schlumberger configuration, all the four electrodes are arranged collinearly and symmetrically placed with respect to the centre (Fig. 2).

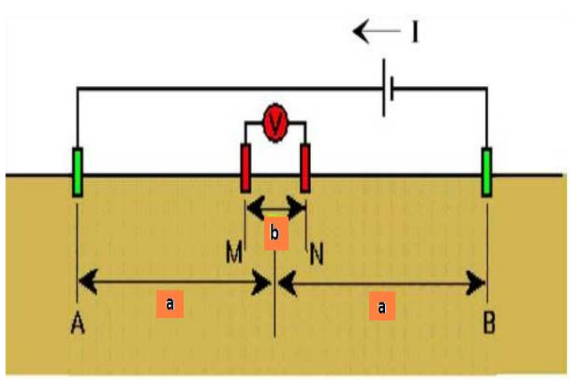

Figure 2. Sketch diagram of the Schlumberger array

In the present study, four vertical electrical sounding results were acquired. The maximum current electrode (AB) spacing ranged from 300 to 580meters. All the soundings were carried out near existing hand-dug wells for comparative purposes to explore the interrelation between lithological sequences with geo-electrical layer sequences (Fig.1). The apparent resistivity (ρa) for the Schlumberger array was calculated using the formula

$$\rho a = \pi R \left(\frac{a^2}{b} - \frac{b}{4} \right)$$ (Keller and Frischnechk, 1979)

Where R= resistance in ohms,

a= half current electrode separation

b= potential electrode spacing

The field data were used to generate sounding curves with the aid of the IPI2Win interpretation software (Fig. 3). Geoelectric sections were drawn using the information obtained from the sounding curves while aquifer thickness was estimated from the geoelectric sections. The hydraulic conductivity (K) of the aquifer was calculated from a simple hydraulic conductivity test (Auger hole test) carried out in the field. The calculated K and the aquifer thickness, derived from the interpretation of resistivity sounding data, were used to calculate aquifer transmissivity (T), using the relation:

T=Kh where h is the aquifer thickness.

3.2. Hydrogeochemical Investigation

Groundwater samples were collected from twelve (12) hand-dug wells in the dry season (February, 2009). The electrical conductivity and temperature of the samples were measured in the field. Total dissolved solids (TDS) were measured using EDTA (ethylenediaminetetraacetate titrimetric method) complexometric method. Cations (Na^+, k^+, Mg^{2+}, Ca^{2+}, Mn^{2+}, Fe^{2+}, Pb^{2+}, Cu^{2+}, Ti) were analyzed using the atomic absorption spectrophotometer (model 210 VGP). Anions (NO_3^-, SO_4^{2-}, Cl^- and HCO_3^-) were analyzed using different methods. NO_3^- and SO_4^{2-} were determined by turbidometric titration, using a spectrophotometer (model Genesys 20). HCO_3 was analyzed by titration with sulphuric acid. pH was determined using a Pye Unican 290MK pH metre. The reliability of the water quality data was determined using the ionic balance or electric neutrality formula:

$$\frac{\sum Cations + \sum Anions}{\sum cations - \sum Anions} x100 \le 5\%$$ (Hounslow, 1995)

From the computation of ionic balance, the water quality data was found to be 86% reliable.

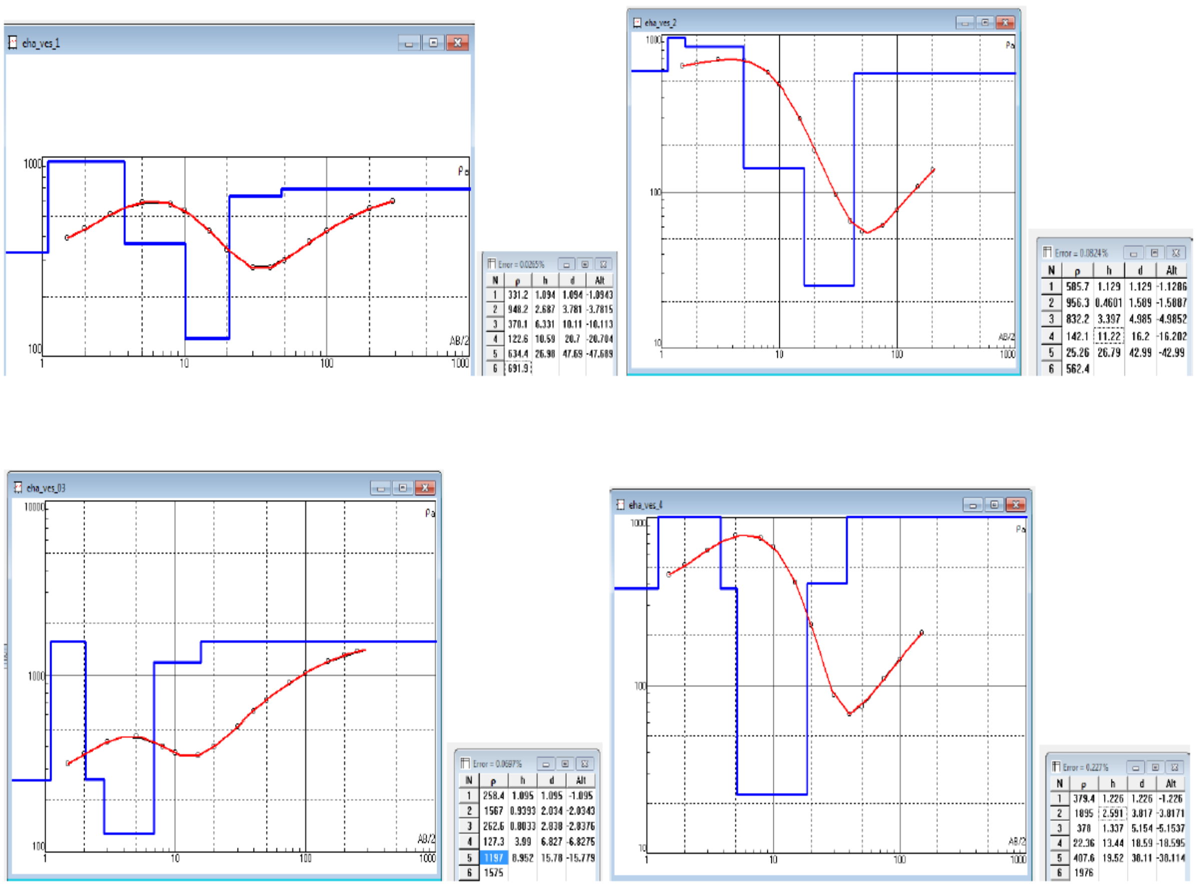

Figure 3. Sounding curves from the study area.

3.3. Auger Hole Tests

Simple auger test was carried out at two locations in the study area in order to estimate the hydraulic conductivity of soils. A known volume of water was introduced into a hole of known depth and diameter. The time taken for the water to permeate completely into the soil was noted. The hydraulic conductivity, K, was calculated by the application of Darcy's law, as given in the equation below:

$$K = \frac{Q_L x \mu_L x L x 1000}{A(P_2 - P_1)} \text{ (the Darcy equation)}$$

where

$$Q_L = \text{flow rate} = \frac{height \quad of \quad water(h)}{time \quad of \quad water \quad to \quad dry(t)} = (ms^{-1})$$

μ_L = viscosity of water (centipoise)

A = Cross-sectional area (m^2)

P_2-P_1 = P_{atm} – P_w = $\wp g\Delta h$

$\therefore$ P_w = P_{atm} - $\wp g\Delta h$

$\therefore P_2 - P_1$ = $\wp g\Delta h$ (atmosphere)

$\wp$ = Density of water

L = height of section (m)

h = height of water (m)

P_2-P_1 = ΔP = $\wp g\Delta h$

P_2 = P_{atm} (Atmospheric pressure) (known)

P_1=P_w (Water pressure) (unknown)

4. Results and Interpretation

We adopted the following procedures in interpreting the results:

- Interpretation of the vertical electrical sounding curves using the IP12WIN Software.
- Generation of geoelectric sections and the inferred lithologies as observed from the hand dug wells.
- Determination of Aquifer thickness and the depth to water from the sounding curves

The sounding curves generated are shown in Figure 3.

4.1. Generation of geoelectric sections and the inferred lithologies as observed from the hand- dug Wells.

4.1.1. VES 1 AT OKPULO EHANDIAGU

The first geoelectric layer with a resistivity of 331Ωm corresponds to the top soil. The second layer consists of lateritic soil with a resistivity value of 948Ωm. The lateritic layer is underlain by a layer of weathered bedrock, which overlies a fractured shale layer (aquiferous layer) with a resistivity of 123Ωm. The fifth geoelectric layer was interpreted as carbonaceous shale because of the recorded high resistivity and the degree of organic richness as observed from scooped samples from a hand –dug well in the area (Fig.4)

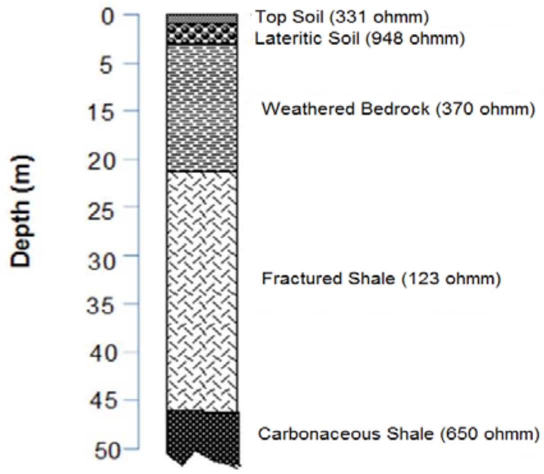

Figure 4. Geo-electric section of VES 1 showing the layer parameters.

4.1.2. VES 2 AT AMUNDIAGU EHANDIAGU

The dry reddish topsoil is underlain by a lateritic soil with resistivities ranging from 832 – 956Ωm. The third geoelectric layer consists of weathered bedrock while the aquiferous layer (fractured shale) has a resistivity of 25Ωm (Fig.5).

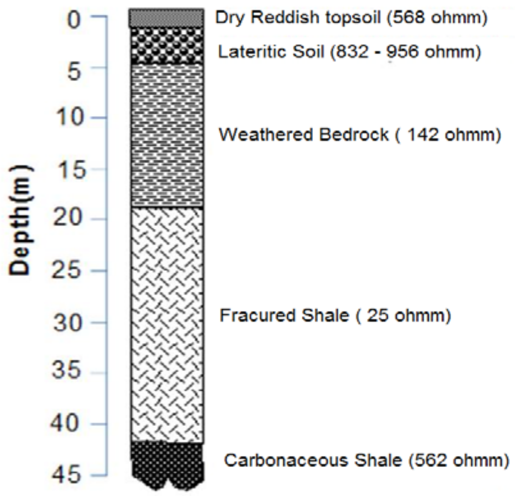

Figure 5. Geo-electric section of VES 2 showing the layer parameters.

4.1.3. VES 3 AT UMUARIMA EHANDIAGU

The first geoelectric layer with a resistivity value of 258Ωm corresponds to a reddish top soil, which is underlain by a consolidated lateritic layer with a resistivity value of 1567Ωm. The third geoelectric layer, with a resistivity value of 263 Ωm, was interpreted as the weathered bedrock, while the fourth layer, with a resistivity of 127Ωm, corresponds to the aquiferous layer. The fifth layer has a resistivity of 1575Ωm and represents carbonaceous shale (Fig. 6)

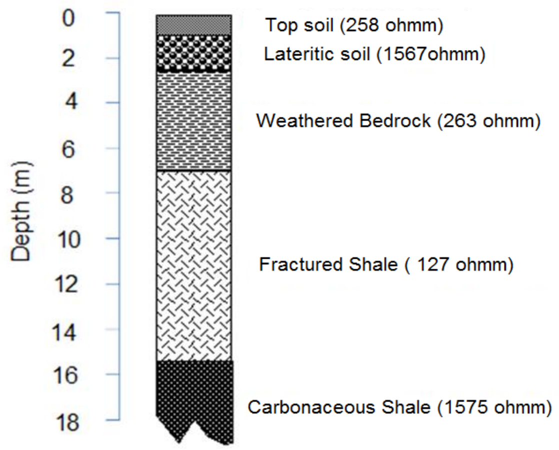

Figure 6. Geo-electric section of VES 3 showing the layer parameters.

4.1.4. VES 4 AT OBINAGU EHANDIAGU

The layered sequences consist of top soil, consolidated lateritic soil, weathered bedrock, and a fractured shaly layer, which constitutes the aquifer layer. The aquifer layer is underlain by a layer of dark carbonaceous shale with a resistivity of 1975Ωm (Fig. 7)

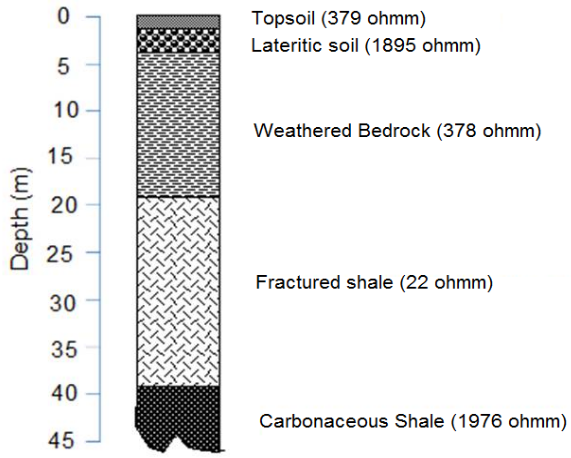

Figure 7. Geo-electric section of VES 4 showing the layer parameters

4.2. Depth to Water and Aquifer Thickness

The depths to water (Fig. 8), across the study area, were determined from the sounding results. The deduction shows that the depth to water is generally shallow in Ehandiagu. It ranges from 6.82m at Umuarima to 20.7m at Okpulo. Aquifer thicknesses range between 8.95m at Umuarima and 26.79 m at Amundiagu (Fig. 9). The above results compare very well with those obtained from hand-dug wells in the area. The depth to water as measured from wells ranges from 6.20m and 15.18m.

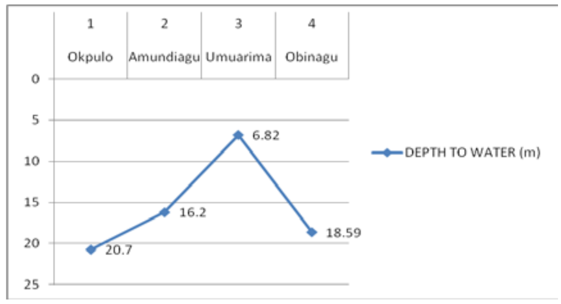

Figure 8. Cross-Section along A-B showing the depth to water

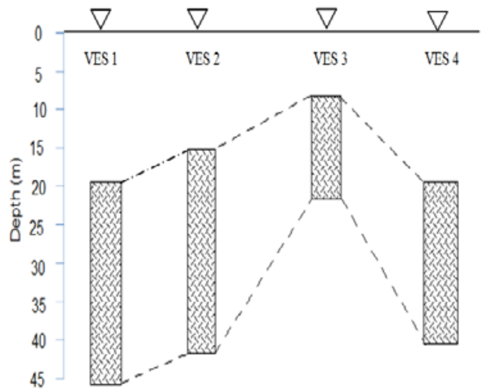

Figure 9. Cross-Section along A-B showing Aquifer thickness.

4.3. Aquifer Characteristics and Hydraulic Properties

From a simple hydraulic conductivity test carried out in the field, a calculated average hydraulic conductivity (K) value of 2.6195 x 10^{-3} was used to determine the transmissivities of all the sounding locations (Table 1). Transmissivity values range from 2.34 x 10^{-2} m^2/day to 7.02 x 10^{-2} m^2/day with an average of 4.31 x 10^{-2} m^2/day. According to Todd (1980), aquifers, with hydraulic conductivity (K) range of 0.05-10^{-3} m/day, are classified as moderately good to poor aquifers. Thus, Ehandiagu is characterized by a moderately good to poor aquifer system that is regionally discontinuous, shallow and thin.

Table 1: Calculated aquifer parameters in the study area.

VES No.	Location	Depth to water (m)	Aquifer thickness (m)	Apparent Resistivity (Ωm)	Transverse resistance (Ωm^2)	Hydraulic Conductivity (m/day)	Transmissivity T=KH (m^2/day)
1	Okpulo	20.7	10.59	122.6	1298.334	-	2.77 x 10^{-2}
2	Amundiagu	16.2	26.79	25.26	676.72	2.4133 x 10^{-3}	7.02 x 10^{-2}
3	Umuarima	6.82	8.95	127.3	1139.34	2.8056 x 10^{-3}	2.34 x 10^{-2}
4	Obinagu	18.59	19.52	22.36	436.47		5.11 x 10^{-2}
					Average	2.6195 x 10^{-3}	4.31 x 10^{-2}

Hydrogeochemical Analysis Results and Interpretation

The result of hydrogeochemical analysis is presented in Table 2.

Charts and graphs were used to present the hydrogeochemical results for easy assessment of water compositions.

Stiff diagrams

Stiff patterns can be a relatively distinctive method of showing water composition differences and similarities (Hem, 1985). The size of the pattern is approximately equal to the total ionic content (Hounslow, 1995). The sizes of the plots in Fig. 6 show that TDS (total dissolved solids) values do not differ significantly for all the samples, except for sample No. 8. The shapes of the stiff diagrams are quite similar, suggesting that the water samples are of the same source, with Na+ and HCO3- as the predominant cation and anion, respectively. A little variation in the shape the patterns can be attributed to fluctuations in the relative concentrations of Ca2+ and Mg2+ in the samples.

Piper diagram

Piper diagram can be used to determine water type, hydrochemical facies and ion exchange (Freeze and Cherry, 1979; Hounslow, 1995). The diamond part of the Piper diagram may be used to characterize waters of different types (Hounslow, 1995). Water plotted at the lower corner of the diamond is primarily composed of alkali carbonates (Na++k+ & HCO3-+ CO32-); this is typical of figure 7. Based on this, the groundwater in Ehandiagu area can be classified as Sodium-Potassium-Bicarbonate type.

Hydrochemical facies are distinct zones that have cation and anion concentrations describable within defined concentration categories (Freeze and Cherry, 1979). The designation of hydrochemical facies is based on the manner suggested by Back (1966) and Back and Hanshaw (1965), in which facies are designated according to the domain in which they occur on the segments of a piper diagram. Thus, the groundwater in Ehandiagu belongs to Sodium-Potassium facies and Bicarbonate facies.

Ehandiagu is underlain by shales, which are made up clay minerals. Clay minerals can have high cation-exchange capacities and may exert a considerable influence on the proportionate concentrations of the different cations in the water associated with them (Hem, 1985). The piper diagram clearly shows that cation exchange softening has increased the sodium (Na) concentration at the expense of calcium (Ca) and magnesium (Mg) concentrations.

Gibbs diagram

Gibbs diagram is a diagram that gives a clear indication of the mechanisms that control groundwater chemistry, considering evaporation, dilution, weathering and precipitation processes. It was developed by Gibbs (1970). In the Gibbs plot (Fig.8), the majority of the points fall within the region of weathering. This clearly shows that weathering is the dominant process that controls the groundwater chemistry. This indicates that the water has possible strong interaction with the geologic material underlying the area (Olayinka and Olayiwola, 2001; Tijani, 2003; Wang *et al*., 2004; Rao, 2006), possibly facilitated by its acidic condition. Weathering gives rise to different products, such as hydrolysates. Hydrolysates (e.g. shale) are secondary products of the chemical breakdown of aluminosilicates, such as feldspar, and they are made up of clay minerals (Hounslow, 1995). According to Todd (1980), clay minerals are one of the major natural sources of cations, such as Na, K, Mg, Ca, Fe; these cations are in significant quantities in the water chemistry data of Ehandiagu.

Table 2: Hydrogeochemical data of sampled wells in the study area.

SAMPLE ID	PH	Temperature Degree Celsius	EC (μ/cm)	Hardness (CaCO3)	CONCENTRATION (mg/l)													
					TDS	Na^+	K^+	Mg^{2+}	Mn^{2+}	Fe^{2+}	Pb^{2+}	Ca^{2+}	Cu^{2+}	Ti	NO^{2-}	$SO4^{2-}$	Cl^-	HCO_3^-
1	6.6	27.2	64	6.26	81	36.9	36.93	0.26	1.88	0.05	ND	2.08	1.9	0.07	3.25	0.7	0.06	56.42
2	4.7	27.1	99	5.6	67	17.65	96.43	0.7	0.95	4.28	0.05	1.09	0.93	0.02	1.45	1.91	0.07	98.75
3	3.4	27.5	35	56.71	13	34.98	7.42	0.31	2.02	0.16	0.02	22.2	0.06	0.04	7.2	1.4	0.06	212
4	3.6	27	26	7.16	22	46.29	22.22	0.46	0.06	0.27	ND	2.11	0.09	0.06	3.6	1.85	0.07	85.18
5	3.7	27.6	30	4.24	15	39.41	28.9	0.4	1.68	0.19	0.13	1.04	0.13	0.09	8	0.4	0.07	176
6	3.8	28	154	11.24	95	57.52	40.31	2.73	0.98	0.27	0.1	ND	0.18	0.1	5.55	0.45	0.13	143.4
7	4.3	27	113	9.1	68	17.12	32.11	1.07	1.65	0.31	0.03	1.88	0.45	0.07	6.1	2.1	0.13	152
8	3.5	27.5	55	8.94	27	8.56	19.45	0.34	1.5	0.17	ND	3.02	0.78	0.04	4.2	0.7	0.05	88.1
9	3.6	27.4	100	11.56	59	49	40	0.26	2.23	0.06	ND	4.2	0.57	0.02	4.3	1.4	0.09	112.6
10	3.4	27.4	138	9.77	88	45.21	22.87	0.76	0.08	0.23	0.11	2.66	0.08	ND	14.7	1.9	0.05	105.5
11	4.5	28.2	654	4.2	1342	21.22	19.45	1.02	0.39	0.52	0.19	ND	0.11	ND	8.4	0.65	0.07	74.79
12	4.4	27.4	60	11.25	35	15.52	19.05	0.72	1.31	0.24	0.04	3.32	0.98	0.01	6.6	0.3	0.06	142.65

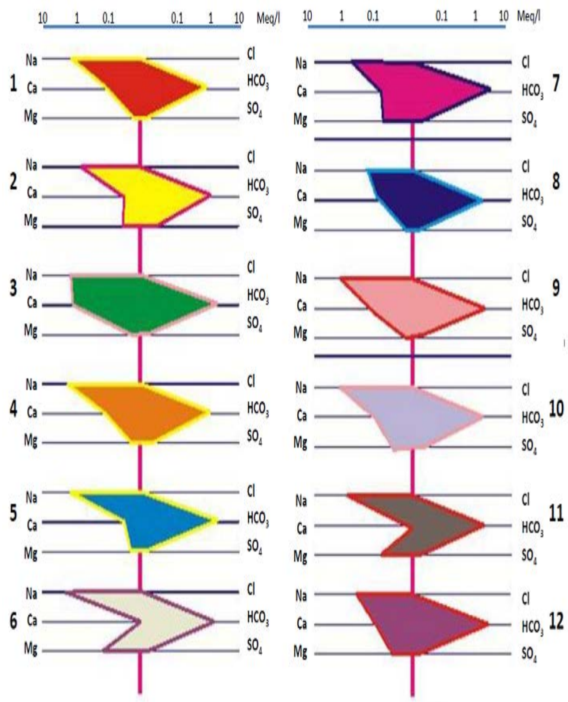

Figure 6: Stiff diagram of water samples.

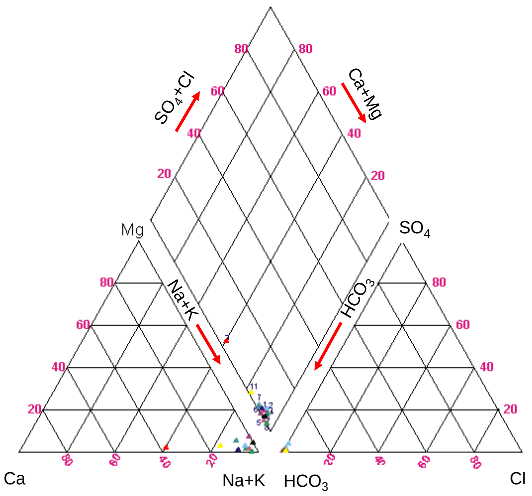

Figure 7: Piper diagram of water samples.

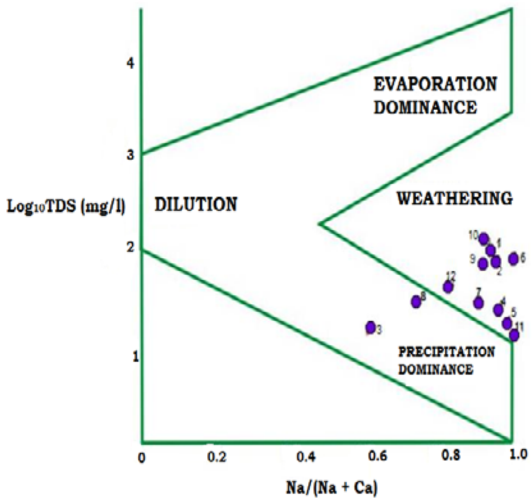

Figure 8: Gibbs diagram of water samples.

Assessment of Groundwater Quality

Hydrochemical results show that the groundwater has pH range of 4-6.5, and thus is moderately acidic. The hardness is <60mg/l, and thus is classified as soft water. Fetter (1990) classified water with TDS of < 1,000mg/l as fresh. The groundwater in Ehandiagu has a TDS range of 13-95mg/l and, thus, can be regarded as fresh water. The concentration of the ionic components was compared with the Nigerian standard for drinking water quality (NSDWQ, 2007) and WHO (2005) standards for drinking water quality. All ionic components in the water samples are within the acceptable limits, with the exception of some heavy/trace metals such as Mn2+ (1.22mg/l), Fe2+ (0.56mg/l), and Pb2+ (0.06mg/l), whose average concentrations are above the acceptable limits for potability. Although heavy metals result from human activities (industrial and agricultural) and radioactivity (Matthes and Miller, 1994), the elevated concentrations of iron, manganese and lead cannot be attributed to any of these sources because Ehandiagu is neither an industrial nor a heavy agricultural area. These metals may have originated from natural process(s). Their high concentrations may be attributed to geochemical redox processes in the area. Hounslow (1995) defined geochemical redox zones as zones, which are of great importance in determining the rate of organic biodegradation that may affect the mobility of trace metals in a predictable way. Hounslow came up with a classification for geochemical redox zones and one of the zones, designated as mildly reducing anaerobic waters, is characterized by the presence of soluble Fe2+, Mn2+, NO3- and absence of H2S. Oxygen-consuming processes such as microbial degradation of organic matter, may give rise to oxygen free reduction zones characterized by the presence of ferrous ion, manganese, ammonia, nitrite, and sulphide; by the deficiency of nitrate; and by a diminished content or absence of sulphate and sometimes chloride also. In such reduction zones, heavy metals are precipitated as sulphides when sulphide ions are present (Schwille, 1976). This explains why Mn2+, Fe2+ and Pb2+ concentrations are high, and suggests that sulphate reduction may have taken place.

Direct measurements of redox potential were not made during the study, but the relative redox status of the groundwater can be inferred from the abundance of redox sensitive solutes such as Fe and Mn. Elevated concentrations of these metals in water are commonly used as indicators of reduced conditions (Neil *et al*., 1991). Moreover, sulphate reduction caused by anaerobic bacteria may have contributed to the elevation of HCO3-, partly at the expense of SO42-, whose concentration in the groundwater is minute relative to HCO3-. This also indicates a reducing environment for the groundwater in Ehandiagu.

5. Summary and Conclusions

The result of the VES survey shows that the study area has shallow groundwater, which explains the abundance of hand-dug wells. The absence of boreholes in Ehandiagu was attributed to the low permeability of the fractured shale aquifer material. The depth to water ranges from 6.82m at Umuarima to 20.7m at Okpulo. Aquifer thicknesses range between 8.95m at Umuarima and 26.79 m at Amundiagu. The hydraulic conductivity of 2.62 x 10-3m/day and transmissivity (T) value of 4.31 x 10-2 m2/day, was used to classify the aquifer as moderately good to poor aquifer. The improved hydraulic conductivity value is closely linked to the existence of fractures, which improved the connectivity between the pores. The depth to water, measured directly from hand-dug wells, varies between 6.20m and 15.18m.

Hydrochemical analysis of water samples from hand-dug wells reveals that all ionic components are within the acceptable limits for potability, with the exception of heavy metals like Fe, Mn, and Pb. Gibbs plot shows that weathering is the major factor that controls the groundwater chemistry. The piper diagram shows that the water type is Sodium-Potassium-Bicarbonate water. The geochemical redox zone that characterize Ehandiagu area, as inferred from the high concentration of heavy metals (Fe, Mn, and Pb), implies that groundwater in the study area occurs in a reducing environment. The very low concentration of sulphate and high bicarbonate suggests that sulphate reduction may have increased bicarbonate at the expense of sulphate. This also indicates that the study area is a reducing environment.

A natural process causes the elevated concentration of Fe, Mn, and Pb. The high concentrations of heavy metals in the groundwater, in addition to the acidity, as indicated by low water pH, portend danger to human health if people continue to drink the water. It is therefore suggested that the groundwater from hand-dug wells be treated before use. Since hand-dug, wells prove to be the major source of potable water in Ehandiagu, the technology of digging and completing the wells should be improved and probably modernized.

References

[1] Ako, A.O. and Olorunfemi, M.O., 1989. Geoelectric survey for groundwater in the Newer Basalts of Vom Plateau State. Nig. Journal of Mining and Geology, vol. 25, nos.1 & 2, pp. 247-450.

[2] Back, W., 1966. Hydrochemical facies and groundwater flow patterns in northern part of Atlantic coastal plain. United States geological survey professional paper, 498-A. 42p.

[3] Back, W. and Hanshaw, B.B., 1965. Chemical geohydrology. Journal of Adv. Hydrosci., vol.1, pp.49-109.

[4] Ekine, A.S. and Osobonye, 1996. Surface Geo-electric sounding for the determination of Aquifer characteristics in parts of Bonny Local Government Area of River State. Nigeria Journal of Physics Vol. 85, pp. 93–97.

[5] Fetter, C.W., 1990. Applied hydrogeology. CBS Publishers and Distributors, New Delhi, India, 567p.

[6] Freeze, R.A. and Cherry, J.A., 1979. Groundwater. Prentice-Hall Press, Austin, Texas, 567p. Ofoma, A.E., Onwuka, O.S., and Egbu O.C., 2006. Hydrogeophysical investigation in Nsukka area, southeastern Nigeria. Journal of research in physical sciences, vol. 2, no. 1, pp. 25-34.

[7] Gibbs, R.J., 1970. Mechanisms controlling world water chemistry. Science, 170 (3962), pp.1088-1090.

[8] Hem, J.D. 1985. Study and interpretation of the chemical characteristics of natural water. United states Geological survey water supply paper 2254, 244p.

[9] Hounslow, A.W., 1995. Water quality data: Analysis and Interpretation. CRS Press, Inc. Lewis Publishers, 397p.Igboekwe, M.U., Okwueze, E.E. and Okereke C.S., 2006. Delineation of potential aquifer zones from geoelectric soundings in Kwaibo river watershed, southeastern Nigeria. Journal of engineering and applied sciences, vol.4, pp.410-421.

[10] Igboekwe, M.U., Okwueze, E.E. and Okereke C.S., 2006. Delineation of potential aquifer zones from geoelectric soundings in Kwaibo river watershed, southeastern Nigeria. Journal of engineering and applied sciences, vol.4, pp.410-421.

[11] Ioannis, F.L., Kerantonis G.A., Nikolaos S.V. and Filippos I.L., 2009. The contribution of geophysical methods in the determination of aquifer parameters: the case of Mornos river delta, Greece. Submitted for publication in the international journal of elelctrical and electronics engineering.

[12] Keller, G. V., and Frischnechk, F.C., 1979. Electrical methods in geophysical prospecting. Pergamon Press, New York, pp 91 - 135.

[13] Loke, M. H., 1999. Electrical imaging surveys for environmental and engineering studies (A practical guide to 2-D and 3-D surveys). Minden Heights, Penang- Malaysia, 57p.

[14] Matthes, G., and Miller, J.C., 1994. Chemical and biological contaminants and their surface behaviour. In Jerosla, V. and Alexander, Z. (eds.), Guidebook on mapping groundwater vulnerability, vol. 16, pp. 11-17.

[15] Murat, R.C., 1972. Stratigraphy and paleogeography of the Cretaceous and Lower Tertiary in southern Nigeria. In Dessauvagie, T.F.T. and Whiteman, A.J. (eds.) African geol. Univ. of Ibadan, pp.251-266.

[16] Neil, M.D., Niel, J.M., Welker, M.C., and Evenson, K.D., 1991. Geochemical relations and distribution of selected trace elements in groundwater of the northern part of the western San Joaquin valley, California. United States water supply paper, 2380.

[17] Nigerian Standard for Drinking Water Quality, 2007. Nigerian industrial standard NIS: 554. 30p.

[18] Niwas, S., and Singhal, D.C., 1981. Estimation of aquifer transmissivity from Da–Zarrouk parameters in porous media. Journal of Hydrology, vol. 50, pp. 393-399.

[19] Obikezie, S.O., 1993. Geochemical investigation of spring waters in parts of Anambra state, Nigeria. Water resources journal, vol. 3, nos.1&2. 2, pp.49.

[20] Offodile, E.M., 2002. Groundwater study and development in Nigeria. Mecon Geology and Engineering Services ltd, 453p.

[21] Ofoma, A.E., Onwuka, O.S., and Egbu O.C., 2006. Hydrogeophysical investigation in Nsukka area, southeastern Nigeria. Journal of research in physical sciences, vol. 2, no. 1, pp. 25-34.

[22] Olayinka, A.I. and Olayiwola, M.A., 2001. Integrated use of geolelectrical imaging and hydrochemical methods in delineating limits of polluted surface and groundwater in a landfill site in Ibadan area, southwestern Nigeria. Journal of Mining and Geology, vol. 37,no. 1, pp.53-68.

[23] Onwuemesi, A.G., and Olaniyan, I.O., 1996. Hydrogeophysical investigation of parts of Anambra State, Nigeria. Water resources journal, vol. 7, nos.1& 2, pp.42-48.

[24] Onwuka, O.S., Uma, O.K., and Ezeigbo, H.I., 2004. Potability of shallow groundwater in Enugu town, southeastern Nigeria. Global Journal of Environmental Sciences, vol.3, nos. 1&2, pp.33-39.

[25] Rao, S.N., 2006. Seasonal variation of groundwater quality in a part of Gunter District, Andhra Pradesh, India. Journal of Environmental Geology, 49, pp.413-429.

[26] Schwiller, F., 1976. Anthropogenically reduced groundwaters. Hydrol. Sci. bull. 21/4, pp. 629-645.

[27] Tijani, M.N., 2003. Bacteriological, chemical and lithologic controls on the water quality in Shagamu area, southwestern Nigeria. Journal of Nigerian Association of Hydrogeologists, 14, pp.93-100.

[28] Todd, D.K., 1980. Groundwater hydrology. John Wiley and sons, United States, 533p.

[29] Wang, B., Wanty, R.B., and Vohden, J., 2004. Geochemical process and geologic framework influencing surfacewater and sediment chemistry in the Fortymile River watershed, eastcentral Alaska. U.S. Geological Survey Professional Paper 1695, pp.3-19.

[30] W.H.O. 1982. Guidelines for Drinking Water Quality W.H.O. Geneva.

[31] Zodhy, A.A.R., Eaton, G.P. and Mabey, D.R., 1974. Application of surface geophysics to groundwater investigations. United States geological survey papers, 123p.

JJEES

Volume 5, Number 2, December. 2013
ISSN 1995-6681
Pages 73- 78

Jordan Journal of Earth and Environmental Sciences

Fracture systems and dissolution cavities in Wadi As Sir Formation, Thughrat Asfour area, Jordan

Abdullah Ali Diabat

Institute of Earth and Environmental SciencesAl al-Bayt UniversityMafraq – Jordan

Received 10 Dec., 2012; accepted 10 Dec., 2013

Abstract

The fracture systems and their relationship with dissolution cavities and/ or karst development in the Turonian Limestone of Wadi As-Sir Formation were studied along abandoned quarries and road cuts in a folded area on the Irbid- Jerash Highway. A total of 740 fracture planes were measured in the field. Among them, sixty striated planes were analyzed for fault-strain by means of the TENSOR structural software. The other fracture data are represented as a rose diagram showing the orientation of the fractures. Four sets of fractures are distinguished in the study area these are: a) Extension fractures (having orientation NNW-SSE (N20°W to N40°W)); b) Release fractures (having orientation ENE- WSW and WNW-ESE (N70°E to S80°E)); c) Shear fractures set-1 (having orientation N- S (N10°W to N10°E)); and d) Shear fractures set-2 (having orientation ESE-WNW (S45°E to S75°E)). Results show that the dextral shear along the ENE-WSW to E-W trend reflects the majority of the analyzed fault-slip data. Plane surfaces of these dextral strike-slip faults are coated with calcite steps and/ or soil staining, suggesting water infiltration and potential dissolution processes. Thus, it can be said that fractures represented by the neoformed dextral strike-slip faults and release joints have been reactivated later and the structural control of the karst development along these structural elements is present in the hard carbonates of the study area.

Keywords: karsts/ dissolution cavities, fractures, paleostresses analysis.

1. Introduction

The growth of some caves is influenced by joints and bedding planes in carbonate rocks, but other cave systems are less obviously joint-controlled in that they exhibit a branching or linear pattern (Zumburge and Nelson, 1976).

The Wadi As-Sir Formation (Turonian limestone) is the main formation cropping out in the study area along Irbid-Jerash Highway (Fig. 1). Dissolution cavities or karst phenomena occur mainly along open fractures. The fractures and associated karstic phenomena in hard limestone and dolomites are generally not obvious on surface outcrops. Their surface expression may be inferred from the negative features in the topography (Arkin, 1980). Fractures, in this study, mean any discontinuity of a rock mass, e.g. faults, joints, cracks and veins. Since these features may be complicated by successive tectonic events and overprinting (Hancock, 1994), it is necessary to examine these weakness surfaces in relation to movement and orientation. The aim of this study is to examine the control of existing fractures along Irbid-Jerash Highway on the development of karstic dissolution cavities. Accordingly, it encompasses the following goals: 1) Measuring and classifying the fractures based on their orientation, 2) Estimating the paleostress orientations that formed these fractures.

2. Geological setting

The Dead Sea Transform (DST) extends from the Gulf of Aqaba in the south to the Taurus Mountain in Turkey in the north. It separates the Arabian plate from Palestine-Sinai Subplate (part of African plate). The DST was formed because of the northward sinistral movement of the Arabian plate associated with the opening of the Red Sea (Garfunkel *et al.*, 1981). The movement started in the Miocene and still active (Quennell, 1959; Eyal, 1996). This fault system is responsible for the formation of different structures in Jordan and in the study area (Fig. 2).

The outcropping rocks in the study area and its adjacent areas are of the Upper- Cretaceous (Cenomanian to Campanian) and belong to two groups; the oldest is the Ajlun Group and the youngest is the Balqa Group.

The age of Ajlun Group ranges from Cenomanian to Turonian. In the study area, the Ajlun Group includes Fuhais, Hummar, Shueib and Wadi As-Sir Formations, while the Balqa Group includes Wadi Umm Ghudran, and Amman Formations (Fig. 1). The Wadi As-Sir Formation covers most of the study area (Fig. 1); it is considered an index horizon in the study area and all over Jordan.

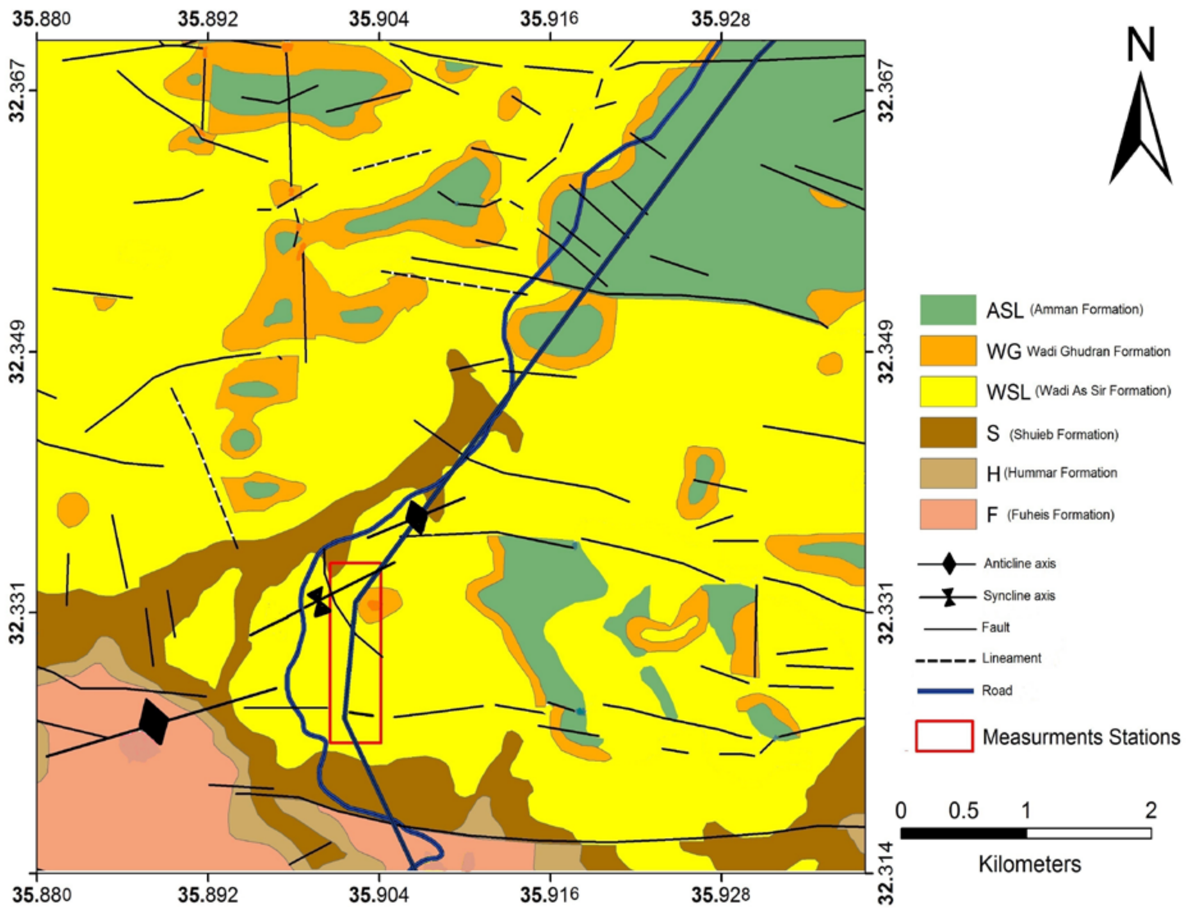

Figure 1: Location and geological map of the study area.

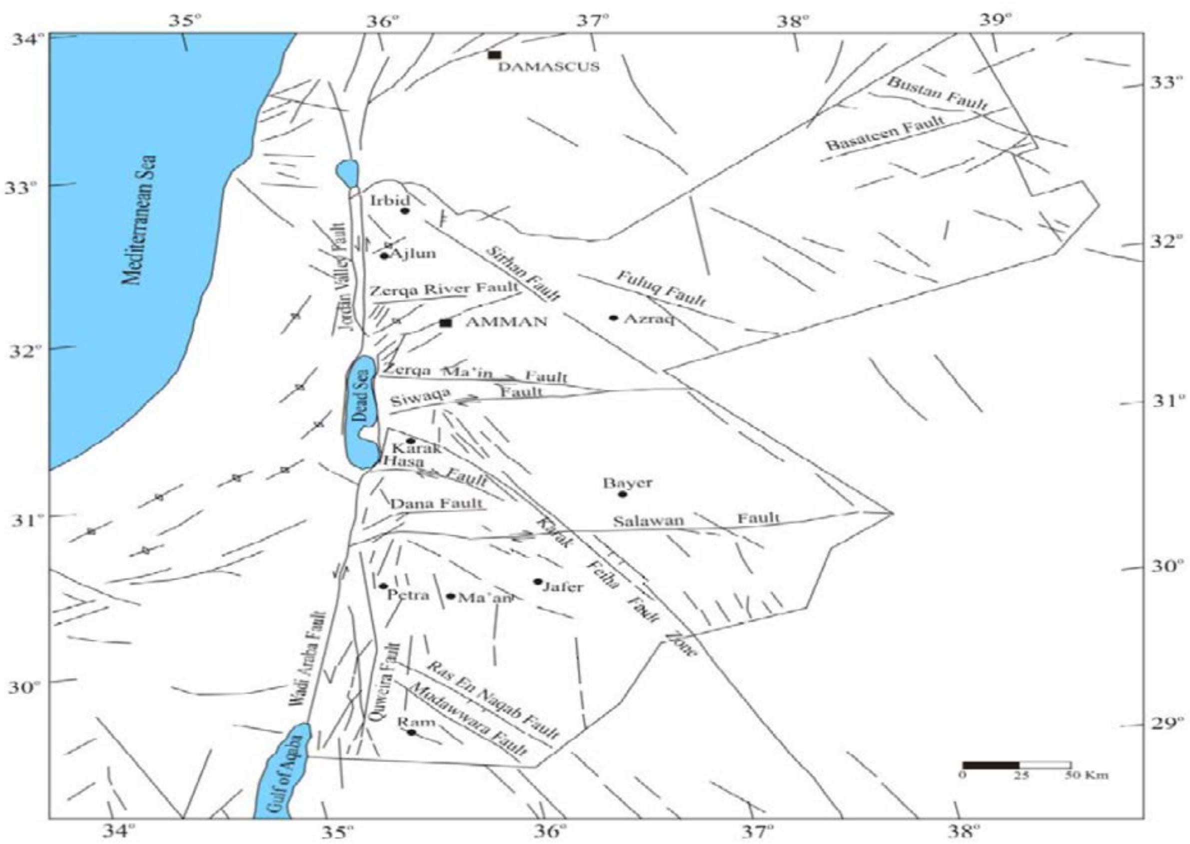

Figure 2: Structural pattern of Jordan (Diabat and Masri, 2005).

The Wadi As-Sir formation is composed mainly of limestone, marly limestone and dolomitic limestone. The upper part consists of thick-bedded crystalline fossiliferous limestone forming a prominent scarp across the study area. The prominent scarp feature of the Wadi As-Sir Formation is overlain by the pelagic deposits of the Wadi Umm Ghudran Formation, which consists of massive chalk beds (in the lower parts) and limestone, chalk and chert (in the upper parts). The youngest rock of the study area belongs to the Amman Formation. It consists of alternations of limestone, marl and chert (Abdelhameed, 1995; Powell, 1989).

3. Methodology

A total of 740 fracture planes were measured in the field using CLAR compass (Fig. 3). The data were collected from abandoned quarries and road cuts along Irbid-Jerash Highway. In particular, the readings encompassing the fractures dominating the hard carbonate rocks (Wadi As-Sir Formation) of the Thughrat Asfor region. The majority of fractures lack any surface striations, thus they were considered as joints. The measurements take into account the strike of their planes. On the other hand, sixty of these fractures showed pronounced striations (i.e. Slickenlines) across their surfaces, thus they were treated as fault-slip data. The plunge, plunge direction and the sense of movement of these fractures have been determined for each fault plane reading (Fig. 3).

Figure 3: Slickenlines show a normal- dextral movement of a fault plane.

4. Fractures

A fracture is a general term for a surface in a material across which there is loss of continuity and, therefore strength (Van der Pluijm and Marshak, 2004). Fractures range in size from grain-scale to continent-scale (Van der Pluijm and Marshak, 2004). The fractures generally are accompanied by various features, which characterize the surfaces of the break and the space between them. These include the degree of curvature, opening, continuity, roughness, surface markings and the type of infillings. These are the most important characteristics that affect the passage or percolation of waters both of meteoric and flowing along the break and the degree of aggressiveness of the water and the potential for solution to occur (Arkin, 1980; 1989).

Open and closed fractures are both observed in the study area (Figs. 4 - 8). Conjugate sets of fractures were also observed. Some fracture planes are stained by soil infillings, vertical solution rills and calcite deposits in the form of stalactites and stalagmites in some (Fig. 4).

Some fractures have preserved slickenlines whereas some fractures have preserved plumose features and tension gashes, which can be classified as shear fractures or extensional fractures, respectively.

These fractures can be divided as follows:

4.1. Release Fractures

When the stress acting on a region of crust is released, the crust elastically relaxes to attain a different shape. This change in shape may create tensile stresses within the region that are sufficient to create release joints or fractures, similar to what occurs in relation to folding; they are also called outer- arc extension joints (Van der Pluijm and Marshak, 2004). Release fracture may also form when overburden load is removed or released (Billings, 1972; Van der Pluijm and Marshak, 2004). In the study area, these fractures are oriented at ENE- WSW and WNW-ESE or have varying strikes from N70°E to S80°E (Fig. 9).

4.2. Extension fractures

This fracture set is oriented normal to the fold axes and is geometrically described as cross fracture (Billings, 1972). These fractures are mainly present at the crestal parts of the folds. Their orientations in the investigated area are NNW-SSE or varied in strikes from N20°W to N40°W (Fig. 9).

4.3. Conjugate shear fractures

A shear fracture is a surface across which a rock loses continuity when the shear stress parallel to the surface is sufficiently large (Van der Pluijm and Marshak, 2004).

Two sets of shear fractures where observed in the study area; set-1 and set-2, conjugate sets (Fig. 9)). Set-1 has orientation mainly N- S, with a range of N10°W-N10°E (Fig. 9). Set-2 has orientation mainly ESE- WNW, with a range of S45°E to S75°E (Fig. 9).

Their intersection planes are parallel to the intermediate stress direction (σ_2), whereas the acute bisector is parallel to maximum stress direction (σ_1).

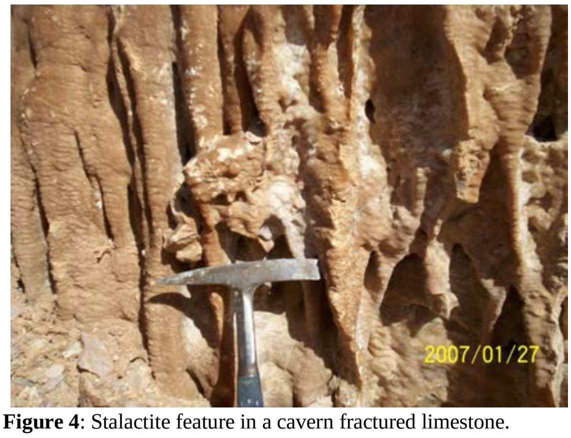

Figure 4: Stalactite feature in a cavern fractured limestone.

  - Volume 5, Number 2 (ISSN 1995-6681)

Figure 5: Open fractures (blue) with dissolution cavities and thin roof at the upper left.

Figure 6: Open fracture (blue) with dissolution cavities and soil staining.

Figure 7: Development of a longitudinal cave on a reactivated dextral strike- slip fault.

Figure 8: Development of a cave as a reactivation of dextral strike-slip fault at later stage as normal fault.

5. Stress Analysis

For stress analysis, the fracture orientation data are plotted on a rose diagram (Fig. 9), whereas the striated fractures were presented as fault-slip data (Fig. 11), using the TENSOR program of Delvaux (1993), and the right Dihedral method of Angelier and Mechler (1977), as well as Angelier (1979).

Rose diagram provides immediate visual estimation of stress orientation regarding any data. The principal stress direction (**σ_1**) is always parallel to extensional fracture sets and normal to release fractures (Billings, 1972; Davis, 1984). Shear fractures are always oblique to the principal stress direction (**σ_1**) (Billings, 1972).

Results show that the predominant trend of the fractures in the rose diagram is NNW-SSE, while the minor trends are E-W and ENE-WSW (Fig. 9).

Analysis of the fault-slip data shows a dominance of a strike-slip tensor which is characterized by the following paleostress orientations: σ_1 = 155/ 08; σ_2 = vertical, σ_3 = 245/17, thus suggesting a NNW-SSE compression (**σ_1**) and ENE- WSW tension (**σ_3**) paleostress state (Fig.10).

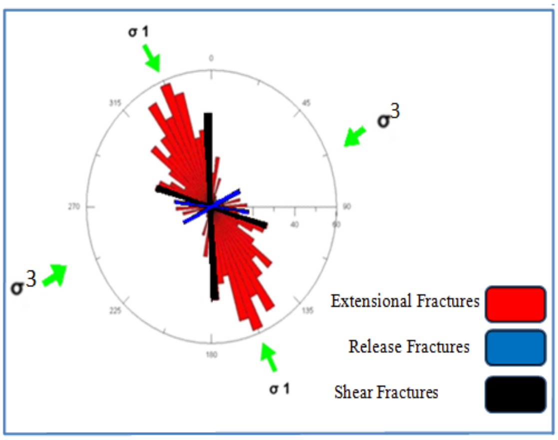

Figure 9: Strike orientation of 740 fracture planes and the generalized direction of maximum principal stress axis (**σ_1**) parallel to extensional fractures and minimum principal stress axis (**σ_3**) parallel to release fractures.

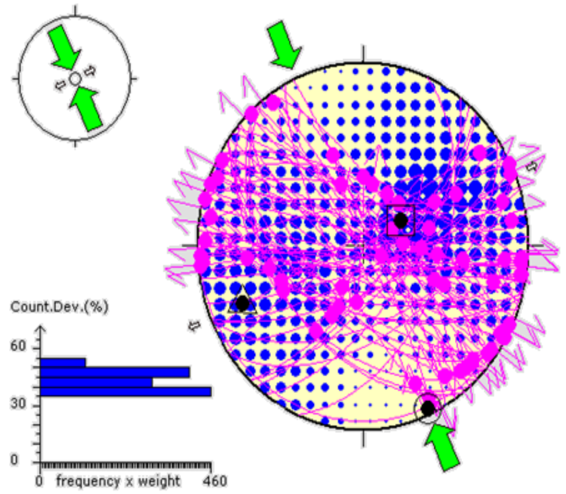

Figure 10: Principal stress axes determination by using the TENSOR program; outward ENE arrows indicate tension (**σ_3**) and inward NNW arrows indicate compression **(σ_1)**, while **σ_2** is vertical.

6. Discussion

In light of their dominant parallel alignment of the investigated fractures with the maximum horizontal compressive stress axis **σ_1** (SH max) of the established regional stress fields (Eyal and Reches, 1983; Eyal, 1996; Diabat, 1999; Diabat *et al*., 2004; Eyal *et al*., 2001; Diabat 2005, 2009, 2013), the NNW-SSE fractures propagated under conditions associated with the Dead Sea stress,which is characterized by NNW- SSE maximum compression **(σ_1)**. The small faults at the study area have estimated paleostress orientations: σ_1 = 155/ 08; σ_2 = vertical, σ_3 = 245/17. They have a similar orientation (but often with slightly steeper dips) to the small faults. Therefore, they are interpreted as extensional or shear fractures with the same paleostress orientations as the small faults and the associated local fold stresses. The coincidence of the NNW-SSE fractures with the maximum horizontal compression (SH max) implies the extensional nature of them. This might be triggering and it might help the karst development mainly along the open fractures of the irregular or undulating surface planes of this trend in the study area.

The ENE-WSW to E-W trend, shown in Figure (9), reflects the majority of fault-slip data that may mainly represent the neoformed dextral strike-slip faults and the release joints. Plane surfaces of the dextral strike-slip faults are coated with calcite steps or slickolites which are of importance as a sense movement indicator. Therefore, the plunge and azimuth of these structural markings were measured and analyzed. Results show that the dextral shear along these fractures (neoformed dextral strike- slip faults and the release joints) has occurred at a later stage/s as a reactivation process. These fault planes are open and calcite curtains or soil staining are observed on their surfaces, suggesting water infiltration and mobility with the subsurface (Figs. 7 and 8). Therefore, the growth of some caves and the development of karstified blocks is controlled by faults reactivated joint structures.

7. Conclusion

Based on the above facts and the relationship of fractures to the fold axes, the general behavior of fractures in the study area is as follows:

1. extension (cross) fractures have orientation NNW-SSE (N20°W to N40°W);
2. release fractures have orientation ENE- WSW and WNW-ESE (N70°E to S80°E);
3. shear fractures set-1 have orientation N- S (N10°W to N10°E); and
4. shear fractures set-2 have orientation ESE- WNW (S45°E to S75°E).

On the basis of both the orientation of release and extension fractures and the fault-slip data, the principal stress direction is swinging around NNW-SSE.

In conclusion, the minor trend (E-W to ENE-WSW) indicates that the reactivated fractures are dextral strike-slip faults, which are the dominant fracture type being affected by the karstification in the study area.

References

[1] Abdelhamid, Gh. 1995. The geology of Jarash Area. Map Sheet (3154-I), Report of Natural Resources Authority.

[2] Angelier, J., 1979. Determination of the mean principal direction of stresses fog a given fault population. Tectonophysics, 56: T17-T26.

[3] Angelier, J., 1994. Fault- slip analysis and paleostress reconstuction. In: Continental Deformation (ed. Hancock, P.L.), 1 edn., pp. 53- 100. Pergamon Press, U.K., Bristol.

[4] Angelier, J., and Mechler, P., 1977. Surune method graphique de recherché des contraintes principales egalemant utilizable en tectonique et en seismology: la methode de diederes droits. Bull. Soc. Geol. Fr. 7:1309-1318.

[5] Arkin, Y., 1980. A survey of karst phenomena, western Judean Mountains. Isr. Geol. Surv. Rep. MM/5/80, 30P.

[6] Arkin, Y., 1989. Large scale tensional features along the Dead Sea-Jordan rift valley. Tectonophysics, 165:143-154.

[7] Billings, M.P., 1972. Structural geology: 3rd ed., Prentice-Hall, Englewood Cliffs, N. J., 606 P.

[8] Davis, G. H., 1984. Structural geology of rocks and regions: 1st ed., John Wiley and Sons, Inc.

[9] Delvaux, D., 1993. The TENSOR program for paleostress reconstruction: examples from the east Africa and the Baikal Rift systems. Terra Abst., Suppl.Terra Nova, 5: 216.

[10] Diabat, A., 1999. Paleostress and strain analysis of the Cretaceous rocks in the eastern margin of the Dead-Sea Transform, Jordan. Ph.D. Thesis, Baghdad University, Iraq.

[11] Diabat, A., 2009. Structural and stress analysis based on fault-slip data in the Amman area, Jordan. Journal of African Earth Sciences 54: 155-162.

[12] Diabat, A., 2013. Fracture systems of granites and Quaternary deposits of the area east of Aqaba: indicators of reactivation and neotectonic activity. Arabian Journal of Geosciences, vol. 6, No. 3: 679- 695.

[13] Diabat, A., and Masri, A., 2005. Orientation of the principal stresses along Zerqa- Ma,in Fault. Mu,ta Lil-Buhuth wad-Dirasat. 20: 57- 71.

[14] Diabat, A., Atallah, M., and Salih, M., 2004. Paleostress analysis of the Cretaceous rocks in the eastern margin of the

Dead Sea transform, Jordan. Journal of African Earth Sciences. 38: 449- 460.

[15] Eyal, Y., 1996. Stress field fluctuations along the Dead-Sea Rift since the middle Miocene. Tectonics, 15: 157-170.

[16] Eyal, y., and Reches, Z., 1983. Tectonic analysis of the Dead Sea Rift region since the late Cretaceous based on mesostructures. Tectonics, 2: 167-185.

[17] Eyal, Y., Gross, M.R., Engelder, T., Becker, A., 2001. Joint development during fluctuation of the regional stress field in southern Israel. Journal of Structural Geology, 23: 279-296.

[18] Garfunkel, Z., Zak, I., Fruend, R., 1981. Active faulting in the Dead Sea rift. Tectonophysics, 80: 1- 26.

[19] Hancock, P.L. (ed.) 1994. Continental Deformation. Pergamon Press, U.K., Bristol. 491p.

[20] Powell, J. H., 1989. Stratigraphy and sedimentation of the phanerozoic rocks in central and south Jordan. Geological mapping division, natural resources authority, Jordan.Bulletin 11, 130p.

[21] Quennell, A., 1958. The structure and evolution of the Dead Sea rift. Quaternary Journal of the Geological Society, 64: 1- 24.

[22] Ramsay, J. G., and Huber, M. I., 1987. The techniques of modern structural geology, volume 2: Folds and Faults. Academic Press, New York, 462 p.

[23] Van der Pluijm, Ben A. and Marshak, S., 2004. Earth structure, an introduction to structural geology and tectonics. 2nd ed., W.W. Norton and Company, Inc. 656 p.

[24] Zumberge, J.H., and Nelson, C.A., 1976. Elements of physical geology. John wiley & Sons, Inc. 395 p.

JJEES

Volume 5, Number 2, December. 2013
ISSN 1995-6681
Pages 79- 86

Jordan Journal of Earth and Environmental Sciences

Tectonic Geomorphology of Alluvial Fans east of the Wadi Araba Fault (Dead Sea Transform), Jordan

Walid A. Saqqa[1], Mohammed Y. Atallah[2,*]

[1]*Department of Earth & Environmental Sciences ,Faculty of Science, Yarmouk University،Irbid-Jordan*

2Department of Earth Sciences, Sultan Qaboos University Al-Khud - Oman

Received 6 April, 2012; accepted 5 October, 2013

Abstract

This study deals with the development of alluvial fans at the foot of the fault-controlled eastern mountainous chain in Wadi Araba Desert (WAD). The alluvial fans are fed mainly by debris flows of ephemeral streams flowing westward across the eastern highlands to the desert plain and/or inland sabkhas. Morphometric analyses showed that fan surface area (FSA) is directly proportional to drainage basin area (DBA), whereas the fan slope (FS) is inversely proportional to 'FSA' or decreases proportionally as the talus cones evolve into fans. The architecture and evolution of the fan/drainage network are controlled by vigorous tectonic forces that began in the Early Miocene. Bedrock geology, history and rates of sediment supply, and the intensity and duration of surface flow more likely contributed to the progressive changes of fans/drainage basin system. The increment of 'FS' towards fan head pertinent to sediment buildup and the occurrence of steep normal fault scarps at mountain edges may reflect recent uplift in the catchment area. The alluvial fans were dislocated apart from drainage basins as a result of strike-slip movement along the Dead Sea transform (DST) and its subsidiary faults. Fanglomerates are compositionally immature and matrix-supported. The angular-subangular shape of clasts indicates a minimum or non-intensive abrasion has been occurred before sedimentation.

Keywords: Wadi Araba , Jordan, Alluvial Fans, Dead Sea.

1. Introduction

1.1. Previous works

Alluvial fans are among the fascinating geological features, like sand dunes, mud pans and saline inland sabkhas that characterize Wadi Araba desert (WAD). The most recent work describing the sedimentology and morphology of alluvial fans in Wadi Araba is the study of Makhlouf *et al.* (2010). Features, other than alluvial fans, have received considerable attention from researchers in modern decades. For instance, the inland sabkhas and sand dunes in 'WAD' are carefully studied by Abed & Al-Hawari (1991) and Saqqa & Atallah (2004), respectively. Until now, little attention has been paid to studying the development of alluvial fans in 'WAD'. The alluvial fans were occasionally reported as part of geology studies in the area (Bender, 1974; Saqqa, 1998). Klinger *et al.* (2000) and Niemi *et al.* (2001) pointed to fan/drainage basin offsets In the northern part of 'WAD' resulted by 4-5 mm/yr slippages of sinistral movement along the Wadi Araba fault. Klinger *et al.* (2003) attributed the development of alluvial deposits and river entrenchment in the Dead Sea area to lake-level fluctuations, which in turn was as a function of late Quaternary climate changes.

McLaren *et al.* (2004) explained modes of sedimentation and landscape evolution of the Quaternary deposits in Wadi Faynan, to the south of the Dead Sea, in view of tectonic setting and paleoclimate. On the western part of 'WAD', Ginat *et al.* (1998) demonstrated incidence of a 15km left-lateral strike-slip displacement along the Dead Sea Transform (DST) in the Late Pliocene to Early Pleistocene. So, dislocation is very likely of the western highlands alluvial fans system away from its original position. Ben-David *et al.* (2002) described Late Miocene fluvial landscapes evolution in view of the tectonic settings in the Central Naqab Desert (west of study area).

Other studies dealing with alluvial fan evolution were done by several authors in neighboring countries. For instance, the study of Ochugi & Ochugi (2004) dealt with the development of Late Quaternary alluvial fan/drainage basin system in Afrin region inSyria and its relation to Late Quaternary climatic change. The study of Beaumont (1972) evaluated the evolution and hydrological conditions of 26 alluvial fans and their drainage

* Corresponding author. e-mail: myatallah@yahoo.com.

basins in the southern margin of Elburz Mountains, SE Tahran. The study of Alçiçek *et al.* (2005) explained the tectonic evolution of the Çameli Basin in SW Anatolia. This basin, which hosts a group of alluvial fans and other fluvial/lacustrine sediments, evolved during three distinct stages of tectonic extensions and resulted in a prominent change in the sedimentation pattern. A recent study on the Quaternary morphotectonics of Wadi Araba by Le Beon *et al*. (2012) identified seven successive morphostratigraphic levels in Wadi Araba. They observed three main phases of alluviation at 102, 163 and 324 ky. Their study estimated the fault slip rate along the Wadi Araba fault to be 5-7 mm/yr.

1.2. Aim of Study

The present work seeks to understand the morphogenesis and tectonic evolution of the alluvial fans system on the eastern rim of Wadi Araba Desert 'WAD', south of the Dead Sea.

1.3. Methods of Study

Aerial photographs (1:10000) and topographic sheets (1:50000) were used to find out the relationship between fan surface area (FSA), drainage basin area (DBA), and fan slope (FS). Areas were measured by dividing the fan surface and basins into polygons. Fan slopes were measured from the contour lines of the 1:50 000 topographic sheets Computations of 'FSA', 'DBA', and 'FS' are essential means for describing morphotectonic evolution of alluvial fans. L ithotype of fanglomerates were described and gravel shapes were analyzed (Zingg method, 1935). G rain size analysis, particularly of the distal part of Wadi Rahma alluvial fan sediments, was carried out using Retsch-type sieve automated shaker.

2. Location and Geological Setting

The investigated alluvial fans rest upon the foot of the e astern m ountainous chain in 'WAD'. The fans emerge at about 10 km away from the northern shorelines of the Gulf of Aqaba and stretch out north along the Dead Sea Rift to the district of Rahma (Fig.1). The bedrock of alluvial fans system and its catchment is the granitic rocks of the Precambrian Aqaba complex and the acidic & mafic dikes and metasediment associations. Thick sequences of Paleozoic–Mesozoic sediments rest non-conformably upon the Precambrian igneous rocks (Jarrar, 1984; Rashdan, 1988; Ibrahim, 1991). Late Quaternary sand dunes, inland sabkhas and mud flats cover extensive areas of 'WAD'.

Wadi Araba-Dead Sea-Jordan Rift Valley province is a narrow depression between Gulf of Aqaba in the south to Lake Tiberias "The Sea of Galilee" in the north. It is about 375 km long and 9-25km width. The Rift is a part of a large-scale fracture zone extending between the East African Rift and southeast Turkey. T he Jordanian Rift aligns the Dead Sea Transform (DST), which is a major left lateral strike slip fault, which runs parallel to the eastern escarpment (Fig.1). The fault has been active since the Miocene and has caused cumulative displacements of about 107km.

The Jordanian Rift is tectonically and seismological active dry region that witnessed several past earthquakes (Garfunkel *et al*., 1981) and is still active.

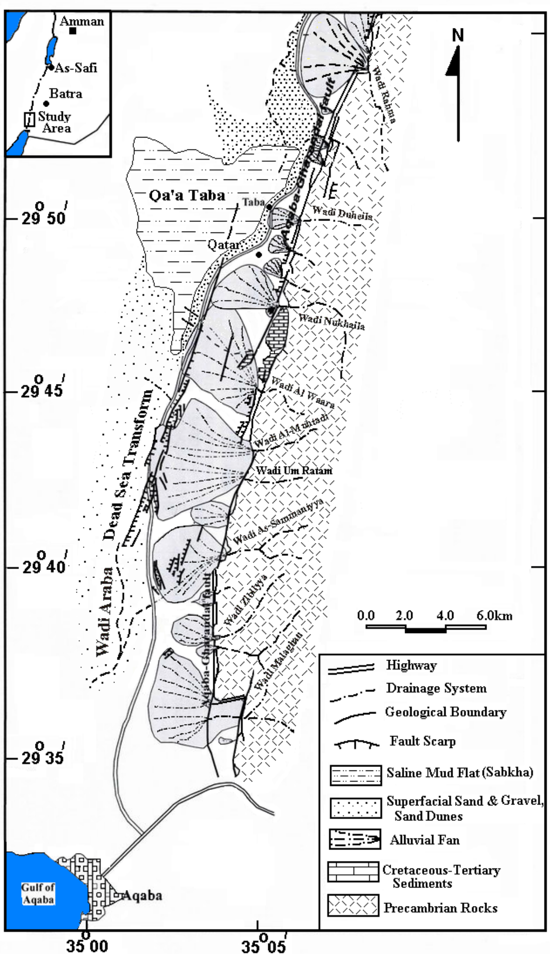

Figure 1. Geologic map of alluvial fans, south of Wadi Araba. Dead Sea Transform (DST) cuts the western parts of some fans forming pull apart basins. Secondary faults of DST cut also fan surfaces.

3. Climate and Geomorphology

Wadi Araba desert 'WAD' and the adjacent Naqab Desert to the west form rain shadow zone between the eastern and western topographic highs. P resent-day climate represents seasons of short dry-cold winter and lengthy dry-hot summer. The maximum temperature may rise up to 50°C in summer and drops to 0.0°C in winter. The diurnal temperature variations are large enough (>30°C) to restrict plant growth. Annual rainfall is normally less than 100mm. Eastern highlands may receive over 200 mm/a. The mean potential evapotranspiration is very high (ca. 2200-2500mm/a) resulted in a rapid loss of soil moisture. Relative humidity fluctuates between 53%-62% in winter and 30%-40% in summer. Localized storms occur mainly in conjunction with active Red Sea troughs or low-pressures centered over the southern parts of Jordan and adjacent regions. Dust storms are principally developed in spring-early summer times (Saqqa and Atallah, 2004).

Several authors stated that universal high rainfalls and fluvial erosions were much more effective during the warm interglacial periods in Late Pleistocene-Early Holocene (Gasse *et al.*, 1987; Glennie, 1987; Petit-Maire and Guo, 1997; El-Baz, 1998; Zhuo *et al.*, 1998).

The western and eastern mountainous chains vary greatly in elevations. The eastern chain has an elevation in excess of 1000m.a.s.l. whereas the western chain is much less (around 300m.a.s.l.) (Abed and Al-Hawari, 1991). The higher elevation of eastern chain referred to as an immediate upwarping along the DST fault during NNE horizontal movement of the Arabian plate (Abed and Al-Hawari, 1991). The eastern mountain range is mainly characterized by the existence of structurally controlled scarps exerted by normal faulting. The eastern highlands are deeply dissected into east-west steep-sided valleys or gorges. The average width: height ratio of the developed valleys is 0.54 (Atallah, 2002). These valleys are practically the catchment of alluvial fans. Stream courses in catchment areas follow, at most, fracture systems. We believe that the configuration of drainage basins and streams was affected by net expansions during active tectonic uplifts.

4. Alluvial Fans Settings

Alluvial fans trap sediments delivered from mountain source areas and affect sediment dynamics downstream, either in relation to distal fluvial systems or to sedimentary basin environments (Harvey *et al.,* 2005 and other references therein). Alluvial fans are common in arid-semi arid regions, but they may occur in arctic, alpine, humid temperate and humid tropical regions (Harvey *et al*., 2005 and other references therein). Alluvial fans of arid environments are usually developed when streams depart the mountainous summits and debouche over desert plains and drop straight away most of their sediments. Alluvial fans indicate periods of heavy rains or flashfloods with a resultant debris-flow and stream-flood deposition. Produced fans range in size from small debris cones (< 50m in length) to fluvially dominated megafans up to 60km in length (Harvey *et al*., 2005 and other references therein). The sizes of alluvial fans which depend basically on rates of sediment supply may be a question of climatic changes (Bull, 1991; Harvey, 1997; Harvey *et al*., 1999; Klinger *et al*., 2003). Oguchi and Oguchi (2004) claimed that a rapid geomorphic response to climatic changes is in the form of talus dissection, debris flow, and fan deposition. Klinger *et al*., (2003) stated that changes of geomorphic systems in arid regions exerted by external variables are slow. Besides climate, a number of factors may also influence aggradations/incision processes and alluvial fan geometry. Among these factors are base-level changes caused by sea-level or lake-level fluctuations and/or tectonics (Merritts *et al*., 1994; Klinger *et al*., 2003), variations in sedimentary processes of fluvial systems (Tucker and Slingerland, 1996) geomorphic adjustment of catchment area and fan systems (Bull, 1991), and temporal as well as spatial extents of aggradations/incision processes in response to vegetation growth and climatic changes (Knox, 1984; Bull,1991). Drainage basins respond very differently to climatic changes. A slightly different climatic change may cause a very different geomorphic response. Such a complexity obscures a clear vision about climatic controls on timing and extent of aggradations/incision episodes (Klinger *et al*., 2003).

Stanistreet and McCarthy (1993) recognized three kinds of subaerial fans. These are expressed in terms of debris flow dominated fans, braided fluvial fans, and low-sinuosity/meandering fluvial fans. This triangular scheme can be compared with the classification of Collinson (1996) expressed in terms of gravity flow, fluvial and terminal fans. Blair and McPherson (1994) recommended limiting the term alluvial fan to steep systems with a slope range of 1.5° - 25° in which debris flow and sheet-floods are common. This has been criticized by others who distinguished alluvial fans based on radial sediment dispersal and their cone shape from fluvial systems with linear-elongated patterns. They stated that alluvial fans are a type of fluvial depositional system in which their geomorphic character is much more important than their fluvial style (Harvey *et al*., 2005, among other references).

5. Methodology

Fieldwork, including geological mapping and lithologic description of alluvial fans system at the foot of the eastern mountainous chain in the southern part of Wadi Araba Desert, was carried out. Aerial photographs were used to delineate depositional patterns, tectonic uplift and dislocations of alluvial fans. Size of alluvial fans and slopes of their surfaces in addition to drainage basin areas were determined, and the relationships between these parameters were identified.

6. Results

6.1. Source of Alluvial Fans Sediments

The main source of alluvial fan sediments is the Precambrian granites of Aqaba complex and the associated volcanic materials and meta-sediments. Eight different types, at least, of clasts were recognized; the most common are granite, granodiorite, rhyolite, schist, and gneiss. Diorite and trachytes are less common.

6.2. Morphometric Analyses and Depositional Pattern of Fanglomerates

Debris flow and stream flood facies are responsible for the formation of alluvial fans. Debris flow facies consist of chaotic mixture of fine-coarse clastic sediments. Clasts are supported with sand-clay matrix, which makes about 40% of the original size, and their sizes vary between granules to very large boulders or blocks. The grain-supported stream flood facies is confined to braided channels cut into fan surface and radiate out down slope from fan apex. The channels may go through periods of down cutting, infilling, and channels migration (Fig. 2).

Grain size analysis of 13 samples along a horizontal transect in the distal part of Wadi Rahma fan is shown in Fig. (3). The percentages of gravel, sand and mud are between 47%-84%, 13%-43%, and 3%-10% with averages as 61%, 33% and 6%, respectively. The low percent of fines (mud size) is more likely attributed to down slope washout by surface running waters, and the washed-out fines discharge into the nearby inland sabkhas or desert plain. The great variation in grain size distribution indicates a wide range of hydrodynamic processes acting during deposition of the fans. Grain size gradation from coarse to fine is from fanhead to fantoe.

Grain shape analysis (Zingg, 1935) demonstrates the lack of actual clustering of any type of clasts to a certain shape regardless the differences in grain size (Fig. 4), but they are randomly distributed between equant (spheroid), oblate (disc), bladed and prolate grain shapes without an aspect of preference.

Concerning the roundness, clasts are mainly angular-subangular being experienced low rates of abrasion through transport. The depositional features and textural attributes of fanglomerates give an impression that the sediments traveled only short distances from the source area and have experienced little modifications before deposition.

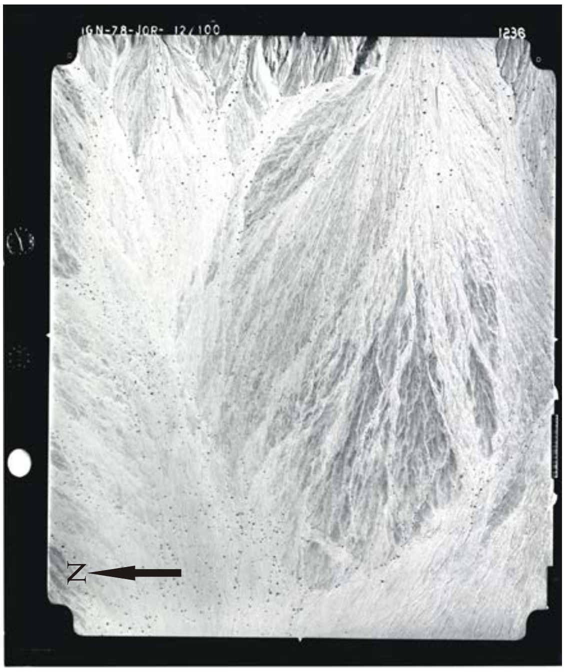

Figure 2. Aerial photograph of Wadi Zibliyya alluvial fan showing color contrast (light-dark) of fan surface due to tectonic uplift.

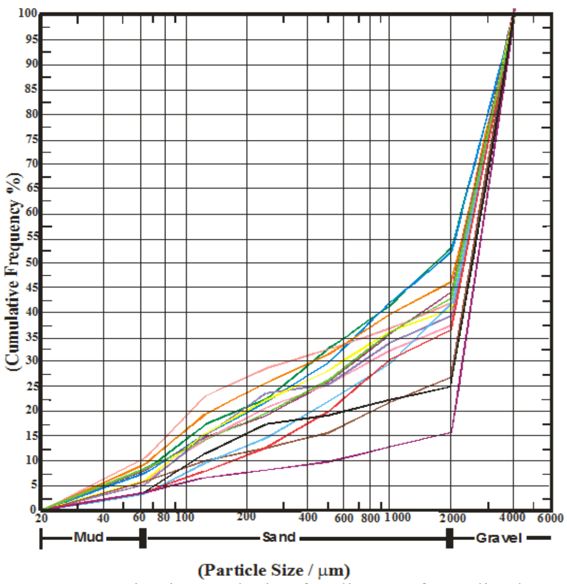

Figure 3. Grain size analysis of sediments from distal part of Wadi Rahma fan.

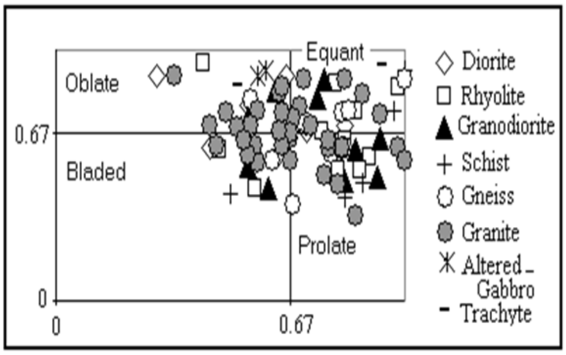

Figure 4. Grain shape analysis Wadi Rahma fanglomerates.

6.3. Geometry of Fans/Drainage Basins

The shape of alluvial fans is generally conical. They concave-up radially (head-to-toe) and concave-down laterally (margin-to-margin. Feeding drainage basins have no definite shapes. They are somewhat elongated in larger drainage basins to semicircular in smaller drainage basins (Fig. 5)..Measurements of fan surface area (FSA), drainage basin area (DBA) and fan slope (FS) pointed to variations in size and slope of the investigated alluvial fans (Table 1). FSA values are between 1.94 km^2 (Wadi Duhaila alluvial fan ‘F8, and 13.81 km^2 (Wadi al-Muhtadi alluvial fan ‘F5,). DBA values are between 5.7 km^2 (Wadi Zibliyya, ‘D2,) and 73.09 km^2 (Wadi Rahma basin ‘D9,). It seems that DBA for all fans with the exception of Wadi Um Ratam fan (F4) is larger than FSA. A direct relationship between DBA and FSA is demonstrated in Fig. (6). The size of the alluvial fans is related to the size of drainage basins, available accommodation space, rates of sediment delivery and style of sediment production in the catchment areas.

Classic alluvial fans of arid regions are usually laid down in tectonically active basins. The available capacity of such basins will be increased if the drainage basins enlarge. Smaller drainage basins deliver sediments to alluvial fans in every transport event more effectively than larger drainage basins can do (Blair and McPherson, 1994; Ritter *et al*., 1995). This can be visualized in the increase of FSA relevant to DBA as it is the case in Wadi Um Ratam fan (Table 1). Fan slope (FS) is a function of lithology in the source area, particle size of debris material, drainage basin area (DBA), rates of discharge (Bull, 1978; Bull and McFadden, 1977) and size of alluvial fan (Bull, 1964; Hooke, 1965). The results of the present study (Table 1) showed that alluvial fans slopes are between 2.6° (Wadi Rahma alluvial fan “ F9”) and 6.3°(Wadi Duheila alluvial fan “F8”). A modest inverse relationship is more likely between FS and FSA (Fig. 6) . This is consistent with the findings of Bull (1964) and Hooke (1965): sizeable alluvial fan surfaces are characterized by low slope angles and vice versa. A decrease in FS may be attributed to systematic variations in debris caliber, depositional processes or an increase of discharge (Hooke, 1965). The alluvial fans of Wadi Al-Muhtadi (F5) and Wadi Rahma (F9) are mainly produced by relatively large discharges resulted in gentler slope fan surfaces. Whereas Wadi Duheila alluvial fan (F8) is more likely produced by a lower discharge and it has a higher-slope fan surface.

Table 1. Fan/Drainage basin areas ((km^2) and fan slope (degrees).

Fan number (F_{1-9})	Name of fan	*Fan area (FA) (km^2)	** Drainage basin area (DBA) (km^2)	Fan slope (degree)
F_1	Wadi Malghan fan.	6.48	21.22	3.2
F_2	Wadi Zibliyya fan.	3.90	5.70	4.6
F_3	Wadi As-Sammaniyya fan.	8.84	11.50	4.3
F_4	Wadi Um Ratam fan.	10.24	5.84	4.3
F_5	Wadi Al Muhtadi fan.	13.81	30.96	3.2
F_6	Wadi Al Waara fan.	5.80	6.31	4.1
F_7	Wadi Nukhaila fan.	7.33	12.07	4.5
F_8	Wadi Duhaila	1.94	7.63	6.3
F_9	Wadi Rahma	11.61	73.09	2.6

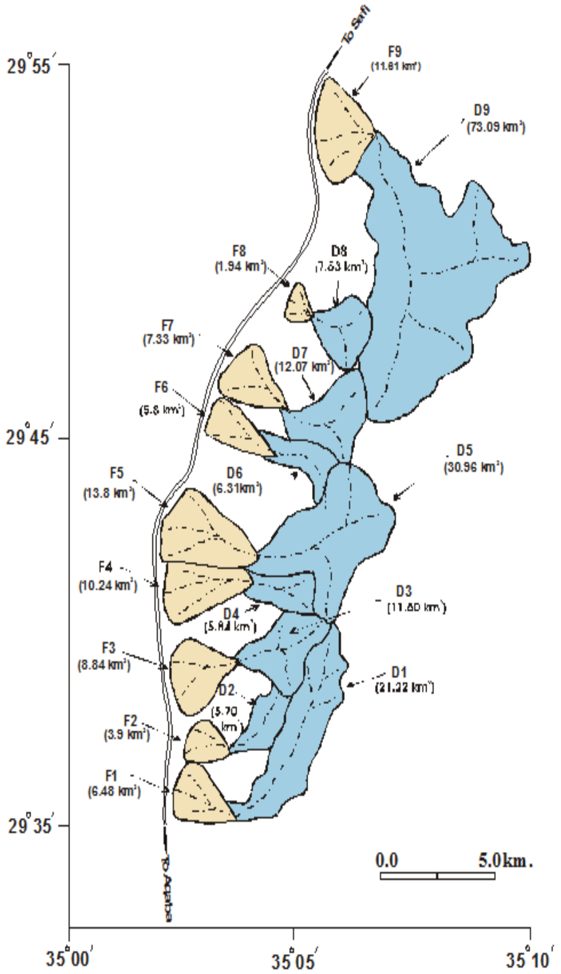

Figure 5. Geometry and surface area of fan/drainage basin system.

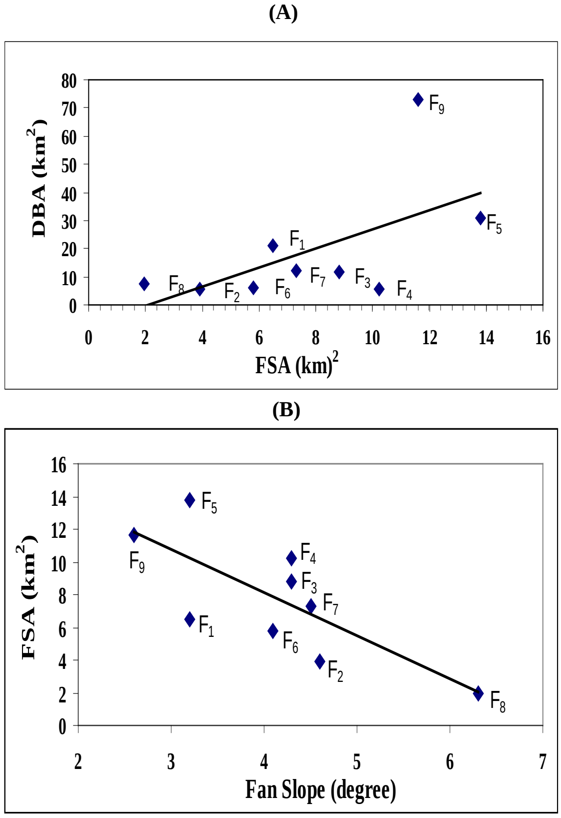

Figure 6. (**A**) Scatter plot of fan surface area (FSA) vs. drainage basin area (DBA). (**B**) Scatter plot of fan surface area (FSA) vs. fan slope (FS).

6.4. Fans Evolution as a Function of Tectonic Setting

Field observations and aerial-photographs analyses show a direct relationship between alluvial fans development and tectonic setting. Active faulting along the DST and its subsidiary faults control strongly sedimentation patterns and evolution of alluvial fans. The Aqaba-Gharandal fault (Fig. 7) is a typical example of an active faulting and scarp development. Fault-controlled scarps, pull-apart basins and narrow grabens hosted talus deposits and fanglomerates are very common in Wadi Ratam, Wadi Al Muhtadi, Wadi Malghan and Wadi As-Sammaniyya in the study area (Atallah and Al Taj, 2004). Mountain-front sinuosity was measured along the mountain front east of Wadi Araba (Atallah, 2002). It is the ratio between the length of the mountain front and the straight- line length of the front (Bull, 1978). The low sinuosity index (1.08) of the adjacent eastern mountain front is a sign for a strong uplift, which was responsible for the development of alluvial fans in the Pleistocene time (Atallah, 2002; Atallah and Al-Taj, 2004). Aerial photographs display color contrasts between younger sediments (light-colored) laid down in alluvial fans proximities and older sediments (dark-colored) in distal parts (Fig. 2). The contrast in colors has been explained by Bull (1978) as a sign of an active uplift in highland regions and fanhead entrenchment. Tectonic forces not only influences the geomorphic setting of alluvial fans, but slopes of alluvial fans surfaces will be affected through uplift and changes in base levels (Calvache *et al.*, 1997; Harvey, 2002).

Type of bedrock, geomorphic adjustment, and geometry of drainage basins as well as the rates and history of sediment supply may all contribute in alluvial fan development. The geomorphic response to climate change in the Quaternary was more likely in the form of fanhead entrenchment or talus dissection. We believe that any excess of stream power relative to sediment load enhances fan entrenchment.

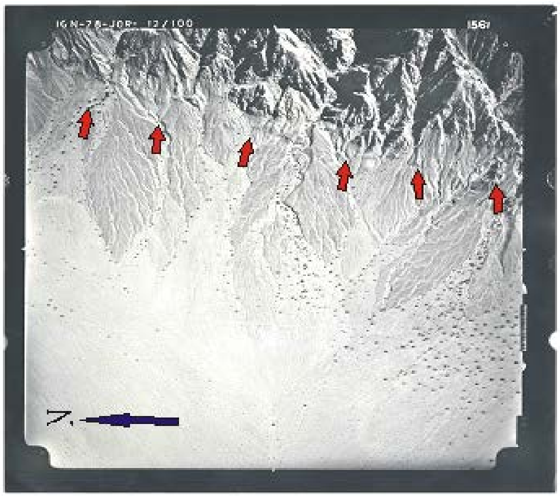

Figure 7. Aerial photograph showing an active fault scarp produced by Aqaba-Gharandal fault (arrows) north of Wadi Rahma.

7. Discussion and Conclusions

The present study relies primarily on the tectonic uplift, and the initiation of the Dead Sea Transform (DST) to explain the geomorphic evolution of alluvial fans at the foot of eastern mountains, south of Wadi Araba Desert (WAD). T he results showed that the fan surface area (FSA) is generally proportional to the drainage basin area (DBA) because of greater sediment inputs delivered to the site of deposition. C oncerning the inverse relationship between fan surface area (FSA) and fan slope (FS), we intimately know that sediment transport in large drainage basins is for longer distances, comparative to short transport in smaller drainage basins. Because of this, the longer transport of sediments leads to the development of relatively larger alluvial fans having more fine sediments and with lower slope angles and vice versa (Bull, 1964; Hooke, 1965). In addition, tectonic uplift and sediment accretion at mouths of streams produce steep-slope and smaller alluvial fans relative to larger alluvial fans with more gentle-slope surfaces. The occurrence of Aqaba-Ghrarandal fault-scarps at the base of the eastern mountains front of Wadi Araba, the tilting of fans due west and the deposition of younger sediments at the proximal part of alluvial fans (e.g .Wadi Zibliyya fan) are all strong pieces of evidence on the tectonic uplift in the catchment areas.

The strike slip movement along the DST (Ginat *et al.*, 1998) caused some dislocations to alluvial fans off their original sites (Fig. 8). Some of the fans were subjected to differential uplift (Fig. 9). In view of the tectonic setting, we may infer to the occurrence of some sequential development of drainage basins through stream capture. Any modification in catchment area affects dramatically the routings and sediment supply to the sedimentary basin. Therefore, the surface area and size of an alluvial fan adjusts to accommodate any change in the catchment area. Tectonic uplift may raise the upper portion of a drainage basin relative to the base level of a stream system. The net effect is to increase the overall gradient of stream and rates of down cutting toward the base level. Therefore, high rates of erosion in catchment area is expected, which is more likely exceed the rates of sedimentation in site of deposition. This conclusion agrees fairly with the obtained results, where DBA is greater than FSA (Table 1). However, the case in Wadi Um Ratam alluvial fan (F4) is dissimilar, where FSA value is nearly twice that of DBA (Table 1, Fig. 6). The reason behind this may refer to a sort of net expansion and stream capture. The capturing in catchment area of Wadi Um Ratam left behind an abandoned drainage basin, which was previously the feeding source of the related alluvial fan. The new-developed smaller drainage basin incorporated within the expanded drainage basin of Wadi Al Muhtadi fan (F5) and drained by t he cat chy stream is no doubt the new supplier f or Wadi U m Ratam a lluvial fan (F4) sediments. Therefore, we believe that Wadi Um Ratam alluvial fan (F4) developed prior to the stream capture. A similar approach was introduced by Mather *et al*. (2000) who studied three modern mountain catchment areas in SE S pain affected by a river c apture. Later, other authors found that the catchment areas were effected by a regional tectonic uplift, most significantly by drainage net expansion and river capture rather than by a l owering of surface relief. Variables other than tectonic uplift may also interact to produce progressive changes in alluvial fan/drainage basin system; these are: the history and rates of sediment supply and the intense and duration of surface flow as a function of climate at time of deposition. Such variables need further assessment. In northern Wadi Araba (Dead Sea area), the story of alluvial fans development might be a little bit different. Klinger *et al*. (2003) looked for better understanding of the late Quaternary climatic changes and active tectonic impacts on morphogenesis of alluvial fans that have been deposited before lake transgression (Lisan period) which started at about 70 KY B.P. The said authors presumed that relative high-stand lake-water levels were interrupted by time periods of fans aggradations. Therefore, the climate change factor seems to have a p riority to explain alluvial fans development in northern WAD.

However, this conclusion does not exactly mean that the tectonic forces did not have a role at that time. Whereas, the geometry and location of these alluvial fans were constrained to some extent, by tectonic forces since they formed at the base of cumulative normal fault scarps similar to the alluvial fans system, south of Wadi Araba. However, Klinger *et al*. (2003) believed that the tectonic control on episodes of alluvial fan aggradations and river entrenchment seems doubtful for the period of interest, since a 1 0m vertical movement along the Dead Sea shorelines was estimated in the post-Lisan period. Another correlation between alluvial fans and Quaternary climatic change (Le Beon, *et al*., 2012) shows that two of the three periods of alluviation are correlated with wet periods that are regionally well documented.

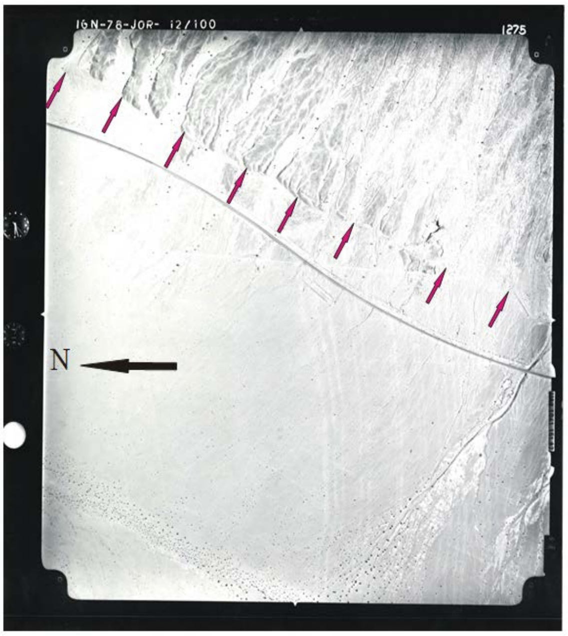

Figure 8. Aerial photograph showing dislocations in the western edge of Wadi Al Muhtadi fan caused by Wadi Araba strike slip fault. The fault is expressed by a prominent westward facing scarp and a horizontal offset of the fan surface.

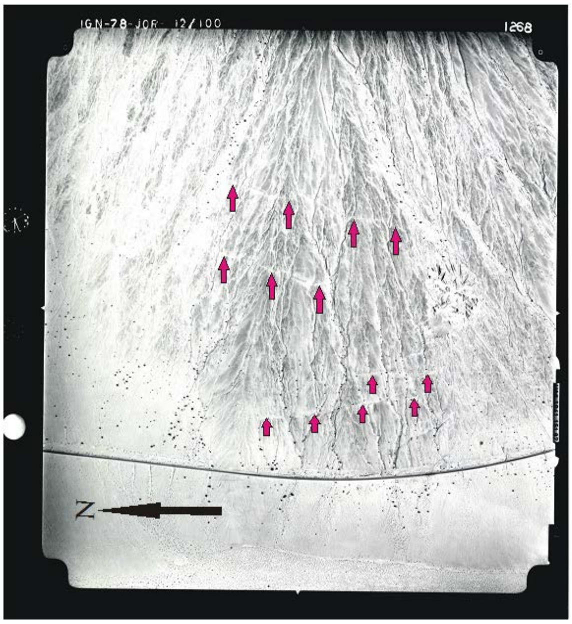

Figure 9. Aerial photograph of fault scarps affecting Wadi As Sammaniyya alluvial fan and causing some differential uplift of fan surface.

Acknowledgments

This work received financial support from Yarmouk University Research Council (Grant No. 1/2003). The authors would like to thank the two reviewers for their constructive comments on this paper.

References

[1] Abed, A.M. and Al-Hawari, Z.K. (1991). Geology and Sepiolite Formation in the Taba Continental Sabkha, Southern Dead Sea–Araba Rift, Jordan. Dirasat 18B, 41-65 .University of Jordan, Amman.

[2] Alçiçek, M.C., Kazani, N., özkul, M. (2005). Multiple rifting pulses and sedimentation pattern in the Çameli Basin, southwestern Anatolia, Turkey. Sedimentary Geology, 409-431.

[3] Atallah, M. (2002). Morphotectonic indices of the eastern Wadi Araba (Dead Sea rift, Jordan). Geogr. Fis. Dinam. Quat. 25, 3-10.

[4] Atallah, M. and Al-Taj, M. (2004). Active surface ruptures of the Dead Sea transform in Wadi Araba, Jordan. Dirasat, series B: Pure Sciences 31 (1), 59-81.

[5] Beaumont, P. (1972). Alluvial fans along the foothills of the Elburz Mountains, Iran. Palaeogeography, palaeoclimatology, Palaeoecology 12, 251-273.

[6] Ben-David, R., Eyal, Y., Zilberman, E., Bowman, D. (2002). Fluvial systems response to rift margin tectonics: Makhtesh Ramon area, Southern Israel .Geomorphology 45,147-163.

[7] Bender, F. (1974). Explanatory notes on the Geological Map of Wadi Araba, Jordan (Scale 1:100,000, 3 sheets). Geol. Jahrbuch B 10, 1-62.

[8] Blair, T.C., McPherson, J.G. (1994). Alluvial fan processes and forms. In: Abraham, A.D., Parsons, A.J. (eds.) Geomorphology of desert environments. London. Champan & Hall, p. 354-402.

[9] Bull, W.B. (1964). Geomorphology of segmental alluvial fans in western Fresno County, California. U.S. Geological Survey, Professional Paper, 352-E, 89-129.

[10] Bull, W. B., McFadden L. (1977). Tectonic geomorphology north and south of the Garlock fault, California. In: Doering, D.O. (ed.) Proceedings of 8th Annual Geomorph. Symp. State University of New York at Binghamton, Binghamton, NY., 116-138.

[11] Bull, W. (1978) - Geomorphic tectonic activity classes of the south front of the San Gabriel Mountains, California. Contract Report 14-08001-G-349, USGS.

[12] Bull, W.B. (1991). Geomorphic Responses to Climat Change. Oxford Univ. Press, Oxford, 326pp.

[13] Calvache, M., Viseras, C., Fernandez, J. (1997). Controls on alluvial fan development- evidence from fan morphometry, Sierra Nevada, SE Spain. Geomorphology 21, 69-84.

[14] Collinson, J.D. (1996). Alluvial sediments. In: Reading, H.G. (Ed.), Sedimentary Environments: Process, Facies and Stratigraphy, 3rd ed. Blackwell Science, Oxford, pp. 37–82.

[15] El Baz, F., (1986). Monitoring of the sand-moving desert winds. In: El-Baz, F., Hassan, M. H. A. (Eds.), Physics of Desertification, Martinus Nijhoff Publishers, Dordrecht, pp. 141-158.

[16] Garfunkel Z., Zak I. & Freund, R. (1981). Active faulting in the Dead sea rift .Tectonophysics 80, 1-26 .

[17] Gasse, F., Fontes, J.C., Plaziat, J.C., Carbonet, P., Kaczmarska, I., De Deckker, P., Soulie-Marche, I., Callot, Y., Dupeuple, P., (1987). Biological remains geochemistry and stable isotopes for the reconstruction of environmental and hydrological changes in the Holocene lakes from the Northern Sahara. Palaeogeography, Paleoclimatology, Paleoecology 60, 1-46.

[18] Ginat, H., Enzel, Y., Avni, Y. (1998). Translocated Plio-Pleistocene drainage systems along the Arava fault of the Dead Sea transform. Tectonophysics 284, 151-160.

[19] Glennie, K.W., (1987). Desert study environments, present and past- A summary. Sedimentary Geology 50, 136-165.

[20] Harvey, A.M. (1997) The role of alluvial fans in arid zone fluvial systems. In: Thomas, D.S.G. (ed.), Arid Zone Geomorphology: Processes, Forms and Change in Drylands. John Wiley & Sons, Chichester, 231–259 .

[21] Harvey, A.M., Wigand, P.E., Wells, S.G. (1999). Response of alluvial fan systems to the late Pleistocene to Holocene climatic transition: contrast between the margins of pluvial lakes Lahotan and Mojave, Nevada and California, USA. Catena 36, 255-281.

[22] Harvey, A.M. (2002). The role of alluvial fans in arid zone fluvial systems. In: D.S.G. Thomas (editor), Arid Zone Geomorphology: Process, Form and Change in Drylands, 2nd edit., Wiley, Chichester, 231-259,

[23] Harvey, A.M., Mather, A.E., Stokes, M. (2005). Alluvial Fans: Geomorphology, Sedimentology, Dynamics. Geological Society, Special Publication 251, pp248, London.

[24] Hooke, R. (1965). Alluvial fans, PhD Thesis, California Institute of Technology, Pasadena, California, 192p .

[25] Ibrahim Kh. (1991). The geology of Wadi Rahma, map sheet no. 3049 IV. Natural Resources Authority, Bulletin 15, Amman, 122pp .

[26] Jarrar, Gh. (1984). Late Proterozoic crustal evolution of the Arabian–Nubian Shield in the Wadi Araba Area, SW Jordan. Braunschweiger Geologisch–Palaeontologishce Dissertationen 2, Braunschweig, Germany. 107 pp.

[27] Klinger, Y., Avouac, J.P., Abu Karaki, N., Dorbath, L., Bourles, D., Reyss, L. (2000). Slip rate on Dead Sea Transform Fault in Northern Araba Valley (Jordan). Geophysics Journal International 142, 755-768 .

[28] Klinger, Y., Avouac, J. P., Bourles, D., Tisnerat, N. (2003). Alluvial deposition and lake-level fluctuations forced by Late Quaternary climate change: the Dead Sea case example. Sedimentary Geology 162, 119-139.

[29] Knox, J.C. (1984). Responses of river systems to Holocene climates. In: Late Quaternary Environments of the United States: Vol. 2, The Holocene, Longman, London, 26-41.

[30] Le Beon, M. , Klinger,Y., Meriaux, A.-S., Al-Qarioti, M., Finkel, R. C., Mayyas, O. and Tapponier P. (2012). Quaternary morphotectonic mapping of the Wadi Araba and implications for the tectonic activity of the southern Dead Sea fault. Tectonics, 31. Tc 5003. Doi 10.1029/2012TC003112.

[31] Makhlouf, I., Amereh, B. Abed, A. (2010). Sedimentlogy and Morphology of Quaternary Alluvial Fans in Wadi Araba, Southwest Jordan. JJEES 2, 79 – 98.

[32] Mather, A.E., Harvey, A.M., Stokes, M. (2000). Quantifying long-term catchment changes of alluvial fan systems. Geological Society of America Bulletin 112, 1825-1833.

[33] McLaren, J.,Gilbertson, D.D., Grattan, J.P., Hunt, C.O., Duller, G.A.T., Barker, G.A. (2004). Quaternary palaeogeomorphologic evolution of the Wadi Faynan area, southern Jordan. Palaeogeography, Palaeoclimatology, Palaeocology 205,131-154.

[34] Merritts, D.J., Vincent, K.R., Wohl, E.E. (1994). Long river profiles, tectonism and eustasy: a guide to interpreting fluvial terraces. Journal Geophysics Research 99, 14031-14050.

[35] Niemi, T., Zhang, H., Atallah, M., Harrison, J.B. (2001). Late Pleistocene and Holocene slip rate of the Northern Wadi Araba Fault, Dead Sea Transform, Jordan. Journal of Seismology 5, 449-474.

[36] Oguchi, T., Oguchi Ch. T. (2004). Late Quaternary rapid talus dissection and debris flow deposition on an alluvial fan in Syria. Catena 55, 125-140.

[37] Petit- Maire, N., Guo, Z.T. (1997). Holocene paleoprecipitation over the present-day Sahara desert. Continental signals in Paleomonsoon Dynamics in Africa, Inter-Hemispheric Perspectives. SIWA Workshop, Paleomonsoon Project 33.

[38] Rashdan M. (1988) . The regional geology of the Aqaba-Wadi Araba area, map sheets 3049 III, 2949 II. Bulletin 7, Natural Resources Authority, Amman, Jordan, 87pp.

[39] Ritter, D.F., Kochel, R.C., Miller, J.R. (1995). Process Geomorphology. 2nd edition, W.C. Brown Publishers, Dubuque, IA, 544pp.

[40] Saqqa, W., (1998). Surface texture of quartz grains from arid continental environments (Wadi Araba area, SW Jordan). N.Jb. Geol. Paläont. Abh., 135-144,

[41] Saqqa, W. and Atallah, M. (2004). Characterization of the aeolian terrain facies in Wadi Araba desert, southwestern Jordan . Geomorphology 62, 63-87.

[42] Stanistreet IG, McCarthy TS (1993). The Okavango fan and the classification of subaerial fan systems. In: Fielding CR (ed.) Current Research in Fluvial Sedimentology. Sedimentary Geology 85, 115-133.

[43] Tucker, G.E., Slingerland, R. (1996). Predicting sediment flux from fold and thrust belts. Basin Res. 8, 329-349.

[44] Zhuo, Z., Baoyin, Y., Petit-Maire, N. (1998). Paleoenvironments in China during the last glacial maximum and the Holocene optimum. Episodes 21, 152-158.

[45] Zingg, Th. (1935). Beitrag zur Schotteranalyse. Schweizerische Mineralogische und Petrologische Mitteilungen 15, 39-40.

التقديم

بعون من الله وتوفيقه يسعدنا أن نقدم العدد الثاني من المجلد الخامس من المجلة الأردنية لعلوم الأرض والبيئة وهي مجلة علمية محكمة ومفهرسة تصدر عن اللجنة العليا للبحث العلمي وبدعم من صندوق البحث العلمي التابع لوزارة التعليم العالي والبحث العلمي في المملكة الأردنية الهاشمية ويشرف على إعداد ونشر هذه المجلة عمادة البحث العلمي والدراسات العليا في الجامعة الهاشمية.

بإسمي واسم أعضاء هيئة التحرير فإنني أتقدم بجزيل الشكر وعظيم الامتنان للزملاء المقيمين وكل من ساهم في إخراج هذا العدد على جهودهم الخيرة التي بذلوها في إنجاح هذه المجلة.

ونحن كهيئة تحرير للمجلة نحرص دوماً على الاستمرار في البحث ونشر الأبحاث العلمية المحكمة والتي ستكون بعون الله ذات فائدة للباحثين في المؤسسات الأكاديمية والتطبيقية المحلية والعربية والعالمية ونتمنى من هذه المؤسسات تزويدنا دوماً بالأبحاث والتي نعدهم بأن يتم معاملتها بكل دقة وأمانة واحتراف مع كل الحرص على سرعة النشر وحسب الأصول العلمية المتبعة، حيث اننا كهيئة تحرير سنبدل كل الجهود للمضي قدما في إصدار الأعداد المنتظمة السنوية من المجلة مما يساعد ويخدم الباحثين ويحقق أهداف المجلة في نشر كل ما هو مميز ومفيد أضافه لمحاولة السير باجراءت الاعتماد على المستوى العالمي والله نسأل العون والسداد.

أ.د. عيد عبد الرحمن الطرزي
رئيس هيئة التحرير
كلية الموارد الطبيعية والبيئة
الجامعة الهاشمية

المملكة الأردنية الهاشمية

الجامعة الهاشمية

المجلة الأردنية
لعلوم الأرض والبيئة

JJEES

مجلة علمية عالمية محكمة

تصدر بدعم من صندوق البحث العلمي

http:// jjees.hu.edu.jo/

ISSN 1995-6681

المجلة الأردنية لعلوم الأرض والبيئة

مجلة علمية عالمية محكمة

المجلة الأردنية لعلوم الأرض والبيئة: مجلة علمية عالمية محكمة ومفهرسة ومصنفة، تصدر عن الجامعة الهاشمية وبدعم من صندوق البحث العلمي – وزارة التعليم العالي والبحث العلمي، الأردن.

ترسل البحوث إلى العنوان التالي:

رئيس تحرير المجلة الأردنية لعلوم الأرض والبيئة

عمادة البحث العلمي والدراسات العليا

الجامعة الهاشمية

الزرقاء ١٣١٣٣ – الأردن

هاتف ٩٠٣٣٣٣-٥-٩٦٢+ فرعي ٤١٤٧

Email: jjees@hu.edu.jo, Website: www.jjees.hu.edu.jo